





DAVID W. TAYLOR NAVAL SHIP RESEARCH AND DEVELOPMENT CENTER



Bethesda, Maryland 20084

AD A068486

CALIBRATION OF 5-HOLE AND 13-HOLE PITOT TUBES BEFORE
AND AFTER A FULL-SCALE WAKE SURVEY
ON THE R/V ATHENA

by

Rae B. Hurwitz Marilyn Dick

APPROVED FOR PUBLIC RELEASE: DISTRIBUTION UNLIMITED

SHIP PERFORMANCE DEPARTMENT

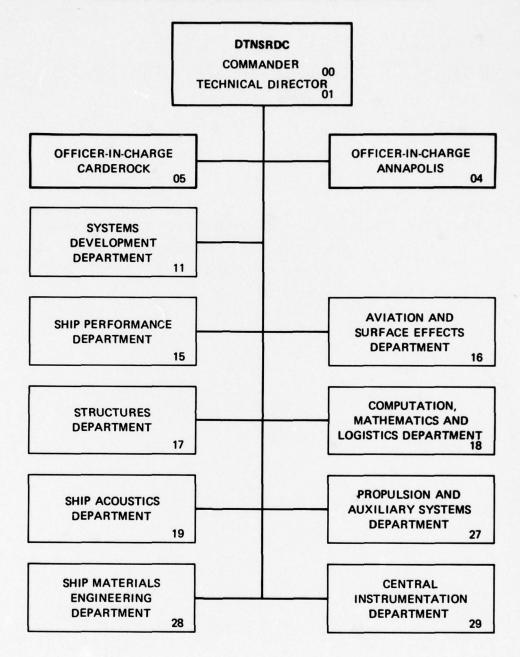
D D C PROCEDURE MAY 11 1979 PEUSISIU ISU

DTNSRDC/SPD-0833-03

December 1978

DDC FILE COPY

MAJOR DTNSRDC ORGANIZATIONAL COMPONENTS



UNCLASSIFIED

SECURITY CLASSIFICATION OF THIS PAGE (When Date Entered) READ INSTRUCTIONS BEFORE COMPLETING FORM (12) REPORT DOCUMENTATION PAGE 2. GOVT ACCESSION NO. 3. RECIPIENT'S CATALOG NUMBER REPORT NUM DTNSRDC SPD-0833-03 TYPE OF REPORT & PERIOD COVERED CALIBRATION OF 5-HOLE AND 13-HOLE PITOT TUBES BEFORE AND AFTER A FULL-SCALE WAKE SURVEY Final ON THE R/V ATHENA ERFORMING ORG. REPORT NUMBER CONTRACT OR GRANT NUMBER(*) AUTHORIA N00600-78-C0440 Rae B. Hurwitz Marilyn Dick PERFORMING ORGANIZATION NAME AND ADDRESS David W. Taylor Naval Ship Research 63508N, S0379001, 19977. and Development Center 1-1524-641 Bethesda, Maryland 20084 REPORT DATE 11. CONTROLLING OFFICE NAME AND ADDRESS Dec Naval Sea Systems Command (NAVSEA 0331G) Washington, D.C. 20362 179 14. MONITORING AGENCY NAME & ADDRESS(If different from Controlling Office) 15. SECURITY CLASS. (of this repo UNCLASSIFIED 15a. DECLASSIFICATION/DOWNGRADING 16. DISTRIBUTION STATEMENT (of this Report) APPROVED FOR PUBLIC RELEASE: DISTRIBUTION UNLIMITED 17. DISTRIBUTION STATEMENT (of the abstract entered in Block 20, if different from Report) 411167 winter, VA 18. SUPPLEMENTARY NOTES This report was prepared by Chi Associates, Inc. under contract with the David W. Taylor Naval Ship Research and Development Center. The contract number was N00600-78-C0440. 19. KEY WORDS (Continue on reverse side if necessary and identify by block number) Polynomial Curve Fitting 5-Hole Pitot Tube Error Tolerance Intervals 13-Hole Pitot Tube Scanivalve Pressure Systems Fluid Velocity Measurement 20. ABSTRACT (Continue on reverse side if necessary and identify by block number) This report presents the results of the calibrations of spherical 5and 13-hole pitot tubes before and after they were used in a full-scale wake survey. Brief descriptions of standard and specifically developed calibration instrumentation and of calibration procedures are included. The purpose of the calibrations was to determine differential pressure ratios COMT which, during a full-scale wake survey, could be used to compute velocity (Continued on reverse side)

DD 1 JAN 73 1473 EDITION OF 1 NOV 65 IS OBSOLETE S/N 0102-014-6601

UNCLASSIFIED 4 16 SECURITY CLASSIFICATION OF THIS PAGE (When Data Entered)

UNCLASSIFIED

LECTIFITY CLASSIFICATION OF THIS PAGE(When Date Entered)

(Block 20 continued)

component ratios. Differential pressure ratios obtained during the calibrations are depicted graphically in terms of angle of inclination for the pitot tubes at 20 fps (6.10 m/s). In addition, one 5-hole pitot tube was run at four velocities ranging from 6 to 25 fps (1.83 to 7.62 m/s). The calibrations were shown to have a small speed dependence at higher speeds but a significant speed dependence at the lower speeds. Finally, the composite test results for the 5-hole pitot tubes were analyzed statistically to obtain the means, spreads and tolerance intervals. Due to the observed spread of the data among different tubes, the application of individual calibrations, as opposed to one average calibration, was recommended.

UNCLASSIFIED

11

TABLE OF CONTENTS

concerns to the most of the most of the concerns of the concer	Page
LIST OF FIGURES	iv
LIST OF TABLES	v
NOTATION	νi
ABSTRACT	1
ADMINISTRATIVE INFORMATION	1
INTRODUCTION	2
EXPERIMENTAL APPARATUS	3
EXPERIMENTAL PROCEDURE	5
PRESENTATION AND DISCUSSION OF RESULTS	7
CONCLUSIONS	12
REFERENCES	13
TABLES	14
FIGURES	25
APPENDIX A: Procedure for Deriving Velocity Component Ratios from Pressure Measurements	165
APPENDIX B: Calibration Constants	170

BY	ARCESSION to				
DISTRIBUTION/ATANAPILITY COORS	8116		nillo Sol	Hee]	X
SY	***		uff book	lw "	o'
DISTRIBUTION/ATANABILITY SOOS	ENDHAUMEN	1			0
	METIFICATION	l		-	
				4	
	NI		1		

LIST OF FIGURES

		Page
1	-	Outline Plan of Deep Water and High Speed Basins 26
2	-	Schematic of 5-Hole Pitot Tube
3	-	Schematic of 13-Hole Pitot Tube
4	-	Instrument Housing of Calibration Rake
5	-	Calibration Rake Showing Horizontal and Vertical Angular Quadrants
6	-	Schematic of Carriage/Cone/Rake Assembly
7	-	Scanivalve Pressure Control and Measurement System 32
8	-	Strip Chart Record of Pressure Measurements from a 5-Hole Pitot Tube
9	-	Pitot Tube During Air Bleed Cycle
10	-	Pitot Tube During Measuring Cycle
11	-	Drag Coefficient for Spheres as a Function of Reynolds Number
12-58		Pre Calibrations of the 5-Hole Pitot Tubes
59-114	١ -	Post Calibrations of the 5-Hole Pitot Tubes 84-139
115-12	26 -	Pre Calibrations of the 13-Hole Pitot Tubes 140-151
127-13	54 -	Post Calibrations of the 13-Hole Pitot Tubes 152-159
135		Pre Calibration Composite for the Horizontal/Tangential Plane
136	•	Pre Calibration Composite for the Vertical/Radial Plane
137	•	Post Calibration Composite for the Horizontal/Tangential Plane
138		Post Calibration Composite for the Vertical/Radial Plane
139		Post Calibration of Tube 13 in the Horizontal/Tangential Plane at Four Different Speeds

LIST OF TABLES

												Pa	ge
1	-	for the Temp	Experimental perature and	Speed Ra	inge	of th	ie					•	15
2	-		ibrated Pitot										
3	-	Statistical	Calibration	Summary	for	(T ₂ -	T ₁)/	(2C -	- T ₂	- 11	T ₁)		17
4	-	Statistical	Calibration	Summary	for	(C -	T ₁)/V	2					18
5	-	Statistical	Calibration	Summary	for	(T ₁ -	T ₂)/	(2C -	т ₁	-	T ₂)		19
6	-	Statistical	Calibration	Summary	for	(C -	T ₂)/V	2					20
7	-	Statistical	Calibration	Summary	for	(R ₂ -	R ₁)/	(2C -	- R ₂	-	R ₁)		21
8	-	Statistical	Calibration	Summary	for	(C -	R ₁)/V	2					22
9	-	Statistical	Calibration	Summary	for	(R ₁ -	R ₂)/	(2C -	- R ₁	-	R ₂)		23
10	-	Statistical	Calibration	Summary	for	(C -	R ₂)/V	2					24

NOTATION

С	Center pitot tube hole pressure							
P{}	Probability of the event {} occurring							
Rn	Reynolds number							
R_1, R_2	Outer pitot tube hole pressure in vertical/radial plane							
T	Sea or basin water temperature							
T ₁ , T ₂	Outer pitot tube hole pressure in horizontal/tangential plane							
V	Velocity							
β	Flow angle from the pitot tube center hole							

ABSTRACT

This report presents the results of the calibrations of spherical 5- and 13-hole pitot tubes before and after they were used in a full-scale wake survey. Brief descriptions of standard and specifically developed calibration instrumentation and of the calibration procedure are included. The purpose of the calibrations was to determine differential pressure ratios which, during a full-scale wake survey, could be used to compute velocity component ratios. Differential pressure ratios obtained during the calibrations are depicted graphically in terms of angle of inclination for the pitot tubes at 20 fps (6.10 m/s). In addition, one 5-hole pitot tube was run at four velocities ranging from 6 to 25 fps (1.83 to 7.62 m/s). The calibrations were shown to have a small speed dependence at higher speeds but a significant speed dependence at the lower speeds. Finally, the composite experimental results for the 5-hole pitot tubes were analyzed statistically to obtain the means, spreads and tolerance intervals. Due to the observed spread of the data among different tubes, the application of individual calibrations, as opposed to one average calibration, was recommended.

ADMINISTRATIVE INFORMATION

This work was performed under the Controllable Pitch Propeller Research Program sponsored by the Naval Sea Systems Command (NAVSEA 0331G) and administered by the David W. Taylor Naval Ship Research and Development Center (DTNSRDC). The project was funded under Task Area S0379001 and DTNSRDC Work Unit Number 1-1524-641.

INTRODUCTION

As part of its overall project to adapt controllable pitch propellers to the needs of high speed combatant ships, the David W.

Taylor Naval Ship Research and Development Center (DTNSRDC) conducted a full-scale wake survey aboard the R/V ATHENA in September 1977. The specific goal of this project was to obtain propeller disk velocity component ratios in the wake of a full-scale ship through the use of 5-hole and specially designed 13-hole spherical pitot tubes. Additional data were derived from the velocity components through a harmonic analysis, from which propeller design criteria could be verified.

Chi Associates, Inc. assisted DTNSRDC in performing the analysis of experimental data from two types of instrumentation calibrations. One was conducted prior to the full-scale wake survey and the second following the survey. These will be referred to in the text as the pre and post calibrations, respectively. The basic purpose of the calibrations was to measure differential pressure ratios which could be converted during the full-scale wake survey into velocity component ratios. The pre calibrations were conducted during June and July of 1977, while the post calibrations were performed during January and February of 1978. Calibrations were conducted at known angles for several speeds, and calibration curves were plotted from the data gathered. The results of these two sets of experiments were compared to determine if significant differences existed.

This report gives background information relevant to both 5- and 13-hole spherical pitot tubes and describes the experimental apparatus used and the procedures employed during calibration. It also contains figures and appendices relevant to the technical details of the experiments.

EXPERIMENTAL APPARATUS

Calibrations were conducted on the towing carriages at DTNSRDC. The pre calibration utilized both Carriage 2 of the Deep Water Basin and Carriage 5 of the High Speed Basin, while only the High Speed Basin was used for the post calibration. Though it would have been more convenient to operate from one carriage for both series of experiments, two carriages were used for the pre calibration due to scheduling conflicts and time constraints. Schematics of the two basins are shown in Figure 1.

Carriage 2, which is mounted over the Deep Water Basin, is capable of operating at speeds up to 20 knots. Its electrohydraulic drive can maintain carriage speeds to within a few hundredths of a knot. Carriage 5, which is mounted over the High Speed Basin, can operate at speeds up to 55 knots. The electric drive is an adjustable voltage DC system with an automatic feedback control, which can regulate the steady speed to within \pm 0.1 percent of its prescribed value. Both carriages are equipped with digital data acquisition systems for collecting experimental data.

Most of the instrumentation in the pre and post calibrations was supplied by the Department of Naval Architecture and Marine Engineering at the University of Michigan. Some of the special equipment, particularly the 13-hole pitot tube, was designed and manufactured specifically for this project.

The principal instrument used in the calibration was the 5-hole brass spherical pitot tube, 19 inches (483 mm) long and 2.375 inches (60 mm) in diameter. Detailed design features are presented in Troesch et al. 1* and a graphic description of the 5-hole pitot tube is given in Figure 2. It can be seen that each of the four holes used for measuring the angles *Complete listing of references given on page 13.

has been drilled 30 degrees away from the center hole and 90 degrees apart from one another.

In addition to the 5-hole pitot tube, a 13-hole pitot tube was specially designed for the full scale wake survey and was calibrated at DTNSRDC. This pitot tube differs considerably from the classical design described by Janes² in that it consists of seven partially redundant 5-hole pitot tube combinations rather than three completely redundant 5-hole pitot tube combinations. Figure 3 depicts the design of the new 13-hole pitot tube and illustrates the seven possible combinations of 5-hole configurations.

The pitot tube was mounted on a calibration jig, shown in Figure 4, which was moveable in five degree increments in the horizontal/tangential and vertical/radial planes, as shown in Figure 5. The calibration jig was suspended on a funnel or inverted cone, which was fastened to the towing carriage structure (bridge). A spacer plate was placed between the funnel and the bridge in order to lower the pitot tube to the proper level of submergence. A schematic showing general design features is included here as Figure 6.

A single pressure gauge with a Scanivalve system was used to measure the pressure in each hole during the running of the experiments. An important feature of this system is that the Scanivalves automatically close off the air bleed. Once the carriage has attained a steady speed, the pitot tube system is manually activated and then operates automatically. Initially, pressurized air is ejected from the pressure tanks. This blows all water out of the system and registers as a high plateau on the pressure gauge. The air bleed is automatically stopped and pressure

in the system decreases until equilibrium is reached for the total pressure of the flow. This registers on the pressure gauge as a rapid decline followed by transition to a lower plateau. At this point, the system signals the computer that equilibrium has been reached and data collection can begin. A complete description of the system is given in Troesch et al. and is depicted in Figure 7.

An Interdata computer was used during the calibrations to collect the data onboard the towing carriage, to calculate the differential pressure ratios and to generate the calibration coefficients after the experiments had been completed. Strip chart recordings of the pressure measurements were also made for each tube. A sample strip chart recording is presented in Figure 8.

EXPERIMENTAL PROCEDURE

The experimental procedures in the towing tanks were identical for both the pre and post calibration runs. Each pitot tube was towed through the water at 20 fps (6.10 m/s) with its axis at different angles in each of two planes, the horizontal/tangential and the vertical/radial. In addition, tube 13 was towed at 6, 11 and 25 fps (1.83, 3.35 and 7.62 m/s) and tube 37 was towed at 6, 11, 25 and 30 fps (1.83, 3.35, 7.62, and 9.14 m/s). Table 1 lists each speed and its corresponding Reynolds number for the pre and post calibrations.

For each calibration, the pitot tube was mounted on a platform in the calibration jig under the carriage, leveled, and lowered into the water where it could be rotated both horizontally and vertically. The pitot tube was submerged approximately three feet (0.91 m) below the water surface and adjusted to the required angle of inclination. The

holes of the pitot tube were connected to the Scanivalve system for pressure measurements. Air was blown through the pressure lines to the pitot tube as the carriage began to move. A brief bleed period preceded each pressure reading, which was taken when the carriage was traveling at a steady speed. Figure 9 shows a pitot tube during the air bleed cycle, and Figure 10 shows the same tube during the pressure measurement cycle.

The towing tank temperatures during the pre and post calibrations were 70 degrees and 67 degrees F (21.1 C and 19.4 C), respectively. Figure 11 shows the experimentally determined drag coefficients of typical spherically shaped bodies in different flow regimes. From this figure, it can be seen that flow speeds of 6 and 11 fps (1.83 and 3.35 m/s) correspond to a subcritical flow pattern, and those of 25 and 30 fps (7.62 and 9.14 m/s) correspond to a supercritical pattern. The supercritical pattern, with much less flow separation, is indicated by the sharp reduction in the drag coefficient.

As stated in the previous section, the differential pressure ratios were calculated on the Interdata computer and manually plotted onboard the carriage. Plotting the data served as a check to determine if the values, or experiment spots, appeared reasonable based upon the expected outcome from previous calibrations. The plots were once again checked and their values entered into program POLYFIT, which is a least squares curve fitting routine. POLYFIT, in turn, generated the final plots of the calibration curves and their coefficients. Appendix A describes how to use the calibration curves to obtain velocity component ratios.

The complete calibration of a tube consisted of runs at five degree intervals within a 60 degree arc, 30 degrees each side of zero, for

both planes. The original plan called for 38 tubes to be calibrated. Tubes numbered 1-35 were 5-hole pitot tubes, and those numbered 36, 37 and 38 were 13-hole pitot tubes. Due to time and scheduling constraints, only twenty-five and twenty-eight pitot tubes were calibrated for the pre and post calibrations, respectively. Table 2 lists those tubes which actually were calibrated. All tubes were calibrated at a speed of 20 fps (6.10 m/s). To study the effect of speed, measurements were also obtained at speeds of 6, 11, and 25 fps (1.83, 3.35 and 7.62 m/s) for tube 13 and at 6, 11, 25 and 30 fps (1.83, 3.35, 7.62 and 9.14 m/s) for tube 37. See page 11 for a discussion of speed effects.

Since seven 5-hole combinations can be derived from a single 13-hole tube, the number of data points for each 13-hole tube is significantly larger. Figure 3 presents the seven combinations of 5-hole tubes and gives a pictorial representation of the relationship of holes on the 13-hole tube. During the calibration, calculations were made for each of the seven combinations so that the redundancy of the data could be examined.

PRESENTATION AND DISCUSSION OF RESULTS

The results of the pre and post calibrations are the differential pressure ratio coefficients, presented in graphical form as a function of angle of inclination at four different speeds. The calibration curves consist of from 7 to 13 data points collected for each of the 25 5-hole pitot tubes in each of the two planes. Each data point on a curve consists of the value for the differential pressure ratio from which flow directions and magnitudes can be calculated for both the tangential and radial components. Appendix A presents the procedure for deriving velocity component ratios from pressure measurements.

In this study, the coefficients for each calibration were generated from the experimental data in the program POLYFIT. Appendix B explains the quantities which the coefficients represent. POLYFIT fairs a curve through the 7 to 13 given data points and computes 100 intermediate points. Curves from third and fourth degree polynomials were examined, and the one with the highest correlation coefficient to the given points was chosen as the calibration curve to be used for a particular tube, plane and speed. In each instance, the curve used gave an accurate fit.

Figures 12-58 present the pre calibrations of the 5-hole pitot tubes. Figures 22-27 show the results for tube 13 at speeds of 6, 11 and 20 fps (1.83, 3.35 and 6.10 m/s). Figures 59-114 present the post calibrations of the 5-hole pitot tubes, with Figures 73-80 showing the results for tube 13 run at 6, 11, 20 and 25 fps (1.83, 3.35, 6.10 and 7.62 m/s). Figures 115-126 present the pre calibrations of the 13-hole pitot tubes and Figures 127-134 present the post calibrations of the 13-hole pitot tubes. The data from Tube 37 for speeds others than 20 fps (6.10 m/s) will be presented in a future report.

The calibrations of Tube 9 in the horizontal/tangential plane, Figures 17 and 68, illustrate the greatest differences between the pre and post calibrations. At $\beta = -10$ deg, $(C - T_2)/V^2$ is equal to 0.0051 in the pre calibration but is 0.0056 in the post calibration. This difference would result in a five percent error in the prediction of the velocity, V. However, Tube 9 results were not consistent with the results of other calibrations in which the differences between pre and post calibration velocity predictions were on the order of one to two percent.

To compare the calibrations of various tubes, composite calibrations

were derived from each individual experiment. The composite data represent a statistical average over all tubes for a given experimental condition and are presented in this report in Figures 135-138. The statistical analysis of the composite data for the 5-hole pitot tube consists of the mean, maximum and minimum values, and tolerance intervals. In the composite plots, the curves have been faired through the mean values which are assumed to be representative of all tubes. Any differences which appear can be attributed to experimental error and/or imperfection in manufacture. The fairing process should average out experimental errors to give an unbiased estimate of the true value.

The population of this statistical analysis has as its elements the pressure readings for the 5-hole pitot tubes in the horizontal/tangential and vertical/radial planes for both the pre and post calibrations. The mean, minimum and maximum values and the tolerance intervals have been calculated for each angle from the samples obtained during the experiment and are presented in Tables 3-10 and Figures 135-138.

Attention is now directed to the accuracy of the calibrations, using the consistency of the data as the main criterion for evaluating the results. Any inconsistency in the data would indicate a tube irregularity due to improper manufacture or damage during the trial.

A 99 percent distribution-free tolerance region has been determined for this analysis. This tolerance interval is a generalization of the confidence interval corresponding to a band of values as opposed to a single value and gives an indication as to the interval in which a given percentage of the population should fall. The 99 percent tolerance interval means that there is 99 percent confidence that 99 percent of the distribution will lie between the indicated bounds.

Mathematically, this probability concentration of the sample population is expressed as follows:

$$P \{f_R dF \ge .99\} = .99$$

Comparing the results of the pre and post calibrations in Figures 135 through 138, the agreement between corresponding data points in both planes, at least for the constant speed of 20 fps (6.10 m/s), can be readily seen. Almost all of the values fall within the bounds of the tolerance intervals. The exceptions are the minimum values corresponding to β angles of ± 25 deg and ± 30 deg of curves 1 and 3 in the pre calibration horizontal/tangential plane (Figure 135) which fall below the tolerance limit. Since this occurs only in this plane and at these angles, the abnormally low values should be attributable to an isolated tube which perhaps had a bad pre calibration.

Comparison of the mean values of the differential pressure ratio coefficients for the pre and post calibrations for each plane, as listed in Tables 3-10, reveals some differences. In general, the post calibration mean values are higher than the pre calibration values. In Table 4, the statistical summary for $(C - T_1)/V^2$ at $\beta = 10$ deg lists the pre calibration mean as 0.00517 and the post calibration mean as 0.00535. This difference would result in an error of less than two percent in the prediction of the velocity, V. For most of the mean values, the differences between pre and post calibration are even less, indicating an even smaller error.

Though the differences between the statistical averages of the pre and post calibration are small, the scatter of the data between different calibrations is large. This scatter is probably due to manufacturing differences in the pitot tubes, though tank turbulence and experimental error do have an effect. The post calibration mean value of 0.00523 and maximum values of 0.00562 for $(C - R_2)/V^2$ at $\beta = -10$ deg are shown in Table 10. The difference in these two values would result in an error in the predicted velocity, V, of almost four percent. Though this example was selected as an extreme case, errors of two to three percent were not uncommon.

To determine the effect of towing speed on the calibrations, tube 13 was run at 6, 11, 20 and 25 fps (1.83, 3.35, 6.10 and 7.62 m/s) in both the pre and post calibrations. The results are presented in Figures 22 through 27 and in Figures 73 through 80. Composite results for the horizontal/tangential plane post calibration, which are typical, are presented in Figure 139. Significant differences are evident, particularly at the lowest speed. The value for $(C - T_2)/V^2$ at $\beta = -10$ deg at 6 fps is 0.0049 and at 20 fps is 0.0054. This difference would result in an error in the predicted velocity of about five percent. However, at the other speeds, the differences are much less significant.

The speed of 20 fps (6.10 m/s) was selected for the calibrations based on the physical limitations of the calibration equipment such as excessive water spray and rake vibrations. Referring to Figure 11, the speed of 20 fps (6.10 m/s) is seen to be in the transcritical flow pattern regime and the speed of 25 fps (7.62 m/s) is seen to be in the supercritical flow regime. However, since the data presented in Figure 139 show that the calibrations at 20 and 25 fps (6.10 and 7.62 m/s) are practically identical, any transcritical effects on the calibrations are assumed to be negligible. Therefore, the complete set of calibrations at 20 fps (6.10 m/s) is considered valid for the analysis of full-scale data.

CONCLUSIONS

As a result of this calibration analysis, the following conclusions can be reached:

- (1) The differences between the pre and post calibrations for a given tube were generally small. The difference in the predicted velocity using the pre and post calibrations at $\beta \approx 10$ deg was typically one to two percent.
- (2) The calibrations of individual pitot tubes contained significant scatter about the mean values obtained by averaging the results of all tubes. The difference in the predicted velocity using the mean and actual calibrations was typically two to three percent.
- (3) The differences between the mean values over all tubes of the pre and post calibrations were small, indicating the absence of a bias between the pre and post calibrations.
- (4) Based on conclusions (1), (2) and (3) above, individual pre and post calibrations for each tube will give more accurate predictions of velocity component ratios.
- (5) At speeds of 20 fps (6.10 m/s) and above, the calibrations were relatively insensitive to speed change. However, at the lower speeds of 11 fps (3.35 m/s) and less, the calibrations were highly speed (or Reynolds number) dependent. Therefore, the validity of the calibrations listed in this report has only been demonstrated in the speed range of 20 to 30 fps (6.10 to 9.14 m/s), though the calibrations should also be accurate at higher speeds.

REFERENCES

- 1. Troesch, A., V.A. Phelps, and J. Hackett, "Full Scale Wake and Boundary Layer Survey Instrumentation Feasibility Study," Department of Naval Architecture and Marine Engineering, College of Engineering Report, The University of Michigan (January 1978).
- 2. Janes, C.E., "Instruments and Methods for Measuring the Flow of Water Around Ships and Ship Models," David W. Taylor Model Basin Report No. 487 (March 1948).
- 3. Schlicting, H., <u>Boundary Layer Theory</u>, McGraw Hill Book Co., New York (1968) p. 17.

TABLES

TABLE 1

REYNOLDS NUMBERS* FOR THE TEMPERATURE AND SPEED RANGE OF THE CALIBRATIONS

SPEED FT/SEC	PRE CAL Rn x 10 ⁻⁵ T = 70 ^o F:FW	POST CAL Rn x 10 ⁻⁵ T = 67° F:FW
6	1.125	1.081
11	2.063	1.982
15	2.813	2.703
20	3.751	3.604
25	4.689	4.505
30	5.626	5.406

Rn = 5.212×10^5 : Full Scale Trial Conditions Sea Water T = 82° F (27.8°C)

^{*} The diameter of the spherical head of the pitot tube is the characteristic length used.

TABLE 2
CALIBRATED PITOT TUBES

PRE CALIBRATION 5-Hole Tube Number		POST CALIBRATION 5-Hole Tube Number
4 6 9		3 4 5 6 9
11		6
12		9 11
13 15	1	12
17		13
18		15
20		16
21 22		17 20
23		21
24		22
26		23
27		24
28		26
29		27
30		28
31		29
32		30
33		31 32
		33
		34
13-Hole Tube Number		13-Hole Tube Number
36		37
37 38		38
30		

Table 3 STATISTICAL CALIBRATION SUMMARY FOR $\frac{T_2-T_1}{2C-T_2-T_1}$

	Standard Deviation			.005	010.	010.	110.	.030	180.	.158		.008	.015	.019	.032	.052	
-	Upper Tolerance Limit			.024	. 358	. 693	1.075	1.585	2.353	3.521		.036	.719	1.105	1.673	2.405	
	Maximum		tion	.018	.346	929.	1.057	1.530	2.189	3.220	tion	.019	989.	1.082	1.526	2.159	
	Mean		Pre Calibration	800.	. 327	199.	1.038	1.487	2.086	3.002	: Calibration	. 009	699.	1.044	1.488	5.105	
	Minimum		Pre	000	.311	.640	1.019	1.390	1.763	2.418	Post	.002	.629	1.006	1.443	2.024	
	Flow Angle Lower Tolerance Limit	10 O		008	. 295	.629	1.001	1.389	1.820	2.482		017	619.	.982	1.302	1.805	
	Flow Angle			0	2	10	15	20	25	30		Ow	10	15	20	25	

Table 4 STATISTICAL CALIBRATION SUMMARY FOR $\frac{C-T_1}{v^2}$

Standard Deviation		.00008 .00009 .00010 .00010 .00010		.00008 .00013 .00004 .00004
Maximum Upper Tolerance Limit Standard Deviation		.00356 .00451 .00547 .00674 .00710		.00357 .00471 .00578 .00649 .00685
Maximum	ion	.0035 .0044 .0053 .0061 .0066	tion	.00349 .00454 .00561 .00634 .00664
	Calibration	.00328 .00425 .00517 .00589 .00643	Post Calibration	.00330 .00435 .00535 .00608 .00660
Minimum	Pre	.0032 .0040 .0058 .0063 .0066	Post	.00314 .00413 .00514 .00589 .00653
low Angle Lower Tolerance Limit Minimum		.00301 .00399 .00486 .00557 .00611		.00303 .00399 .00492 .00566 .00634
Flow Angle		0 10 15 25 30		0 10 15 20 25

Table 5 STATISTICAL CALIBRATION SUMMARY FOR $\frac{T_1-T_2}{C-T_1-T_2}$

Standard Deviation	.005 .010 .010 .011 .025 .081		.008 .011 .016 .026 .068
Maximum Upper Tolerance Limit on	.024 .359 .704 1.077 1.576 2.355 3.563		.035 .363 .704 1.090 1.623 2.491
Maximum Upper	.018 .345 .692 1.060 1.531 2.157 3.215	ion	.040 .363 .693 1.076 1.506 2.175
Mean Ma Calibration	.008 .327 .669 1.042 1.494 2.090 3.001	Post Calibration	.009 .326 .669 1.038 2.092
Minimum	.000 .307 .651 1.021 1.426 1.758 2.310	Post	.003 .306 .652 1.011 1.432
Flow Angle Lower Tolerance Limit	008 .296 .635 1.007 1.413 1.825 2.439		017 .289 .635 .987 1.315
Flow Angle	-10 -15 -26 -25 -30		-5 -10 -20 -25

Table 6 STATISTICAL CALIBRATION SUMMARY FOR $\frac{C-T_2}{\sqrt{2}}$

Standard Deviation			.00008	21000.	11000.	.00013		60000.	. 00012	.00021	.00024
Upper Tolerance Limit Standard Deviation			.00356	.00626	08900	.00713		.00358	,00576	.00794	.00841
Maximum	13.8	ion	.0034	.0055	7900.	.0070	ion	.00349	.00573	.00702	.00741
Mean		. Calibration	.00328	.00521	.00643	.00676	Post Calibration	.00330	.00536	.00670	.00700
Minimum		Pre	.0032	.0051	.0063	9900.	Post	.00312	.00522	.00644	.00682
Flow Angle Lower Tolerance Limit			.00301	.00483	.00607	.00639		.00302	.00497	.00547	.00561
Flow Angle			O	<u>ا</u> د	-20	-22		oĸ	9:	-15	-25

Table 7 STATISTICAL CALIBRATION SUMMARY FOR $\frac{R_2}{2C-R_2-R_1}$

viation			
Standard Deviation		.010 .016 .017 .034 .039	.013 .016 .018 .041
Limit			
Maximum Upper Tolerance Limit		.048 .390 .733 1.173 1.584 2.244 3.302	.066 .387 .748 1.122 1.762
Upper			
Maximum	ion	.039 .369 .710 1.192 1.560 2.193 3.151	.059 .388 .730 1.114 1.571 2.216
Mean	Calibration	.014 .336 .677 1.063 1.511 2.115 3.002	Post Calibration 4 .025 9 .350 6 .696 9 1.063 1 0 1.523 1 7 2.118 2
Minimum	Pre	.004 .296 .638 1.030 1.454 2.067 2.811	Post .004 .329 .656 1.039 1.460 2.047
Tolerance Limit		020 .283 .621 .953 1.437 1.986 2.701	016 .314 .644 1.003 1.284
Lower			
Flow Angle Lower Toleran		0 110 30 30 30 30	0 15 20 25 25

C - R,	12
	FOR
	N SUMMARY FOR
	STATISTICAL CALIBRATION
	STATISTICAL
	Table 8

	Standard Deviation		01000.	. 00009	11000	. 00012			.00062	.00020	.00007	
>	Maximum Upper Tolerance Limit Standard Deviation		.00356	. 00549	62900	.00717			.00367	.00680	.00751	
	Maximum Up	ration	.0034	.0054	7900.	.0073		oration	.00357	.00629	.006/9	
	Mean	Pre Calibration	.00326	.00519	.00644	.00679		Post Calibration	.00351	.00615	.00569	
	Minimum		.0031	.0051	.0063	9900.			.00326	.00595	.00649	
	Flow Angle Lower Tolerance Limit		.00394	.00489	01900	.00641			.00311	.00550	00900	
	Flow Angle L		0.50	012	20	30 30	3		0 5 0	15	20 25	

Table 9 STATISTICAL CALIBRATION SUMMARY FOR $\frac{R_1-R_2}{2C-R_1-R_2}$

Standard Deviation		010.	910.	.013	.020	.023	.052	991.		.012	.013	.021	.021	.037	950.	
Upper Tolerance Limit		.048	.367	869.	1.093	1.555	2.270	3.608		.063	.348	.716	1.093	1.678	2.423	
Maximum L	tion	.039	.352	.674	1.064	1.518	2.189	3.325	tion	.059	.328	. 689	1.058	1.498	2.161	
Mean	Pre Calibration	.014	.315	.654	1.027	1.480	2.100	3.058	Post Calibration	.025	308	.648	1.025	1.463	5.096	
Minimum	P	.004	. 282	.627	166.	1.438	2.017	2.751	Pos	.004	.277	.604	686.	1.412	2.007	
Flow Angle Lower Tolerance Limit		020	.263	119.	096.	1.404	1,930	2.509		012	.267	. 580	.956	1.247	1.769	
Flow Angle		0	ځ.	-10	-15	-20	-25	-30		0	-5	-10	-15	-20	-25	

Table 10 STATISTICAL CALIBRATION SUMMARY FOR $\frac{C-R_2}{\sqrt{2}}$

Standard Deviation		60000.	.00013	.00023	91000.	61000.	.00024		00000.	.00013	.00013	01000.	. 00011
Upper Tolerance Limit		.00356	.00559	.00655	.00687	.00730	99200.		.00371	.00563	.00639	.00705	.00740
Maximum	ion	.0034	.0054	1900.	2900.	1,000	.0075	ion	.00357	.00562	.00663	.00657	.00693
Mean	Calibration	.00326	.00422	.00581	.00636	99900.	.00688	Calibration	.00338	.00523	96500	.00645	.006/8
Minimum	Pre	.0031	.0040	.0057	.0062	.0064	900.	Post	.00319	.00504	.00582	.00631	.00663
low Angle Lower Tolerance Limit		.00296	.00468	.00506	.00584	.00603	60900.		.00305	.00483	. 00553	.00584	31900.
Flow Angle		01	٠ ٩-	-15	-20	-25	-30		ဝနှ	-10	-15	-20	-52

FIGURES

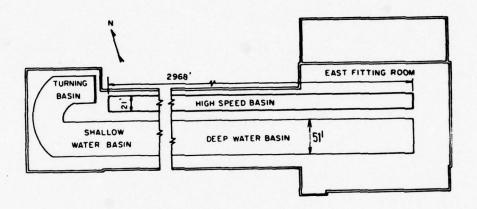
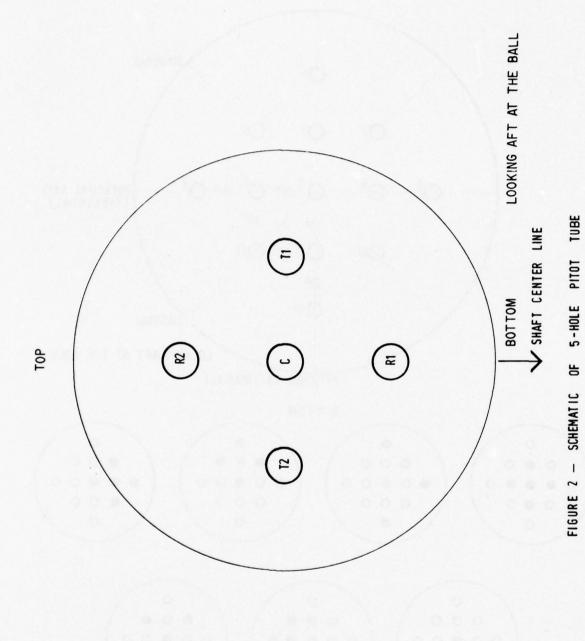


Figure 1 - Outline Plan of Deep Water and High Speed Basins



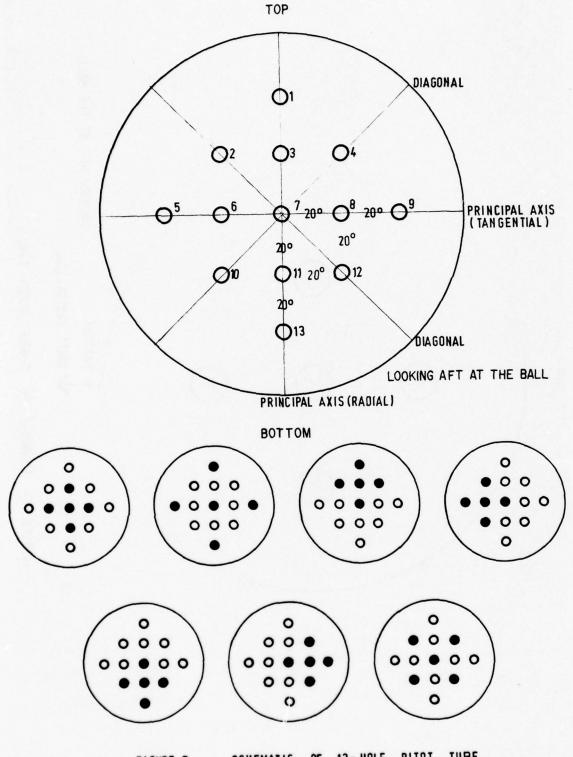


FIGURE 3 - SCHEMATIC OF 13-HOLE PITOT TUBE

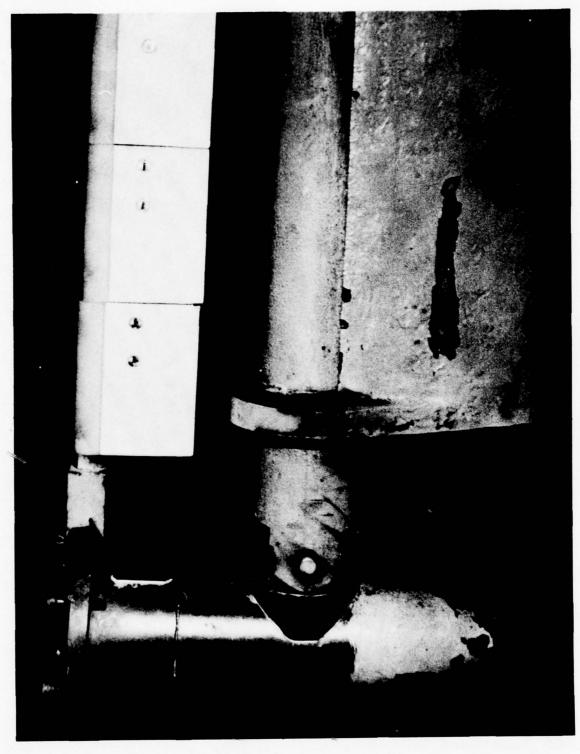


Figure 4 - Instrument Housing of Calibration Rake

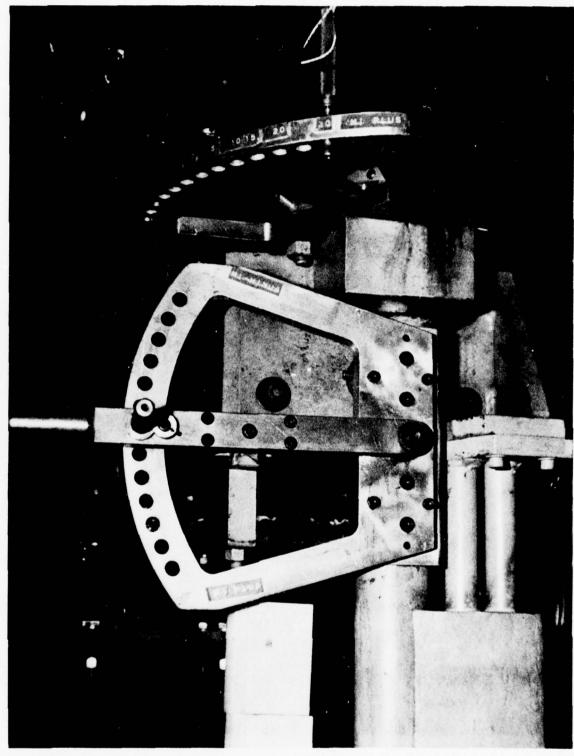


Figure 5 - Calibration Rake Showing Horizontal and Vertical Angular Quadrants

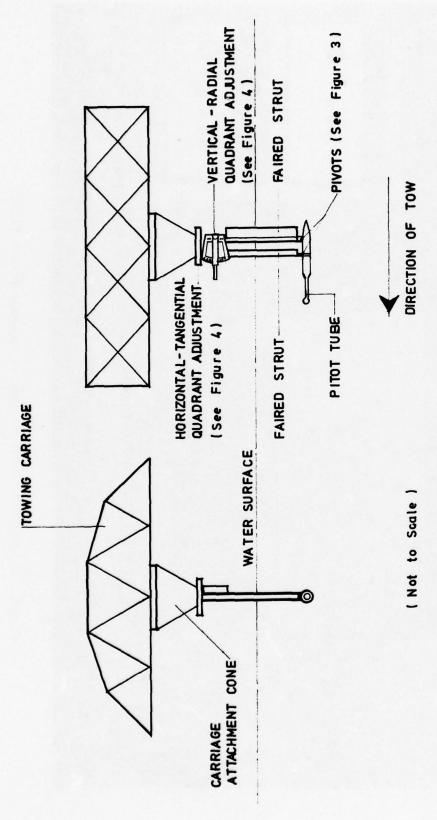


FIGURE 6 - SCHEMATIC OF CARRIAGE / CONE / RAKE ASSEMBLY

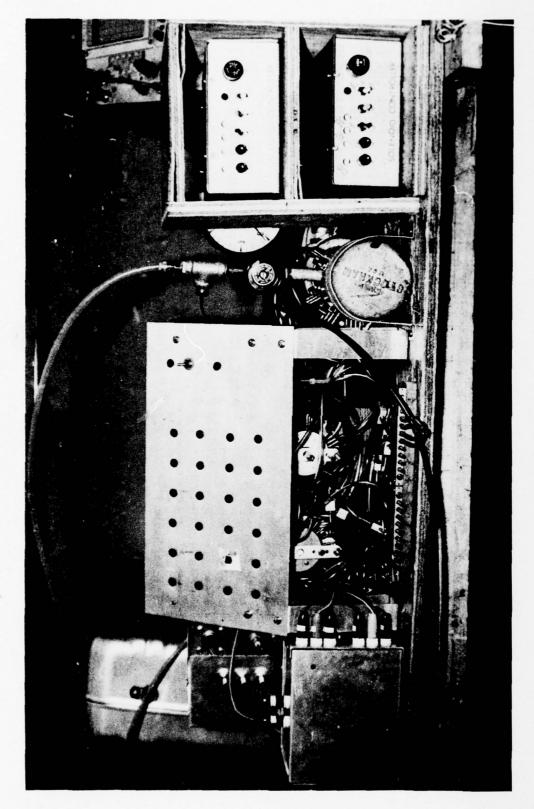


Figure 7 - Scanivalve Pressure Control and Measurement System

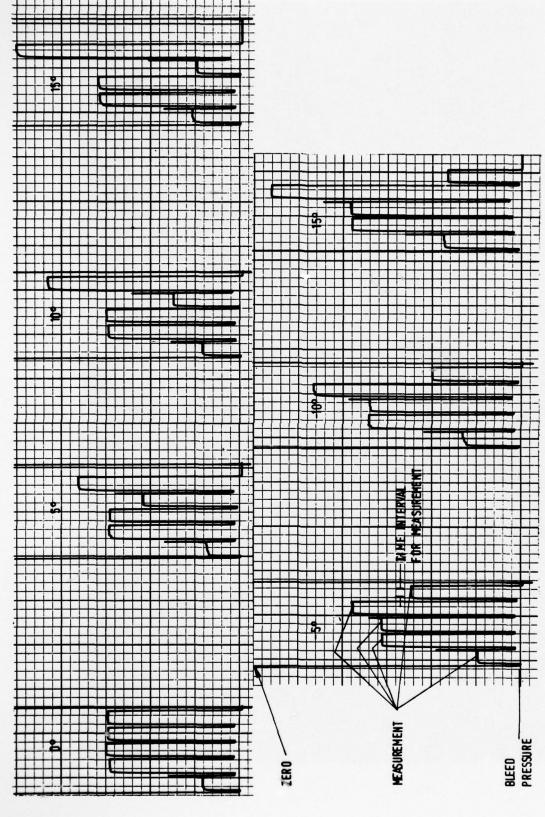


Figure 8 - Strip Chart Record of Pressure Measurements from a 5-Hole Pitot Tube

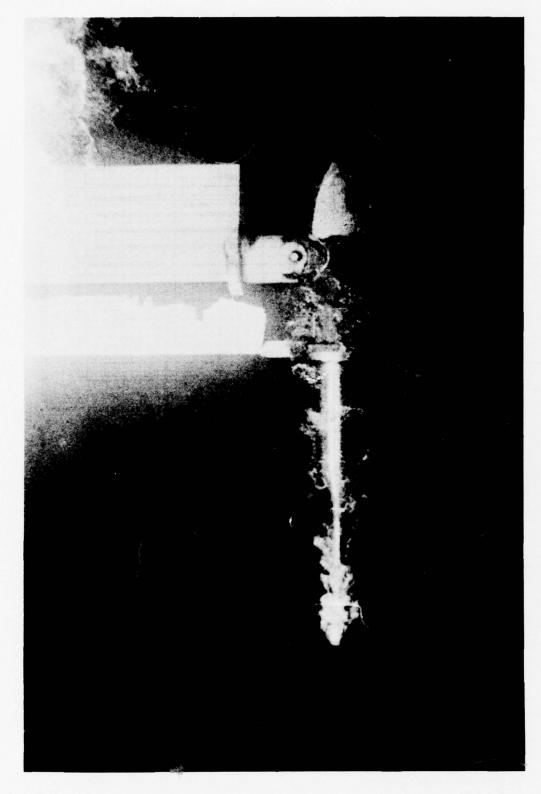


Figure 9 - Pitot Tube During Air Bleed Cycle

PSD 34744-

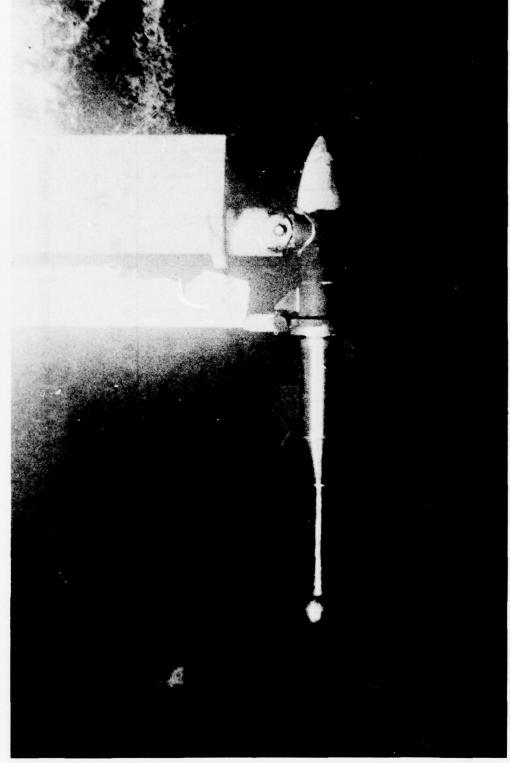


Figure 10 - Pitot Tube During Measuring Cycle

PSD 34744-

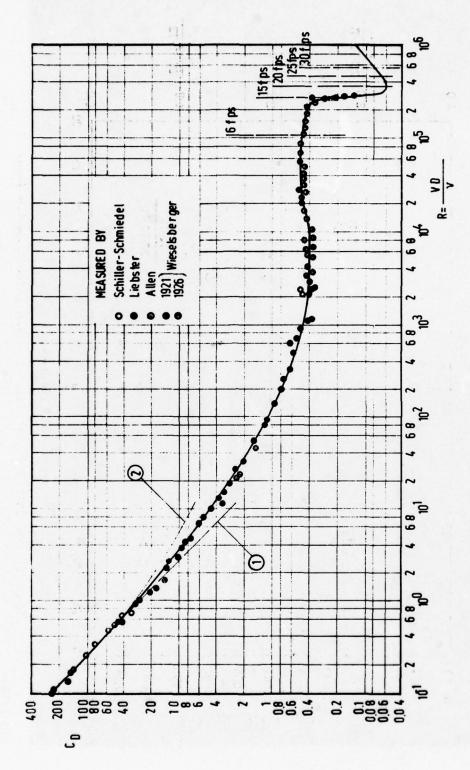


FIGURE 11-DRAG COEFFICIENT FOR SPHERES AS A FUNCTION OF REYNOLDS. NUMBER *

* FROM REFERENCE 3

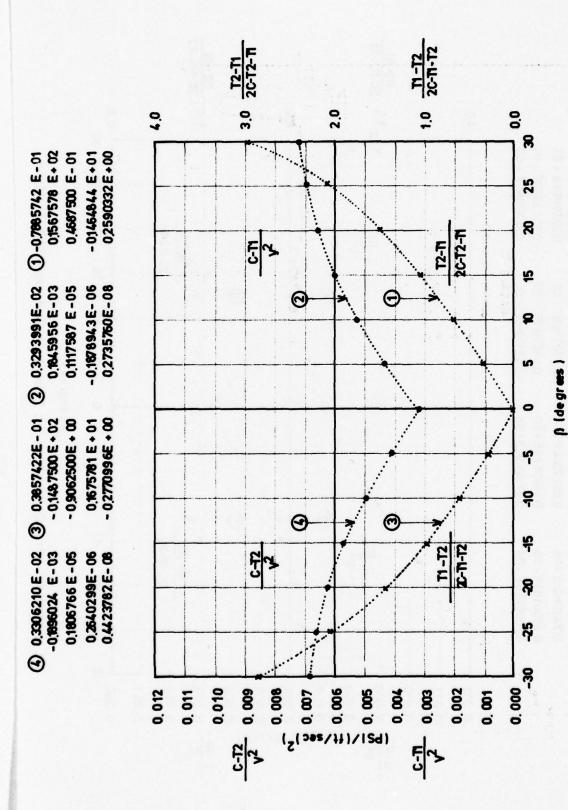


Figure 12 -Pre Cali bration of Tube 4 in Horizontal-Tangential Plane

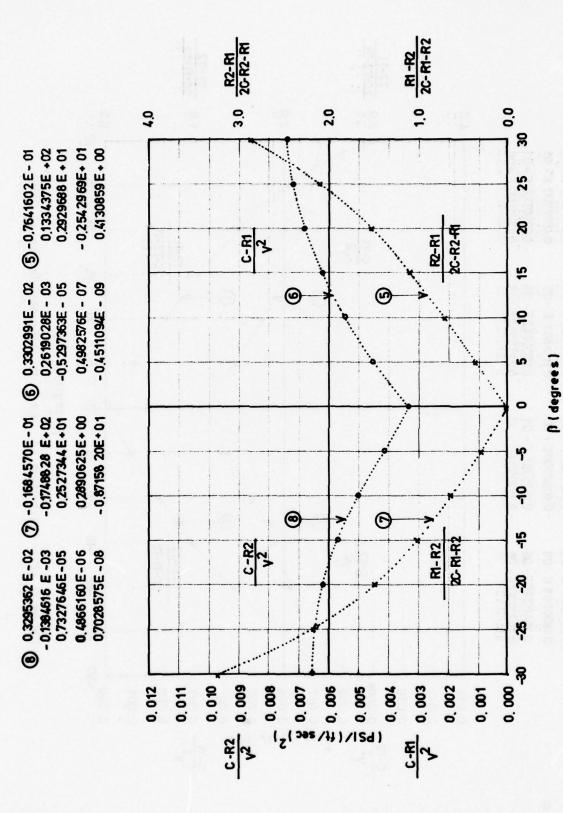


Figure 13 -Pre Calibration of Tube 4 in Vertical - Radial Plane

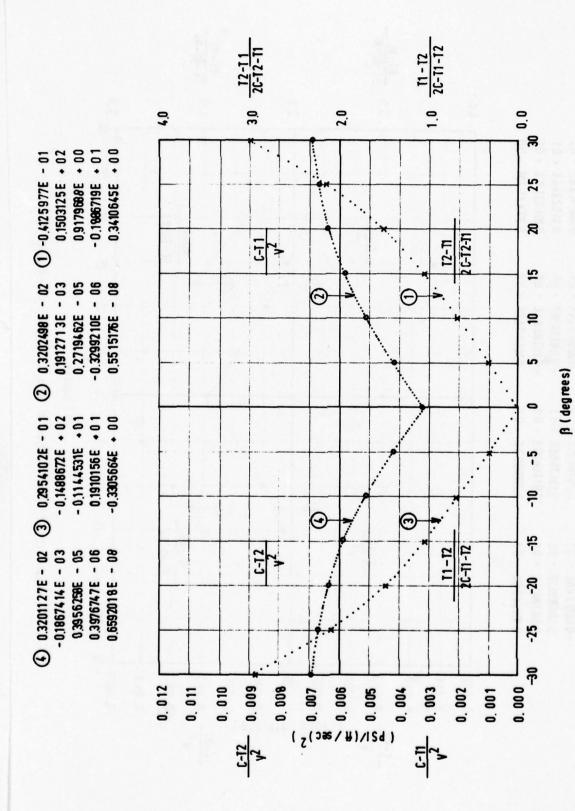


Figure 14 - Pre Calibration of Tube 6 in Horizontal - Tangential Plane

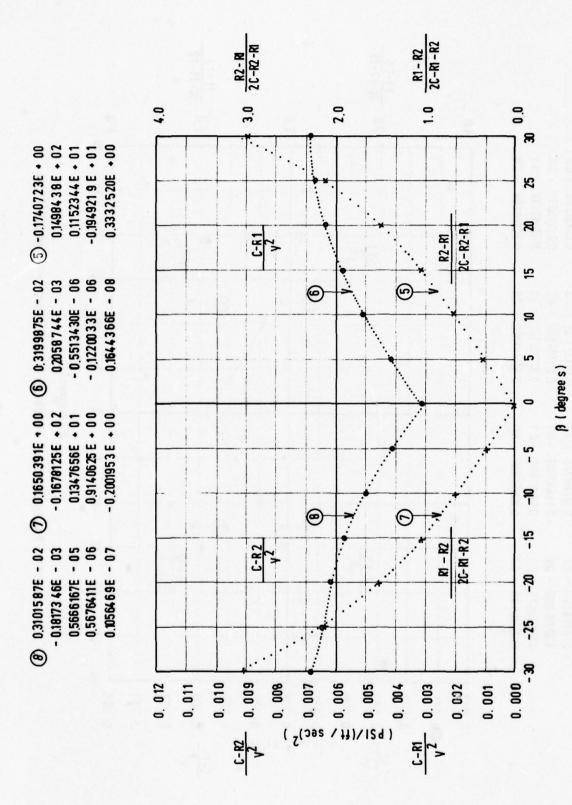


Figure 15 - Pre Calibration of Tube 6 in Vertical-Radial Plane

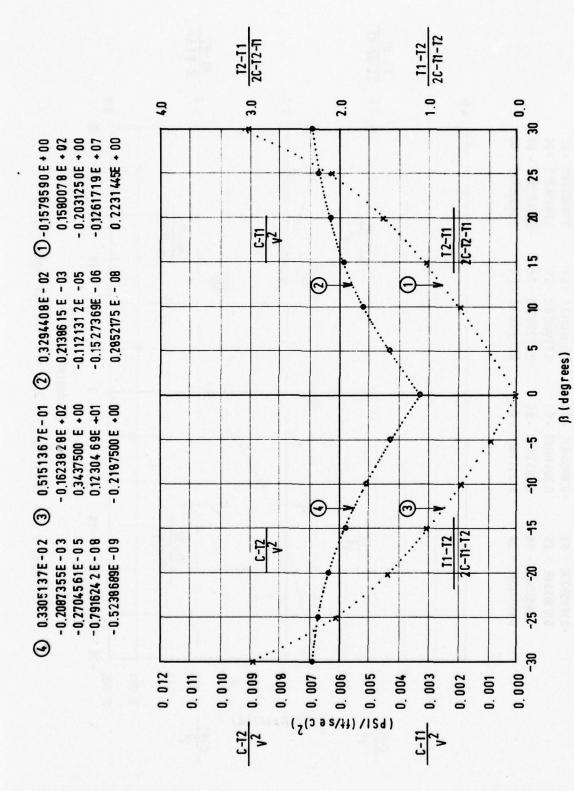


Figure 16 - Pre Calibration of Tube 9 in Horizontal-Tangential Plane

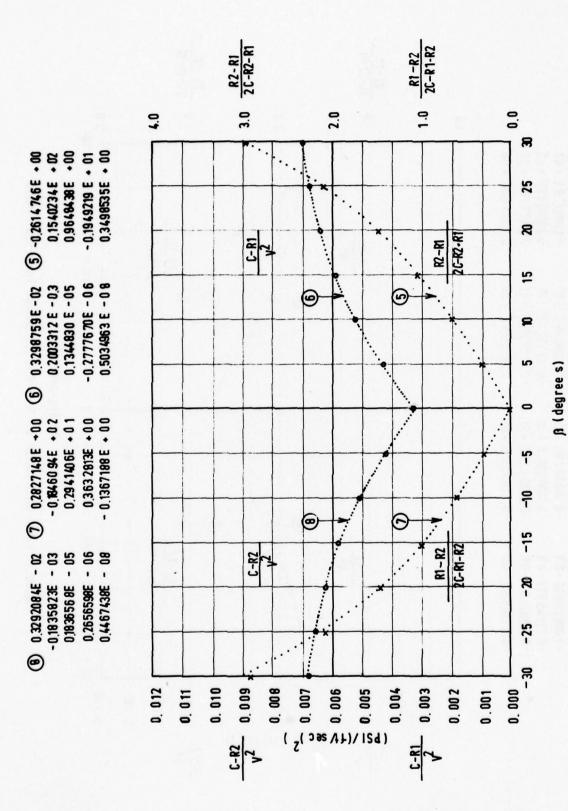
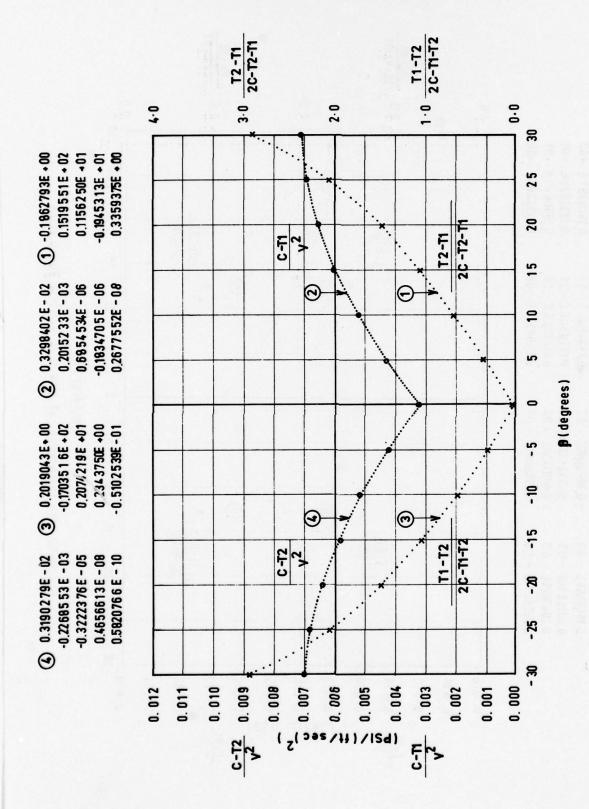


Figure 17 - Pre Calibration of Tube 9 in Vertical -Radial Plane



ののでは、一般のでは、一般のでは、一般のでは、一般のでは、一般のでは、一般のでは、一般のでは、一般のでは、一般のでは、一般のでは、一般のでは、一般のでは、一般のでは、一般のでは、一般のでは、一般のでは、

Figure 18 - Pre Calibration of Tube 11 in Horizontal-Tangential Plane

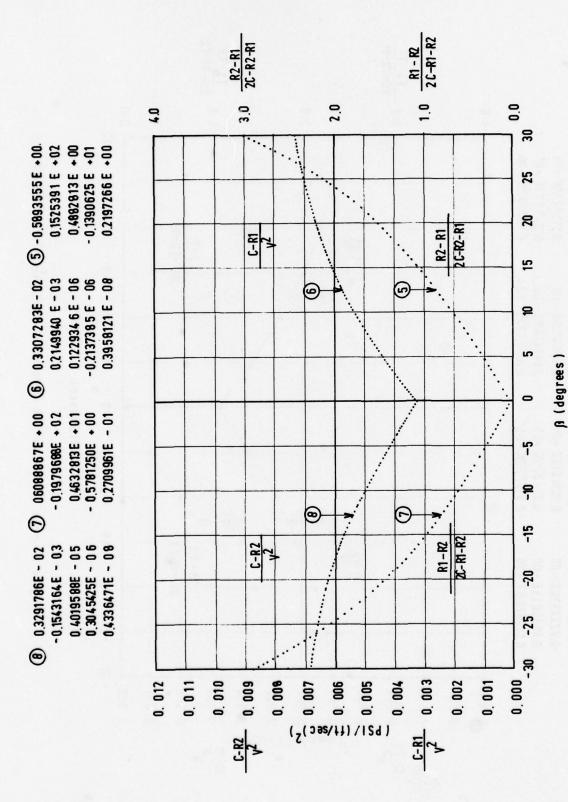


Figure 19 - Pre Calibration of Tube 11 in Vertical-Radial Plane

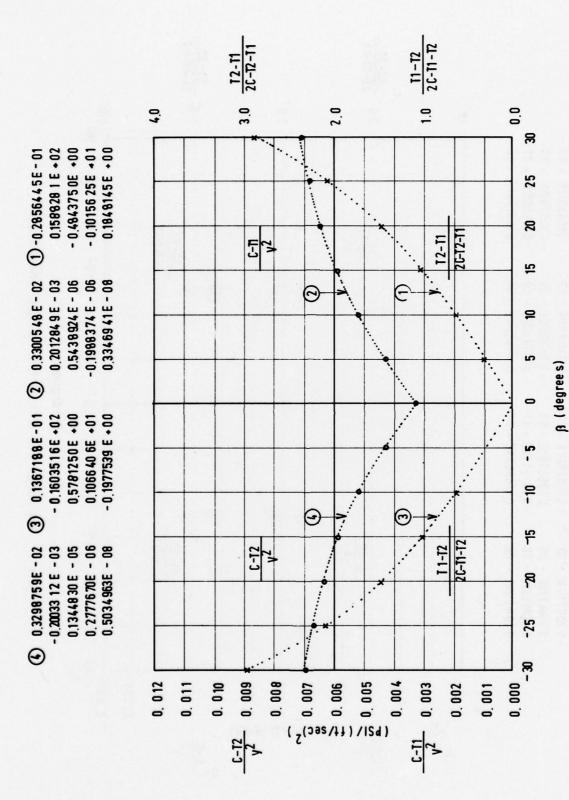


Figure 20 - Pre Calibration of Tube 12 in Horizontal-Tangential Plane

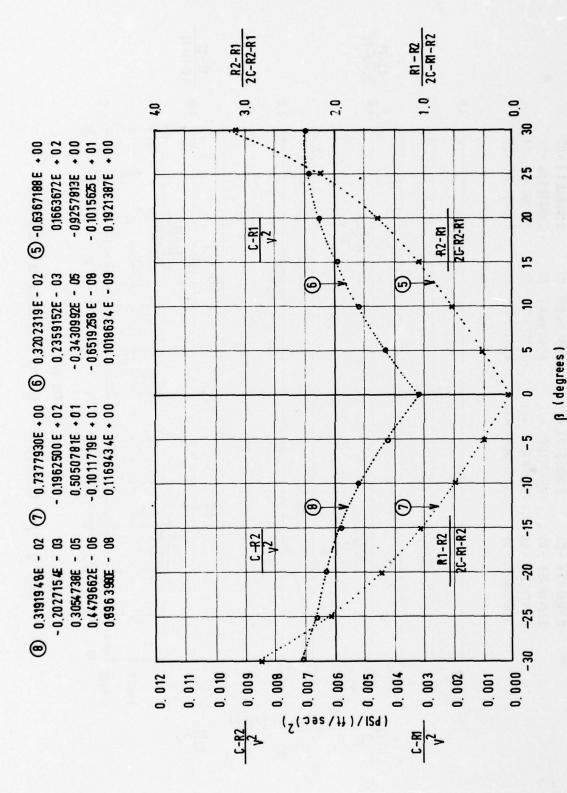


Figure 21 - Pre Calibration of Tube 12 in Vertical -Radial Plane

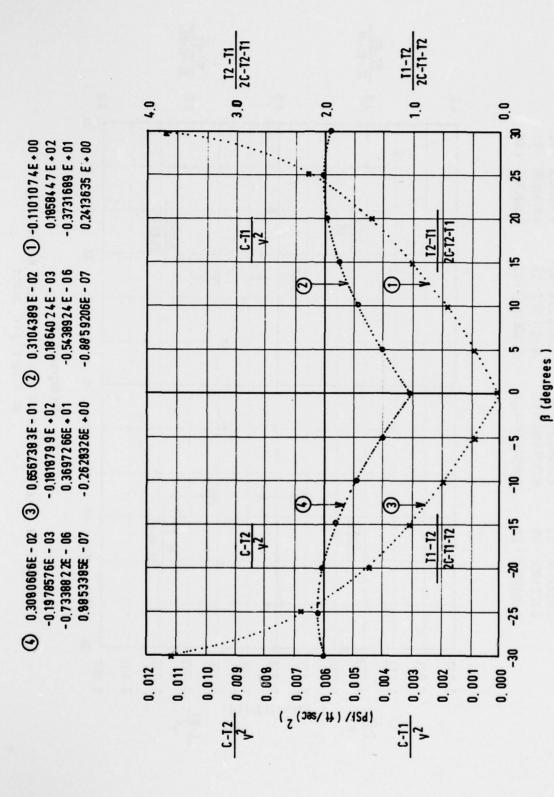


Figure 22 -Pre Calibration of Tube 13 in Horizontal-Tangential Plane at 6 feet per second

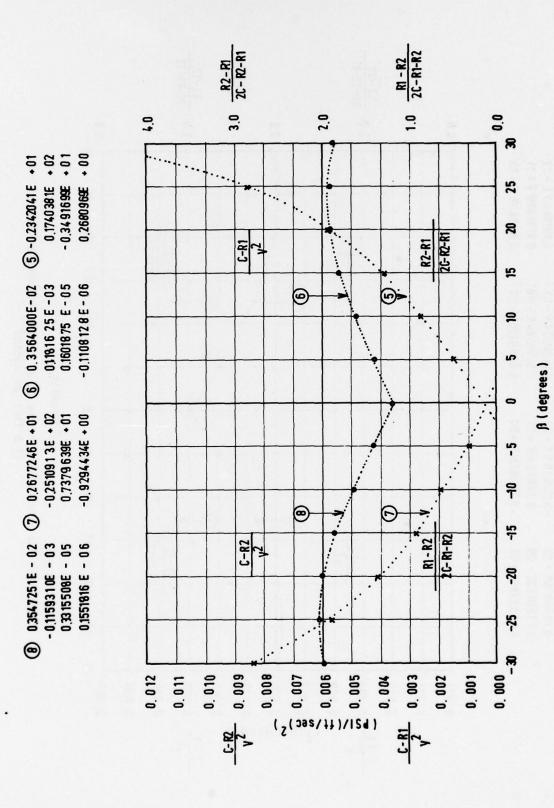


Figure 23 -Pre Calibration of Tube 13 in Vertical -Radial Plane at 6 feet per second

48

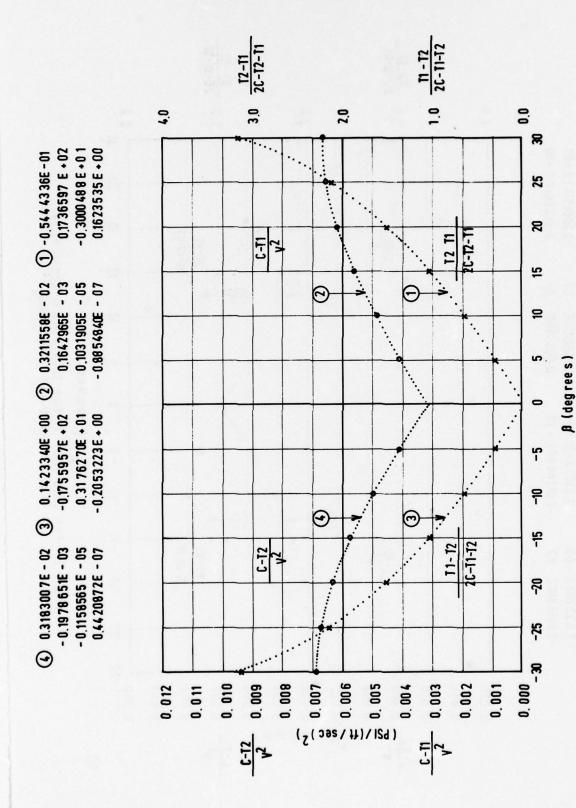


Figure 24 -Pre Calibration of Tube 13 in Horizontal-Tangential Plane at 11 feet per second

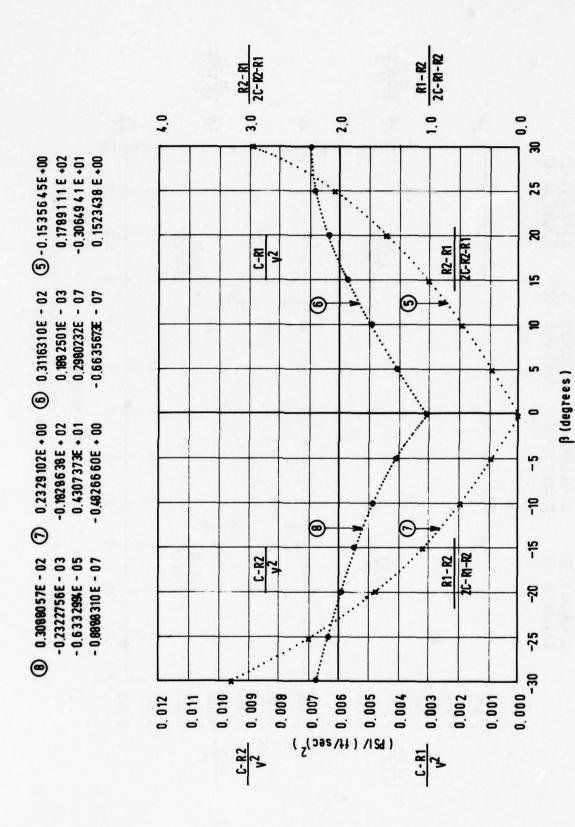
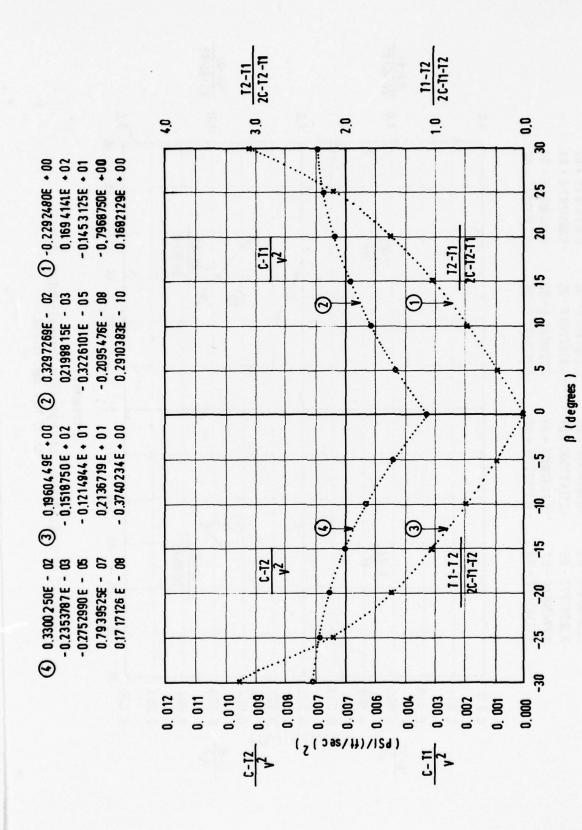


Figure 25 -Pre Calibration of Tube 13 in Vertical-Radial Plane at 11 feet per second

50



of Tube 13 in Horizontal-Tangential Plane at 20 feet per second

Figure 26 -Pre Calibration

51

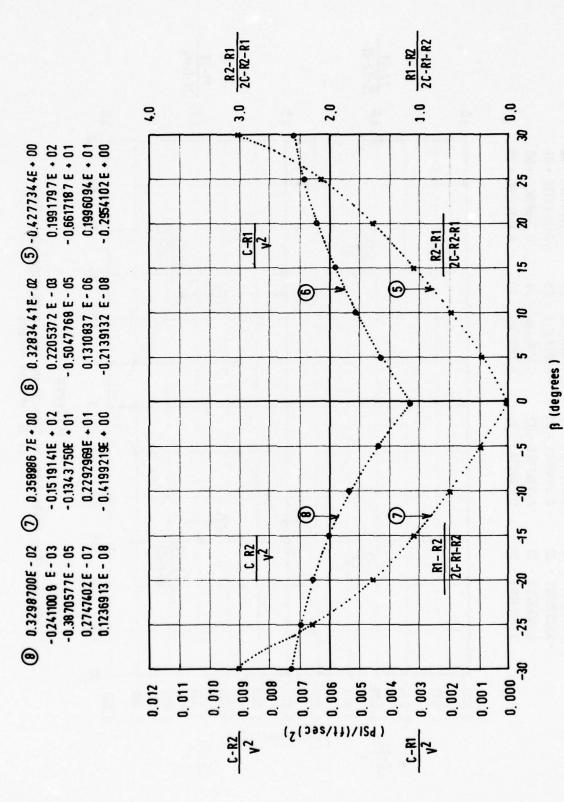
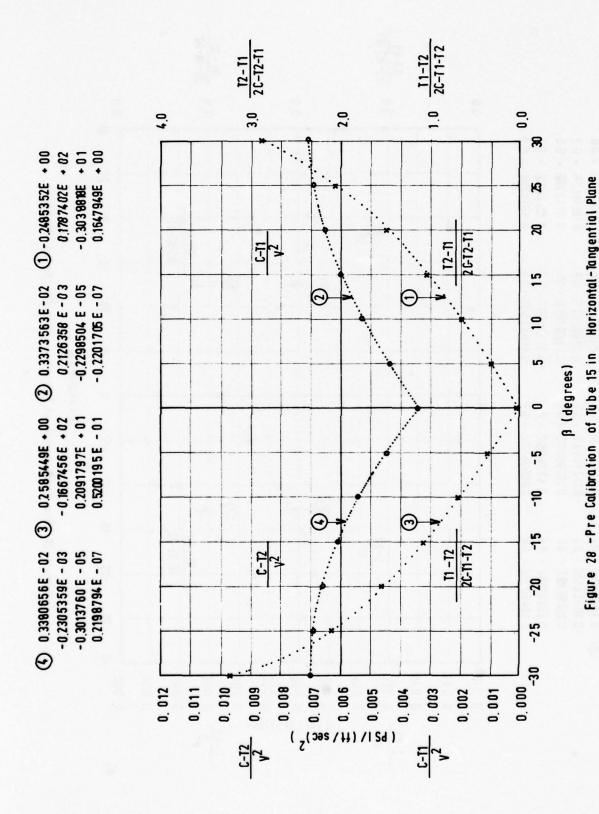


Figure 27 -Pre Calibration of Tube 13 in Vertical-Radial Plane at 20 feet per second



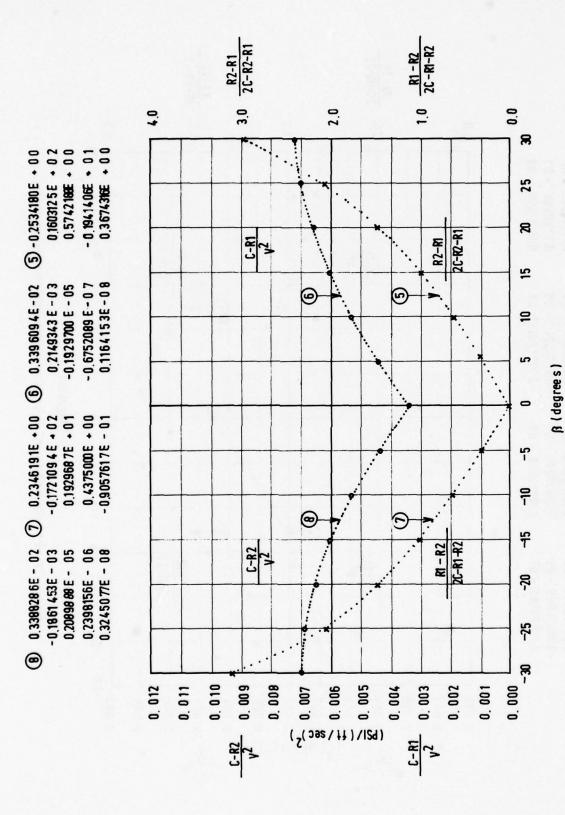


Figure 29 - Pre Calibration of Tube 15 in Vertical-Radial Plane

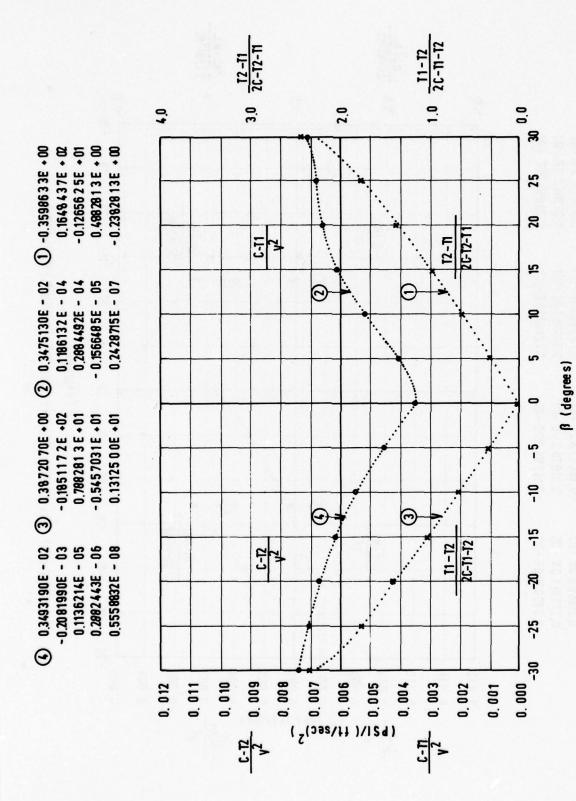


Figure 30 -Pre Calibration of Tube 17 Horizontal Fangential Plane

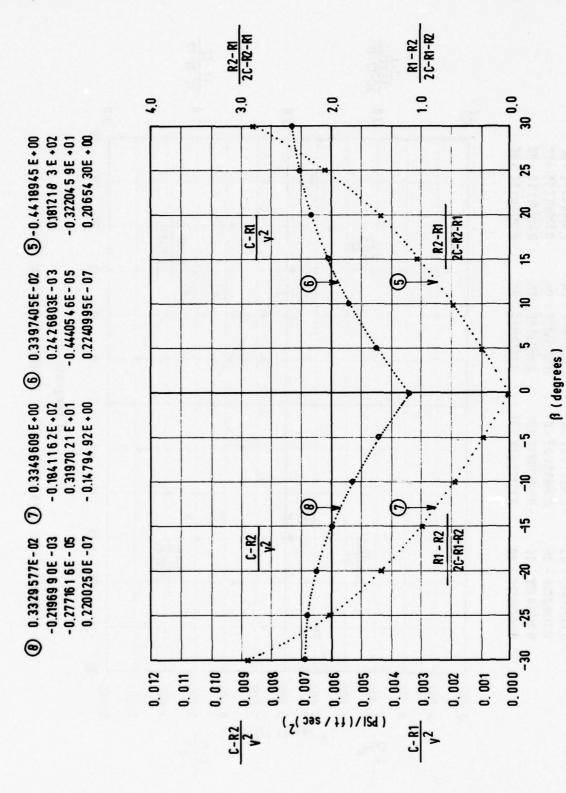


Figure 31 -Pre Calibration of Tube 17 in Vertical-Radial Plane

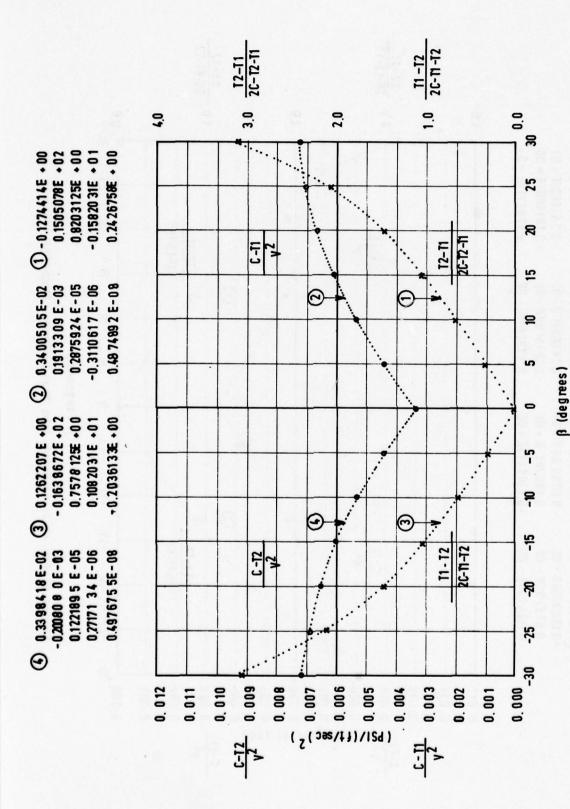


Figure 32 -Pre Calibration of Tube 18 in Horizontal-Tangential Plane

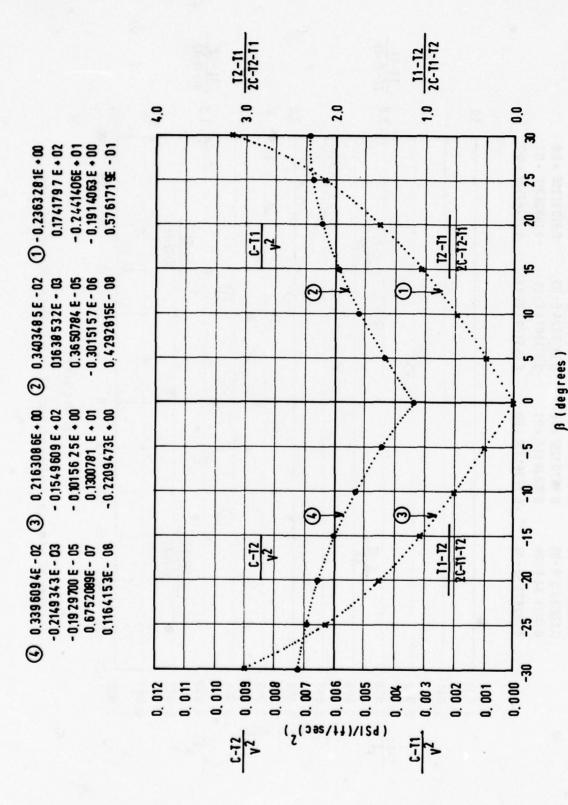


Figure 33 -Pre Calibration of Tube 20 in Horizontal-Tangential Plane

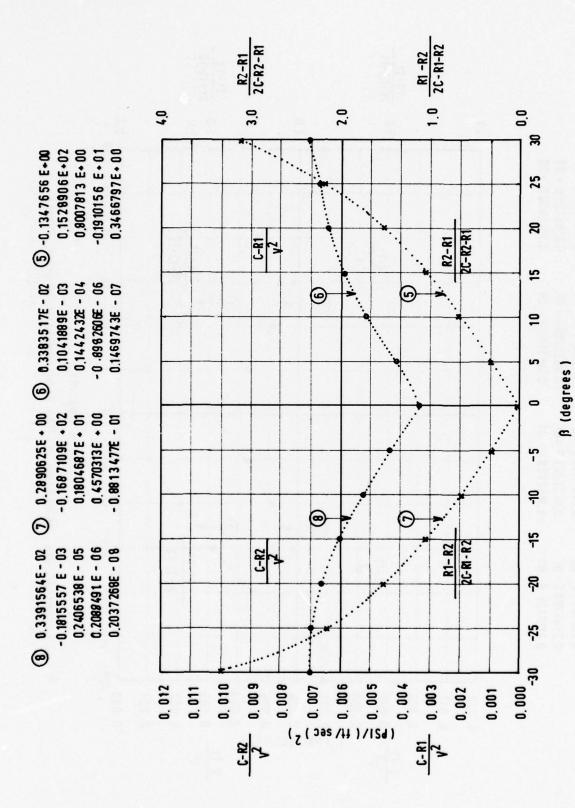


Figure 34-Pre Calibration of Tube 20 in Vertical-Radial Plane

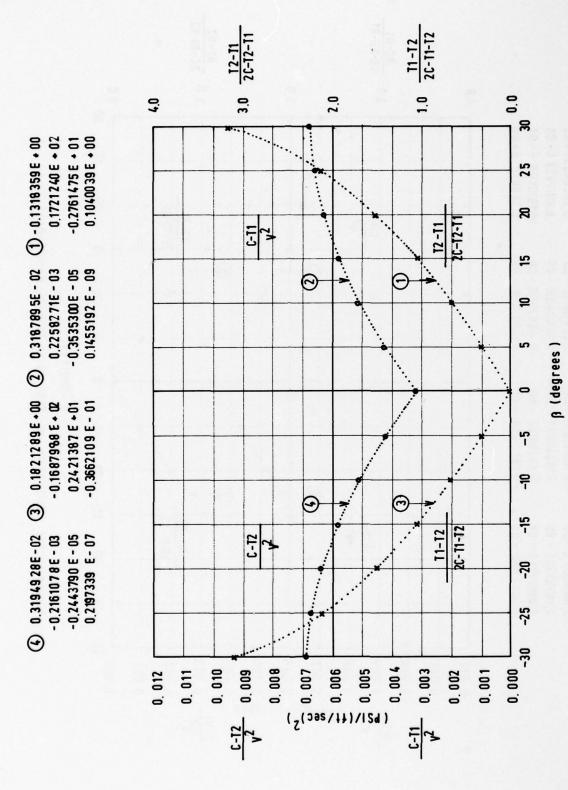


Figure 35 -Pre Calibration of Tube 21 in Horizontal-Tangential Plane

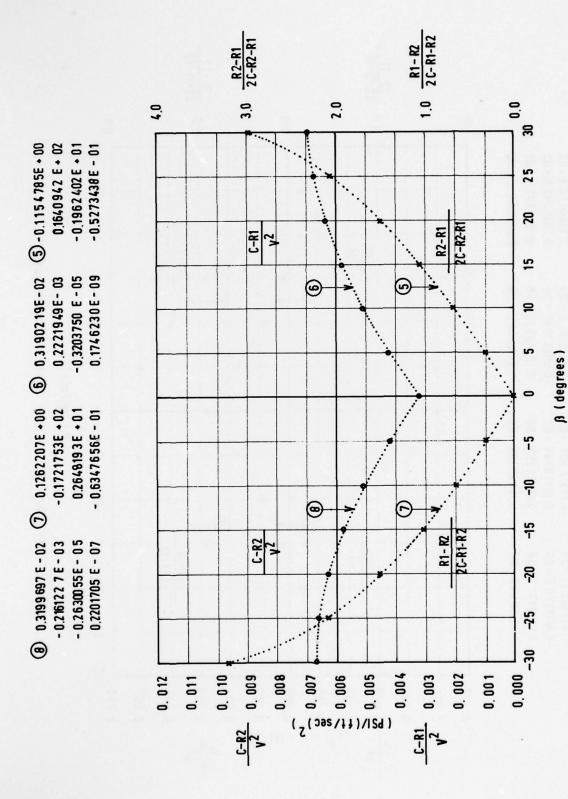


Figure 36 -Pre Calibration of Tube 21 in Vertical-Radial Plane

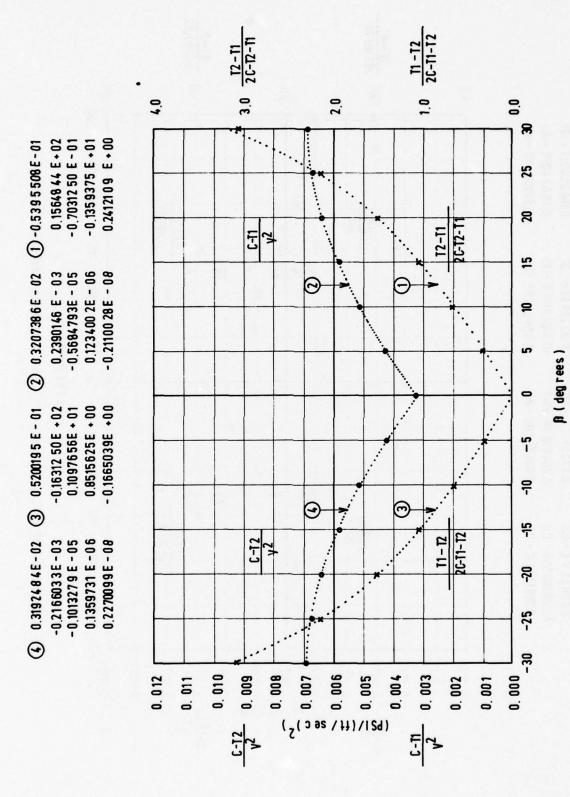


Figure 37 -Pre Calibration of Tube 22 in Horizontal-Tangential Plane

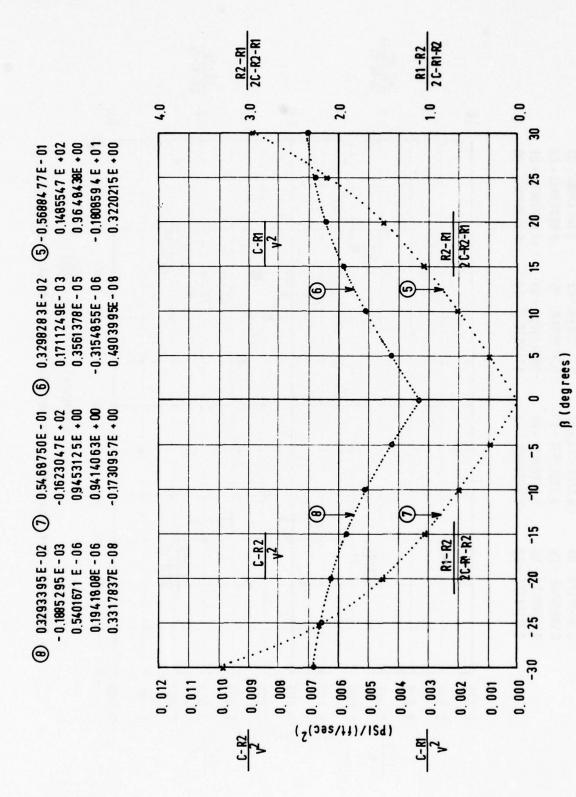


Figure 38 - Pre Calibration of Tube 22 in Vertical-Radial Plane

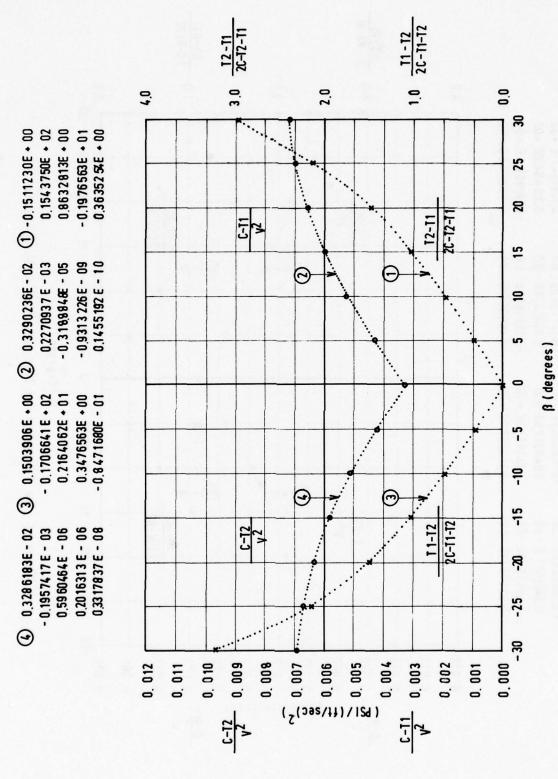


Figure 39 - Pre Calibration of Tube 23 in Horizontal-Tangential Plane

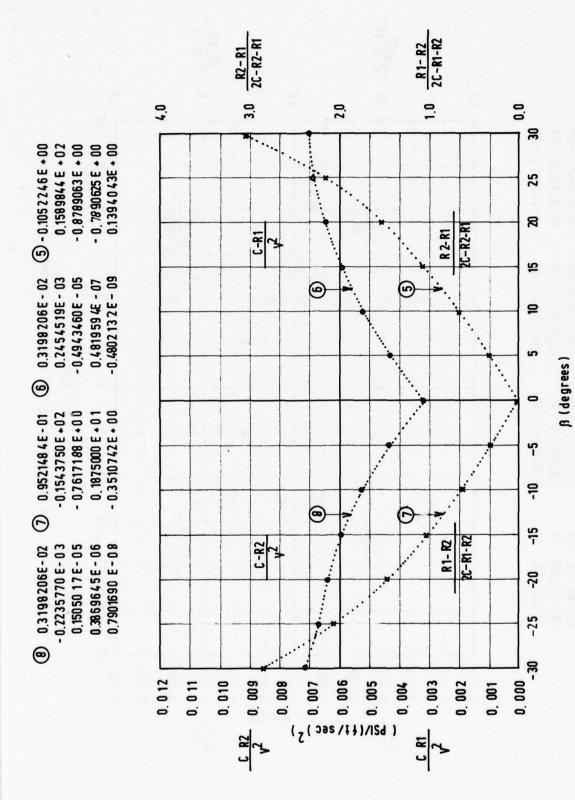


Figure 40 -Pre Calibration of Tube 23 in Vertical-Radial Plane

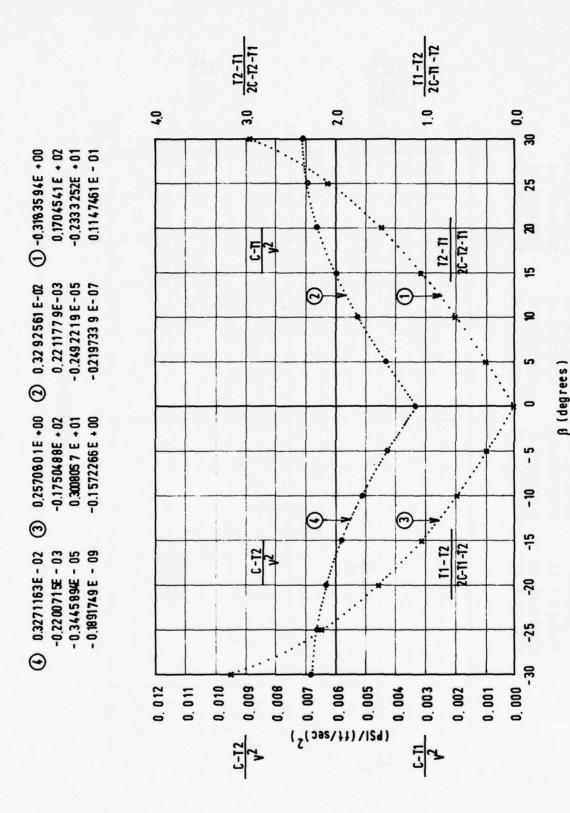


Figure 41 -Pre Calibration of Tube 24 in Horizontal-Tangential Plane

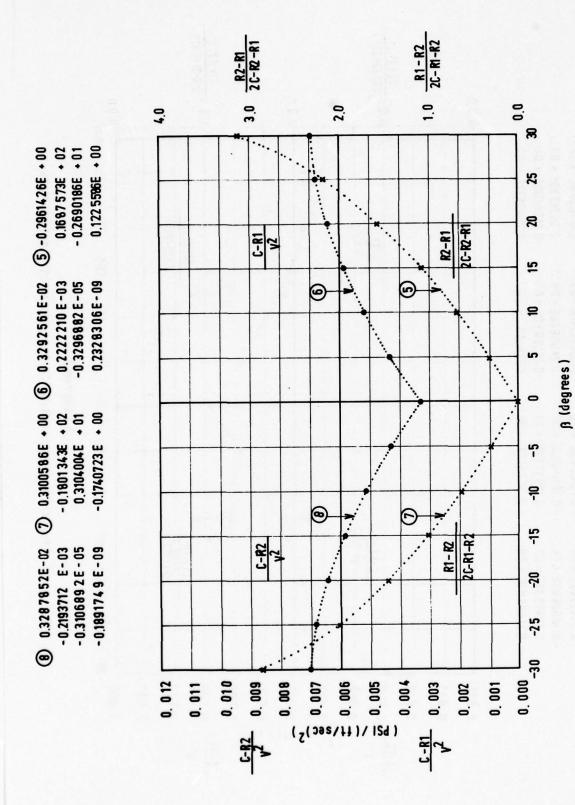


Figure 42 -Pre Calibration of Tube 24 in Vertical-Radial Plane

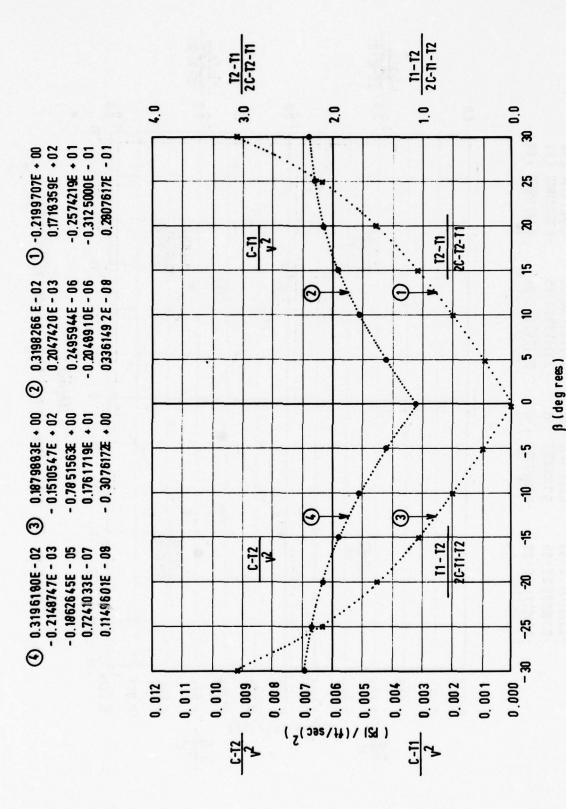


Figure 43 -Pre Calibration of Tube 26 in Horizontal-Tangential Plane

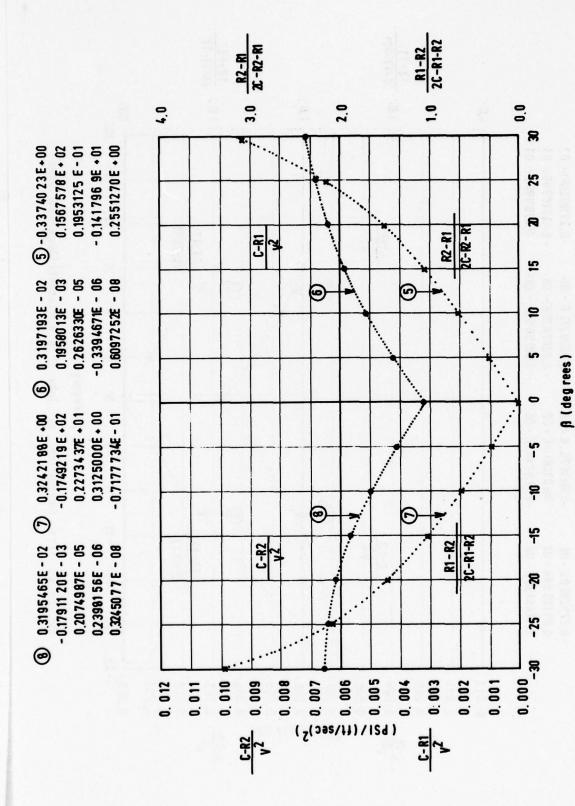


Figure 44 - Pre Calibration of Tube 26 in Vertical-Rodial Plane

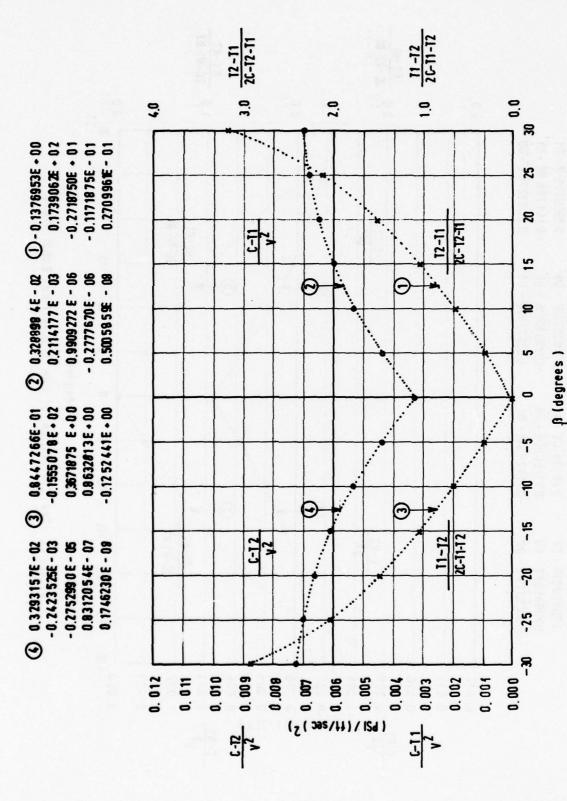


Figure 45 - Pre Calibration of Tube 27 in Horizontal-Tangential Plane

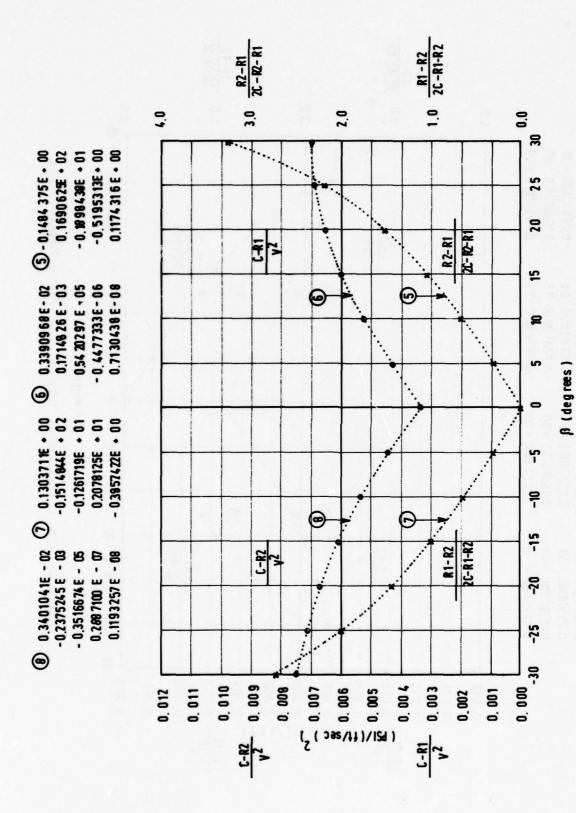


Figure 46 -Pre Calibration of Tube 27 in Vertical-Radial Plane

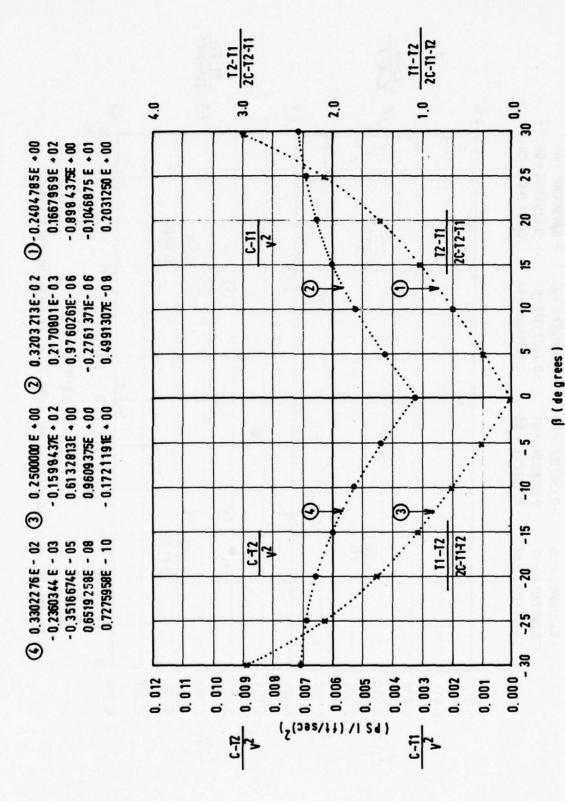


Figure 47 - Pre Calibration of Tube 28 in Horizontal-Tangential Plane

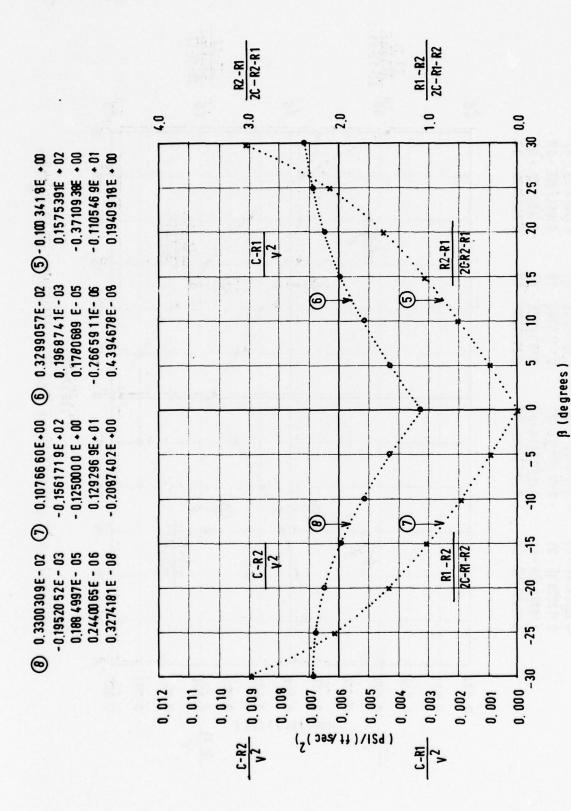


Figure 48 -Pre Calibration of Tube 28 in Vertical-Radial Plane

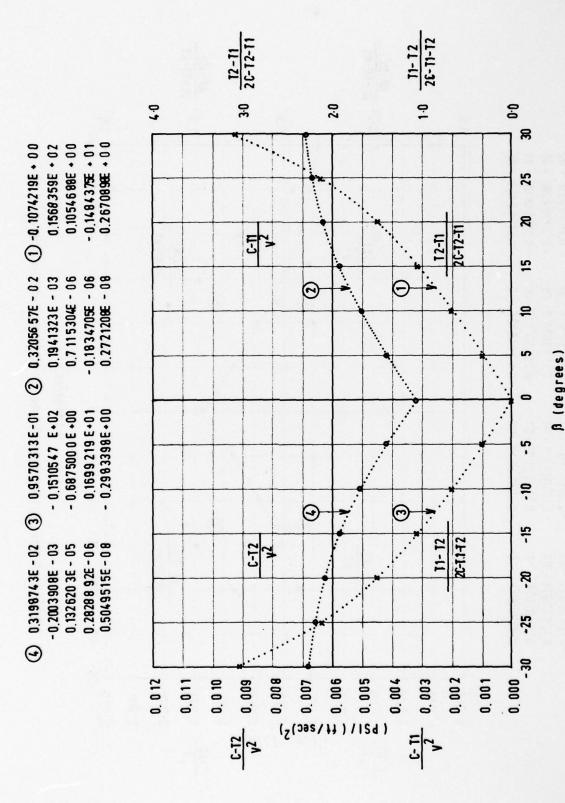


Figure 49 -Pre Calibration of Tube 29 in Horizontal-Tangential Plane

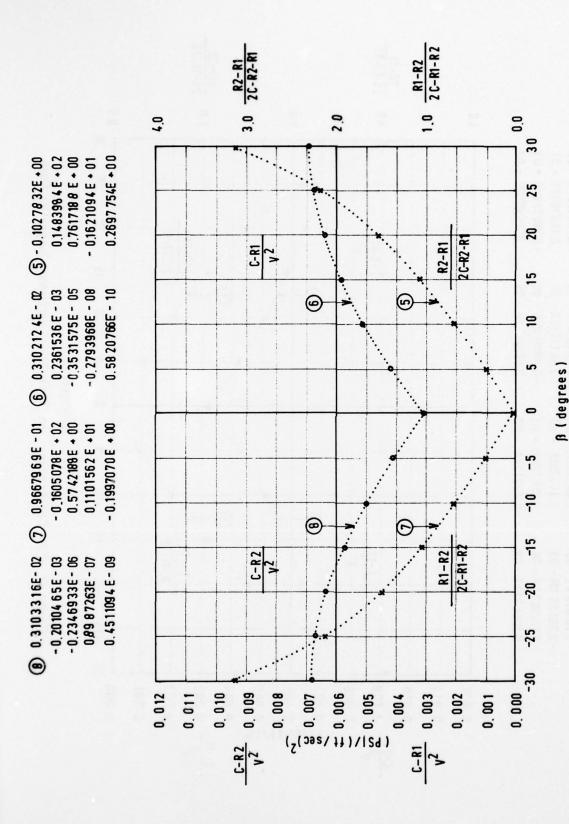


Figure 50 - Pre Calibration of Tube 29 in Vertical-Radial Plane

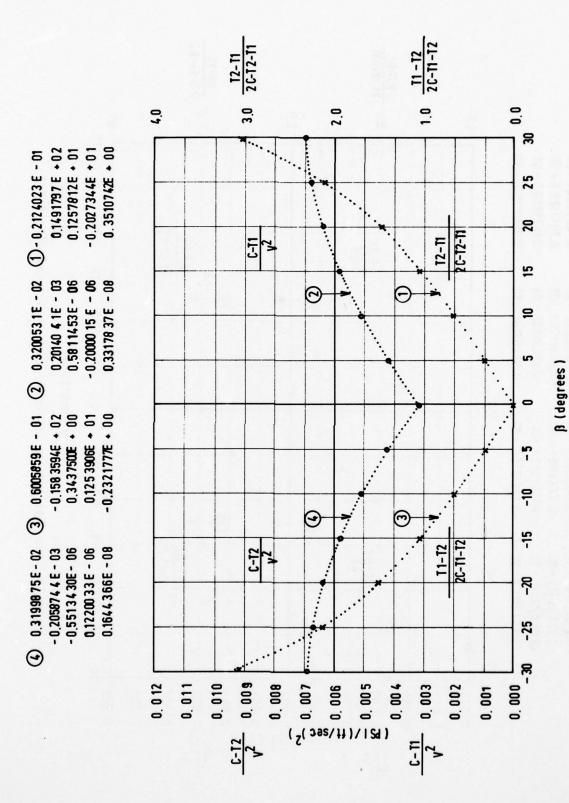


Figure 51 -Pre Calibration of Tube 30 in Horizontal-Tangential Plane

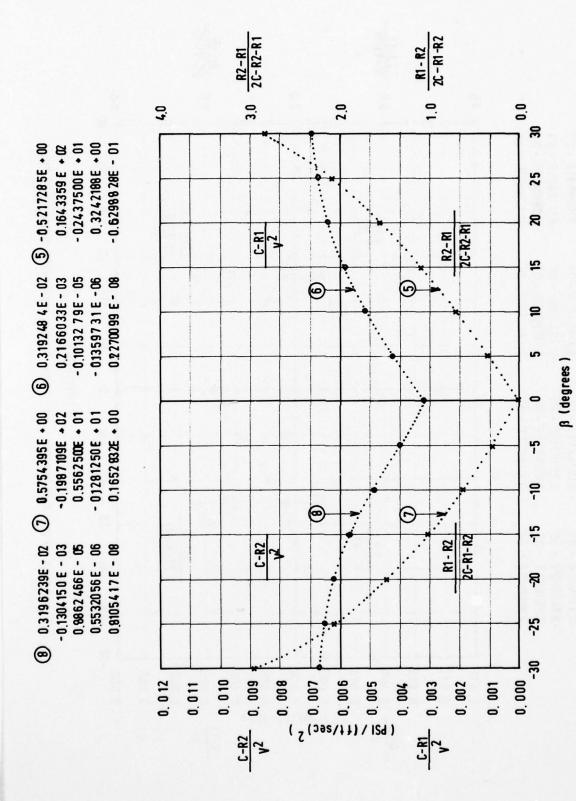


Figure 52 -Pre Calibration of Tube 30 in Vertical-Radial Plane

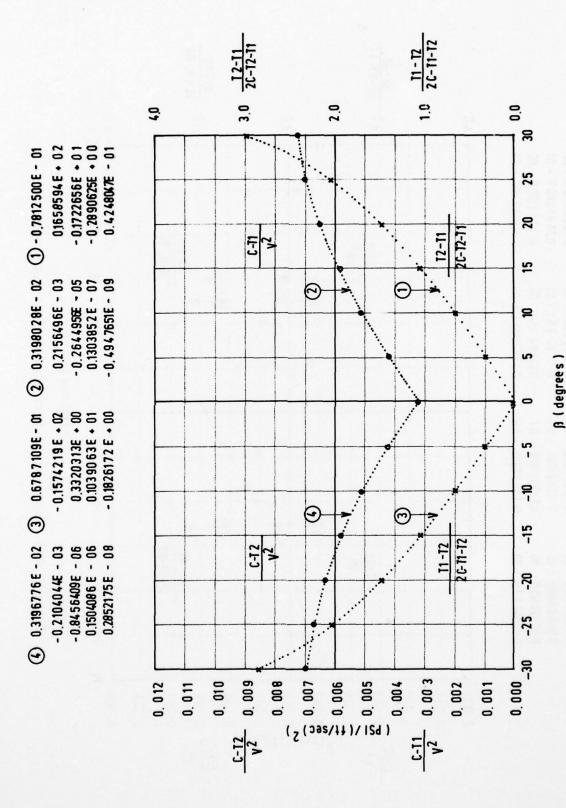


Figure 53 -Pre Calibration of Tube 31 in Horizontal-Tangential Plane

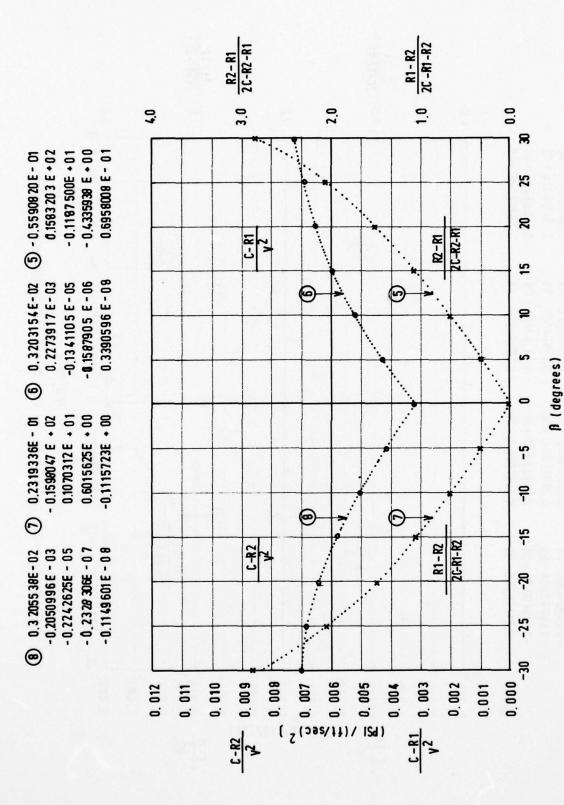


Figure 54 -Pre Calibration of Tube 31 in Vertical-Radial Plane

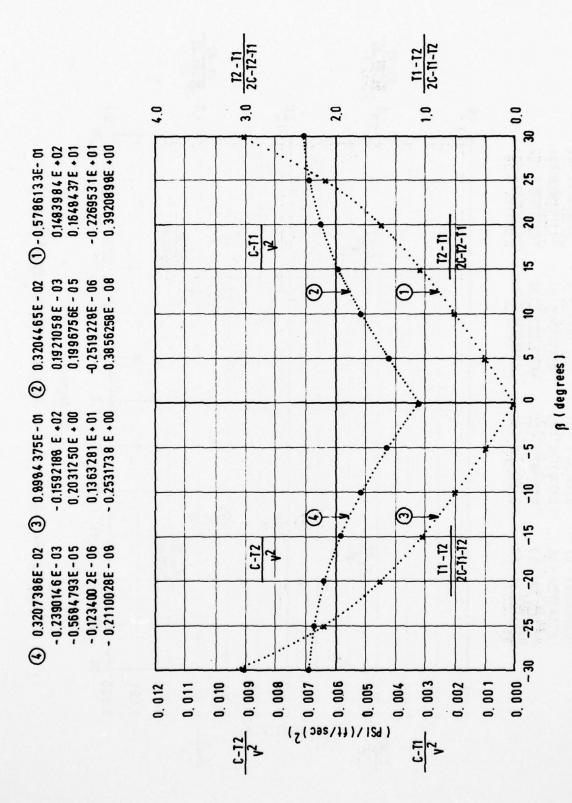


Figure 55 - Pre Calibration of Tube 32 in Horizontal-Tangential Plane

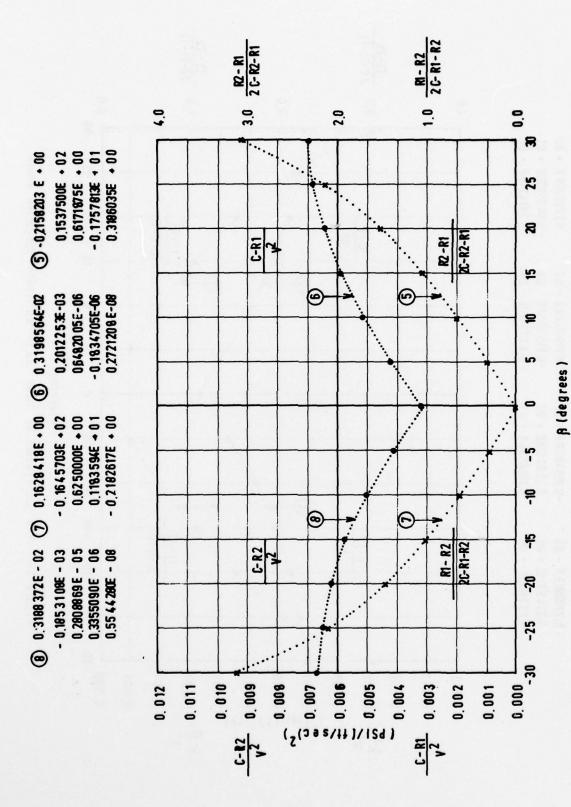


Figure 56 - Pre Calibration of Tube 32 in Vertical-Radial Plane

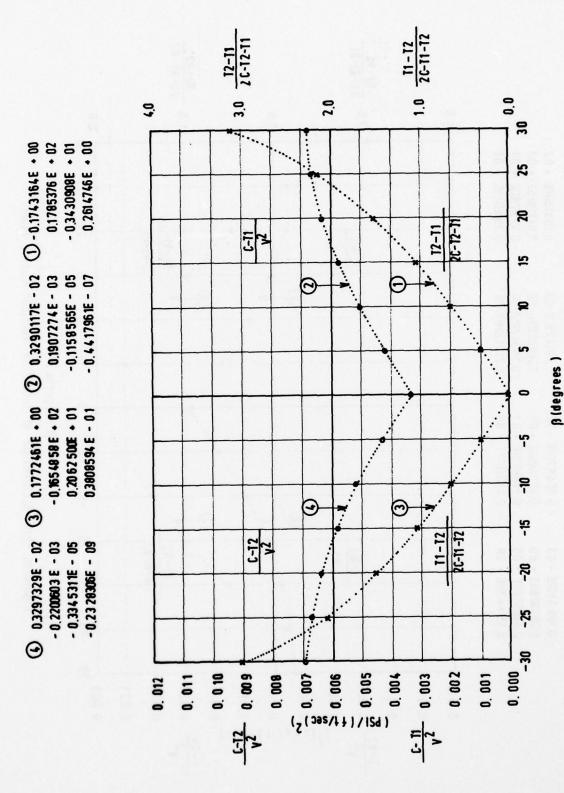


Figure 57 - Pre Calibration of Tube 33 in Horizontat-Tangential Plane

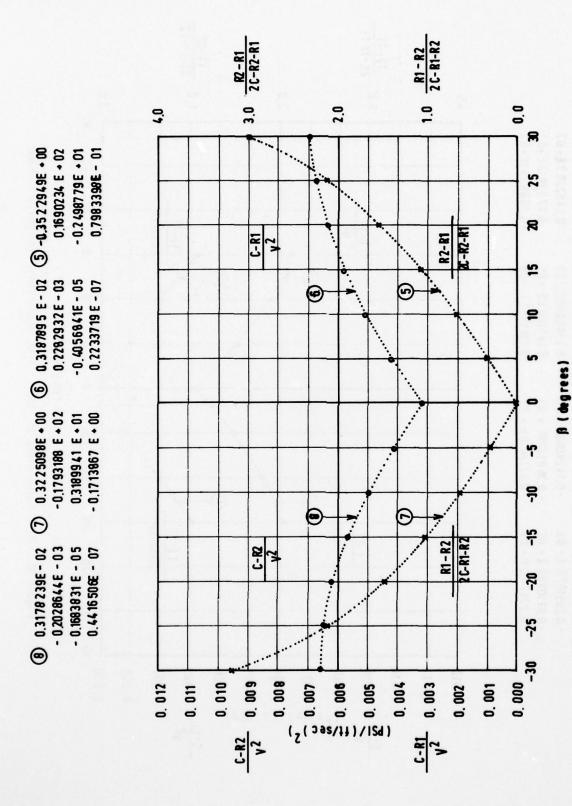


Figure 58 -Pre Calibration of Tube 33 in Vertical-Radial Plane

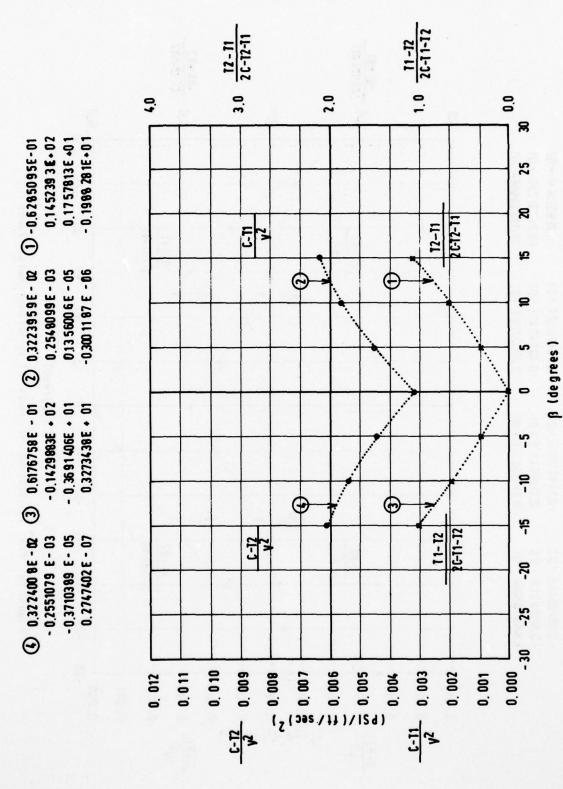


Figure 59 - Post Calibration of Tube 3 in Horizontal-Tangential Plane

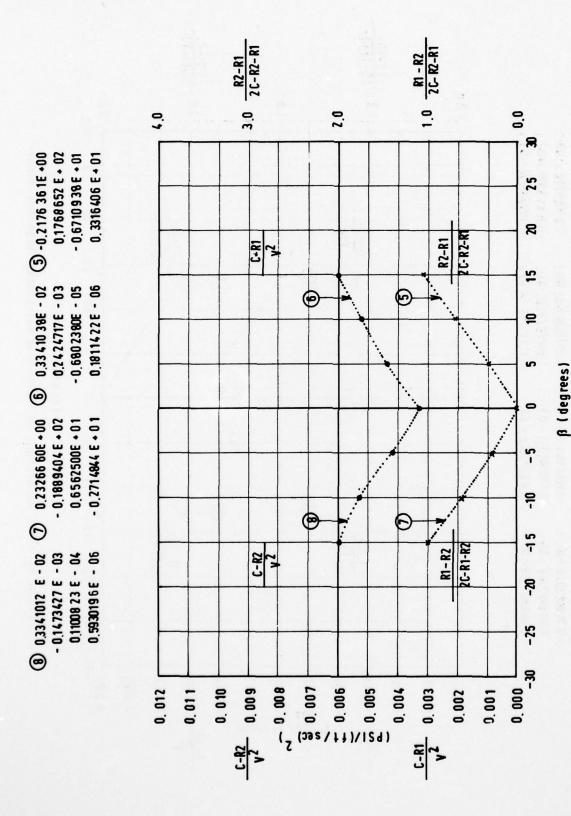


Figure 60 -Post Calibration of Jube 3 in Vertical-Radial Plane

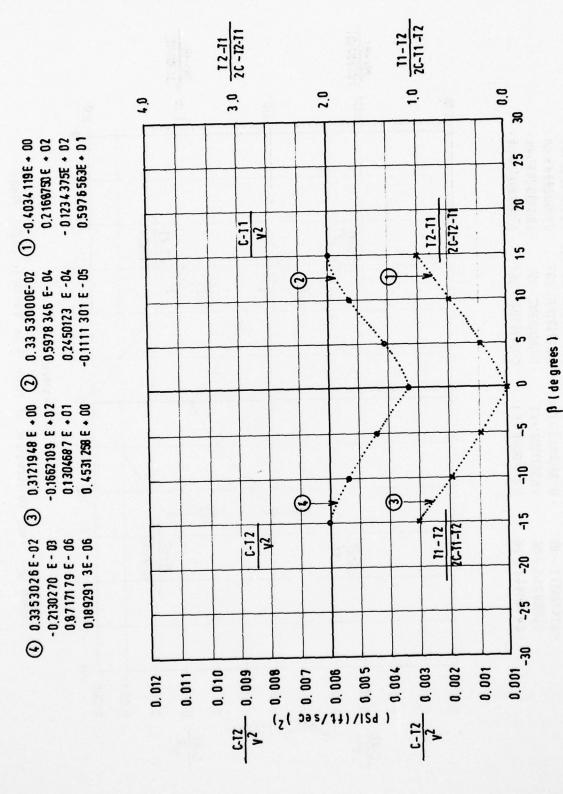


Figure 61 -Post Calibration of Tube 4 in Horizontal-Tangential Plane

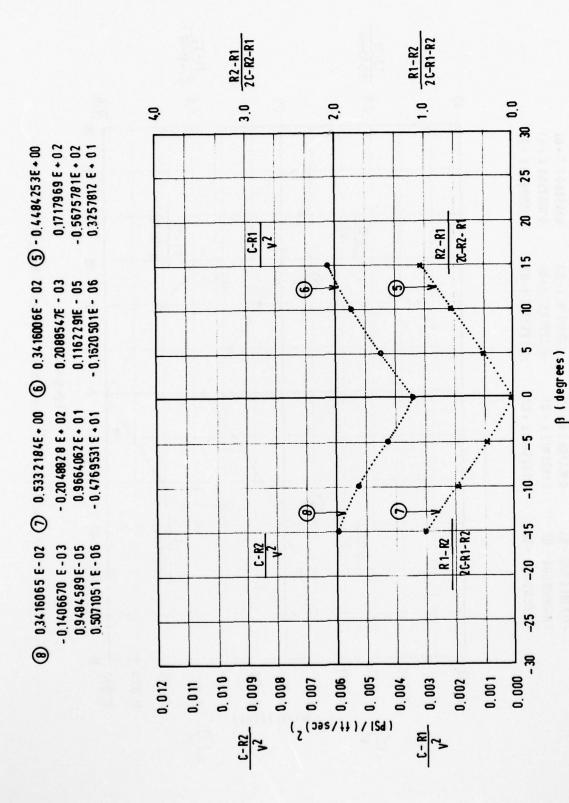


Figure 62 -Post Calibration of Tube 4 in Vertical-Radial Plane

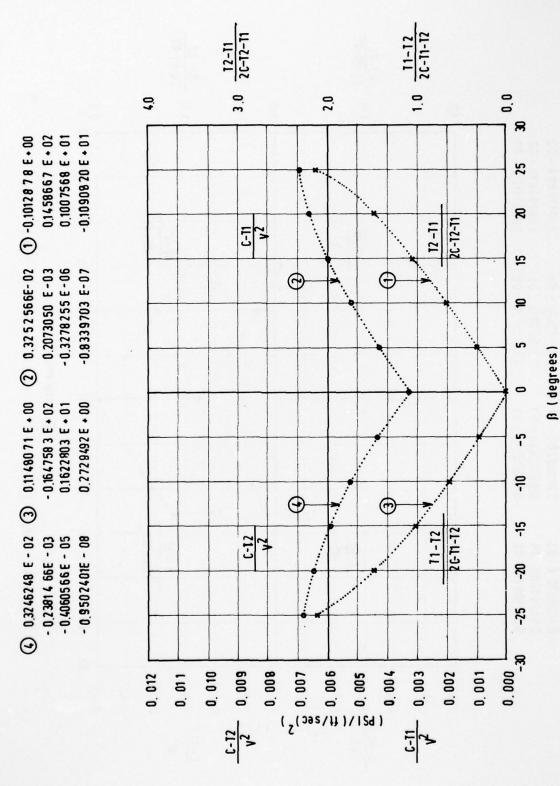
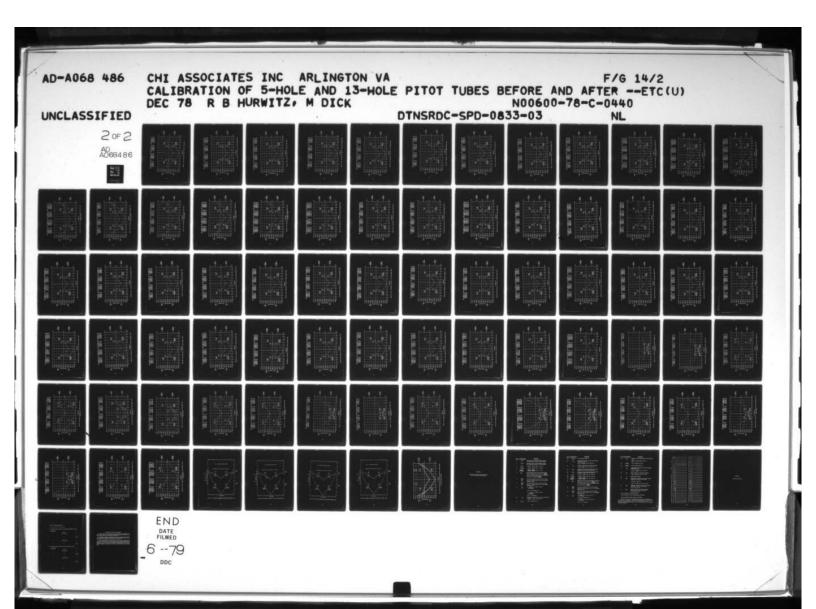


Figure 63 - Post Calibration of Tube 5 in Horizontal-Tangential Plane



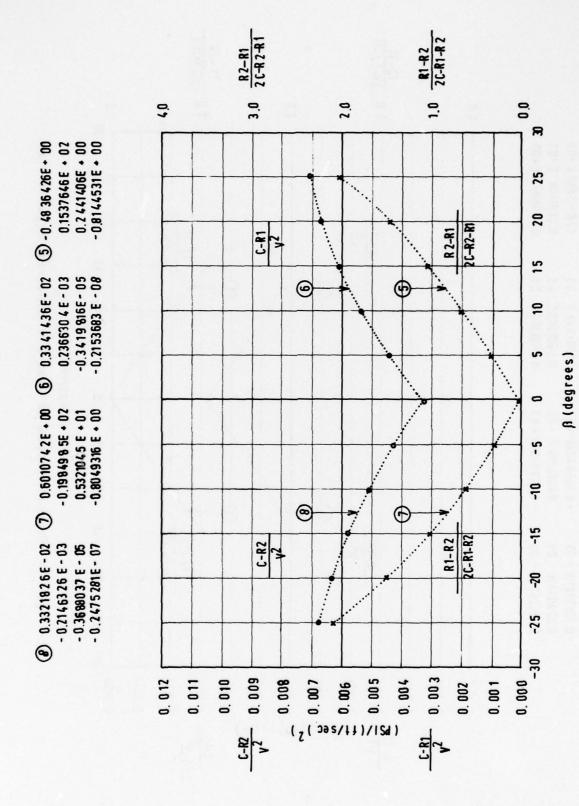


Figure 64 -Post Calibration of Tube 5 in Vertical-Radial Plane

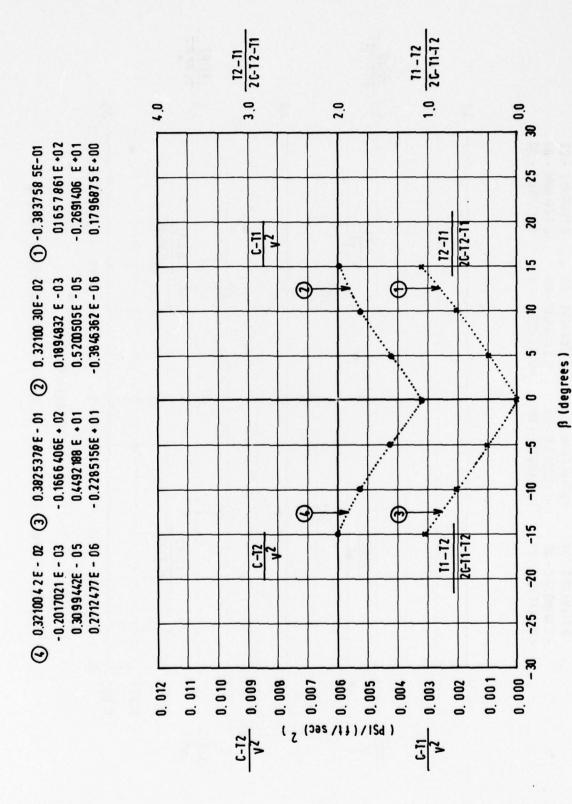


Figure 65 -Post Calibration of Tube 6 in Horizontal-Tangential Plane

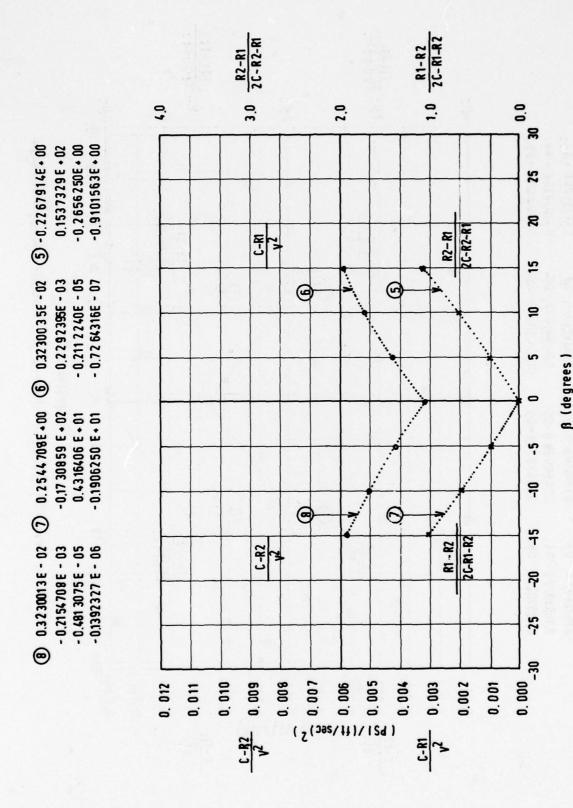


Figure 66 -Post Calibration of Tube 6 in Vertical-Radial Plane

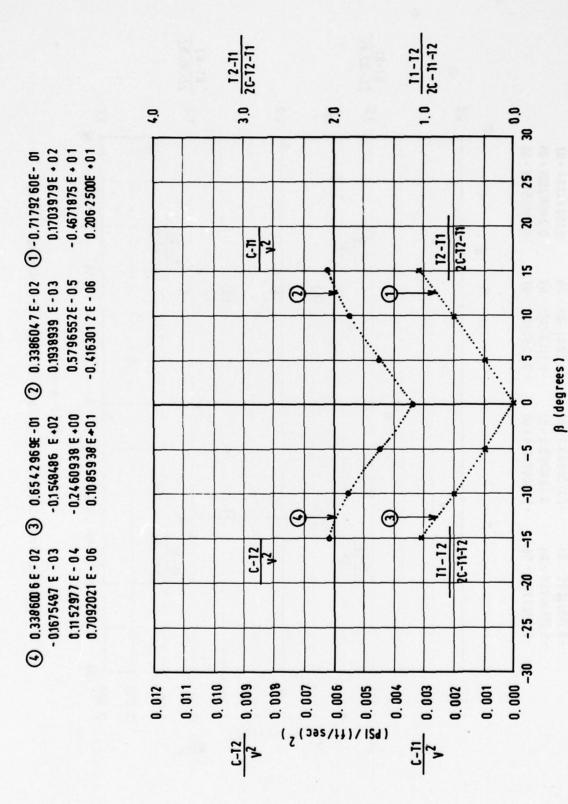


Figure 67 -Post Calibration of Tube 9 in Horizontal-Tangential Plane

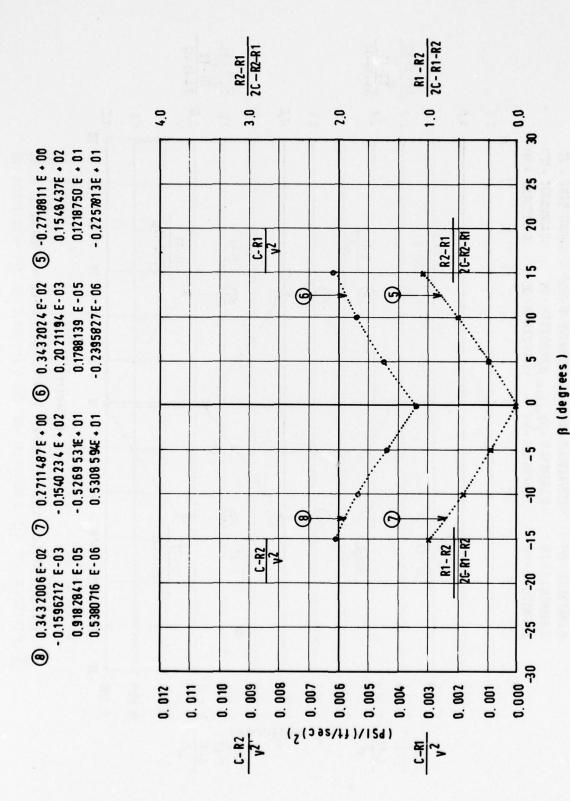


Figure 68 -Post Calibration of Tube 9 in Vertical-Radial Plane

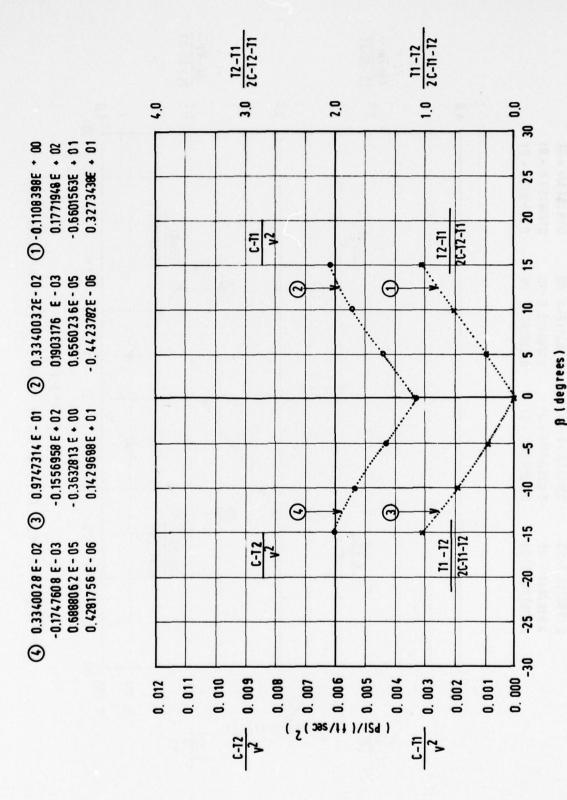


Figure 69 - Post Calibration of Tube 11 in Horizontal-Tangential Plane

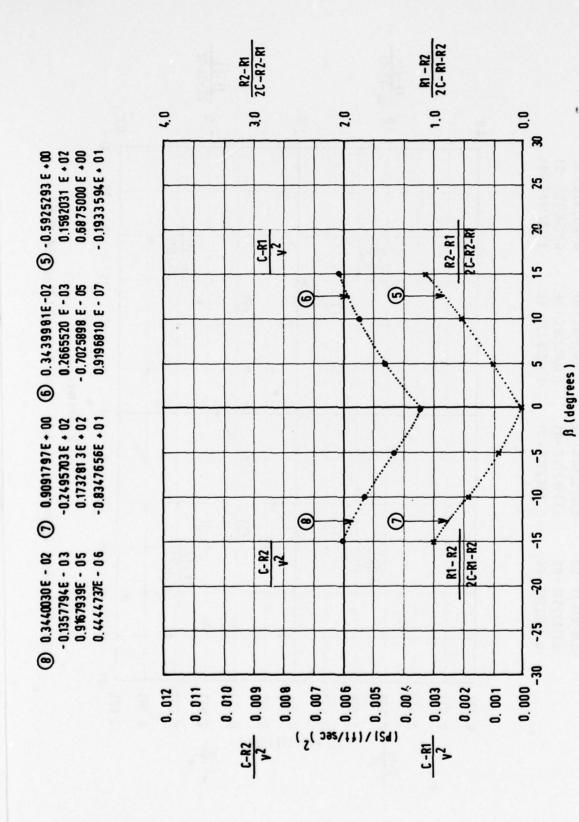


Figure 70 -Post Calibration of Tube 11 in Vertical-Radial Plane

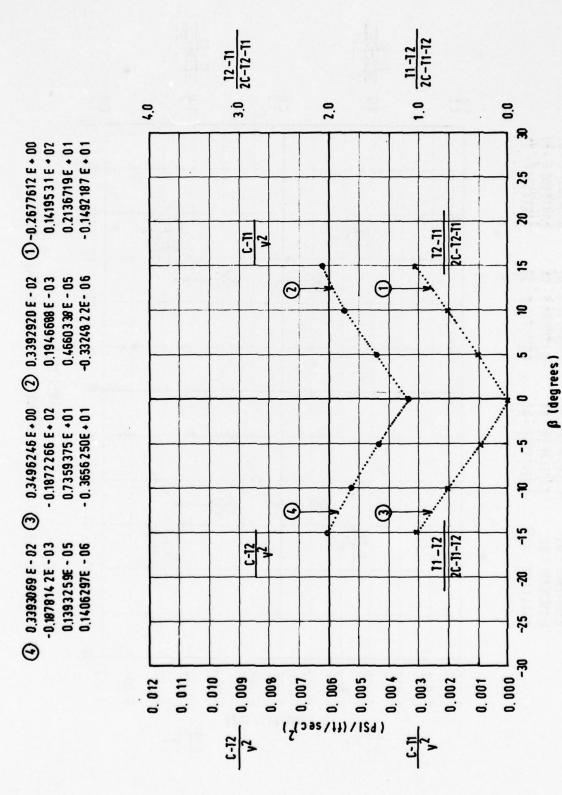


Figure 71 -Post Calibration of Tube 12 in Horizontal-Tangential Plane

96

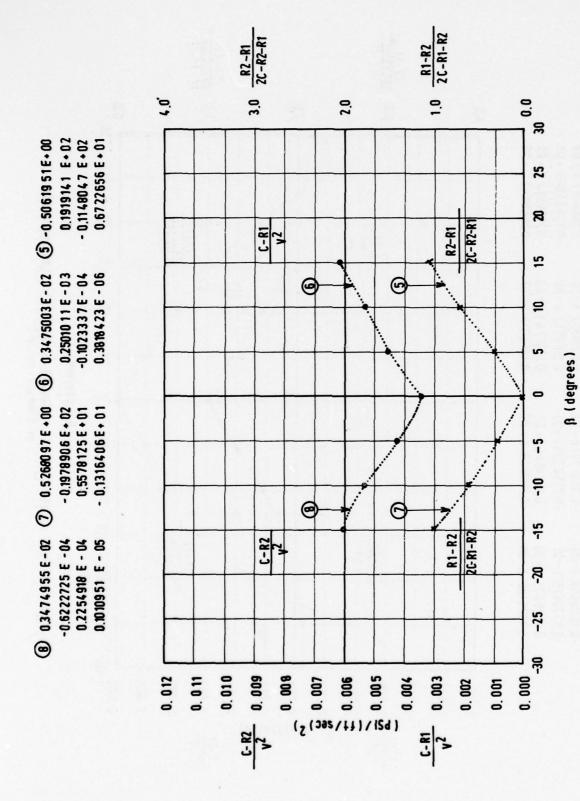


Figure 72 -Post Calibration of Jube 12 in Vertical-Radial Plane

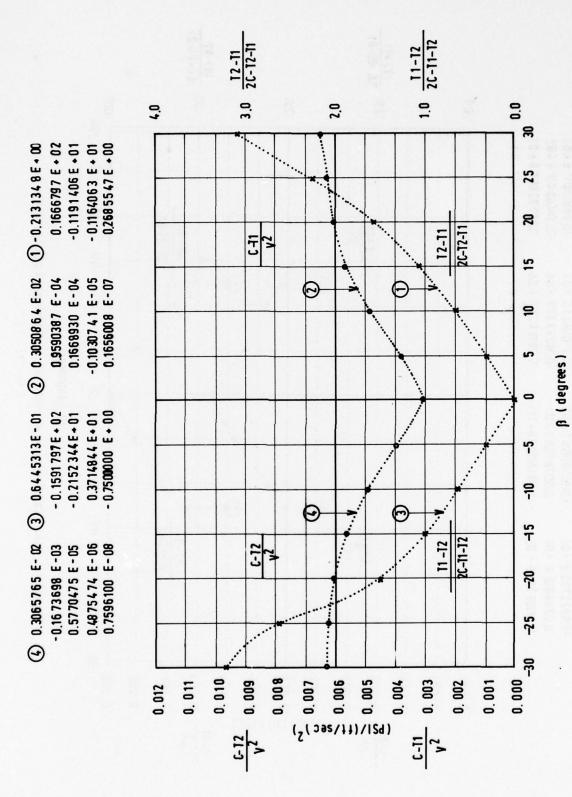


Figure 73 - Post Calibration of Tube 13 in Horizontal-Tangential Plane at 6 teetper second

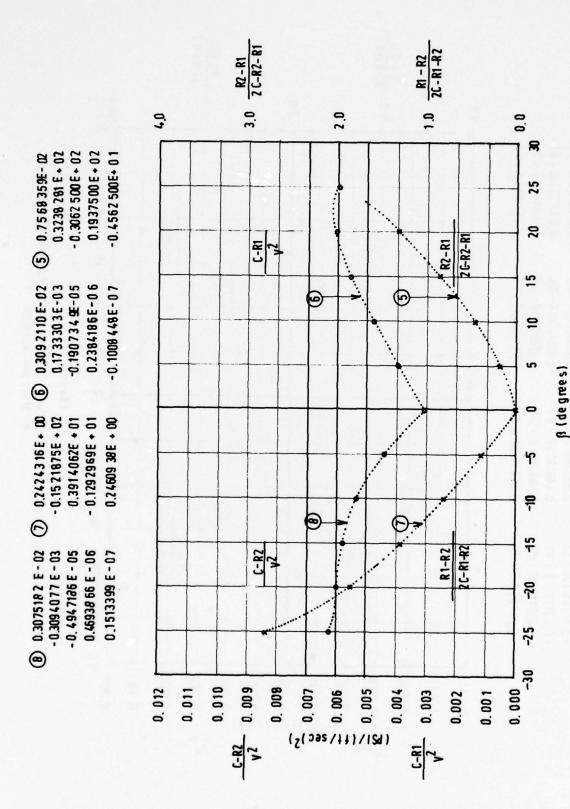


Figure 74 -Post Calibration of Tube 13 in Vertical-Radial Plane at 6 feet per second

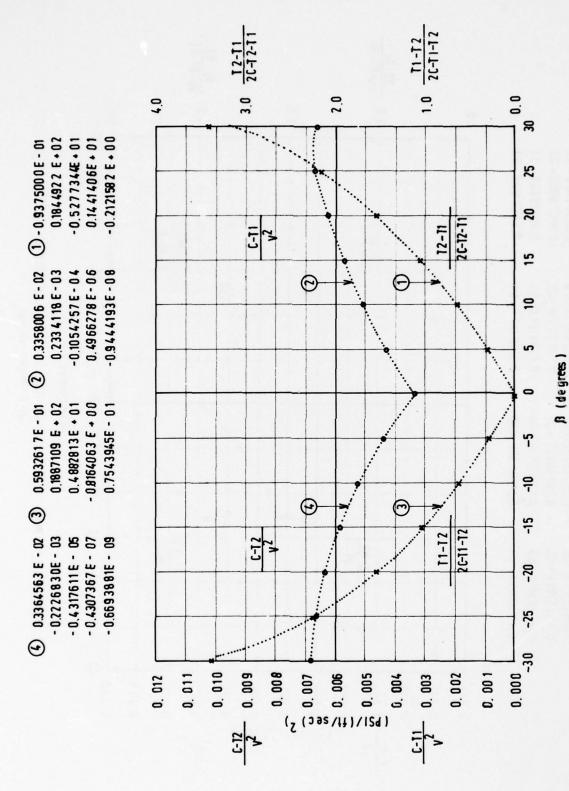


Figure 75 -Post Calibration of Tube 13 in Horizontal-Tangential Plane at 11 feet per second

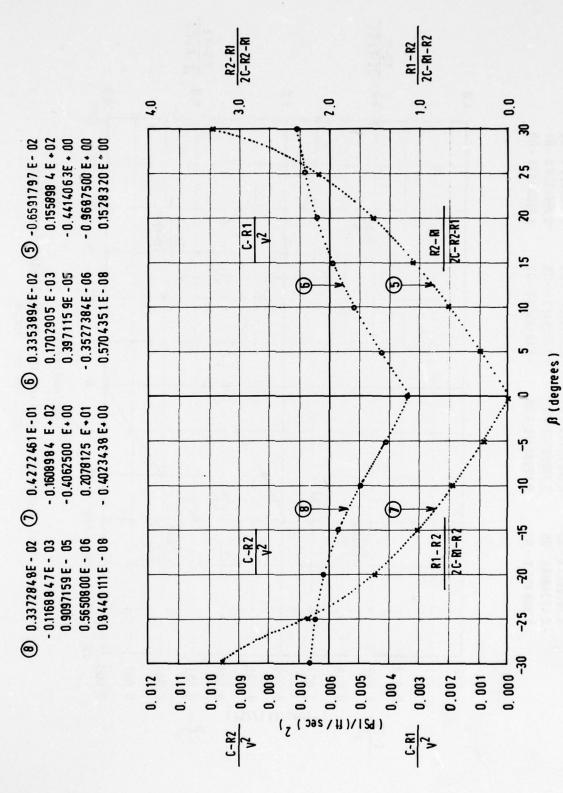


Figure 76 -Post Calibration of Tube 13 in Vertical-Radial Plane at 11 feet per second

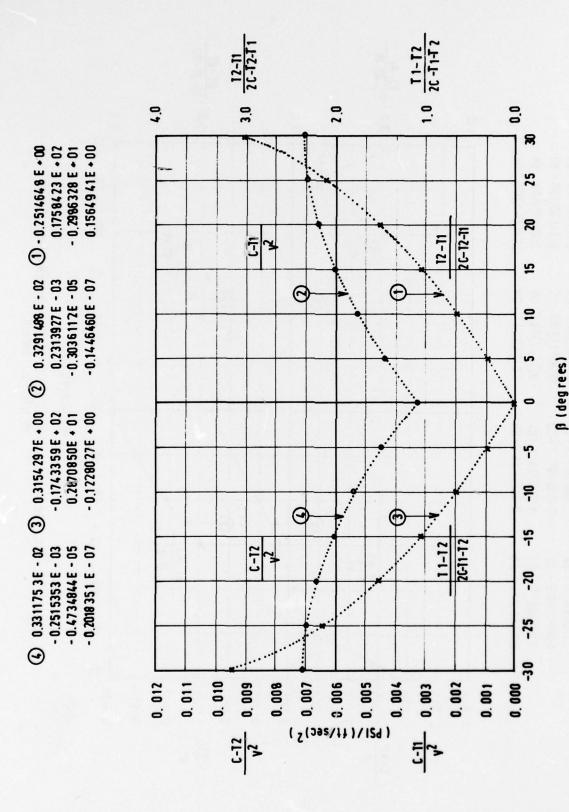


Figure 77 - Post Calibration of Tube 13 in Horizontal-Tangential Plane at 20 feet per second

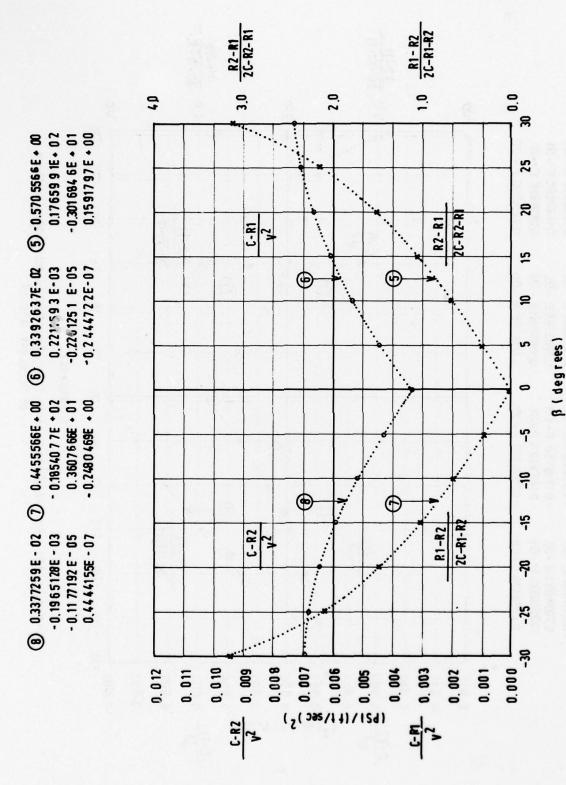


Figure 78 -Post Calibration of Tube 13 in Vertical-Radial Plane at 20 feet per second

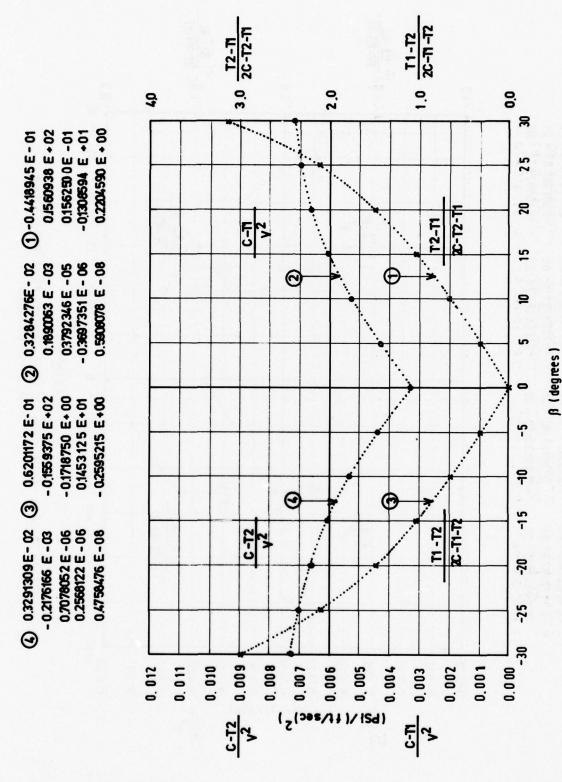


Figure 79 - Post Calibration of Tube 13 in Horizontal-Tangential Plane at 25, feet per second

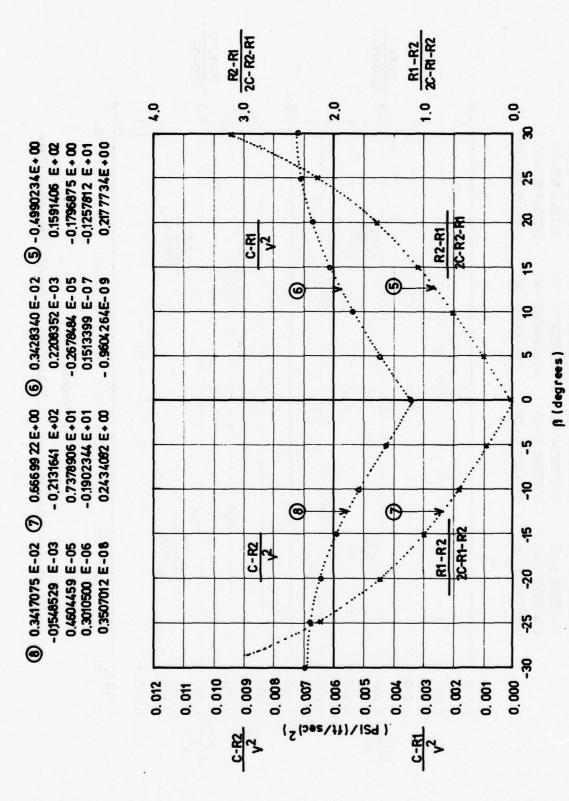


Figure 80 - Post Calibration of Tube 13 in Vertical-Radial Plane at 25feet per second

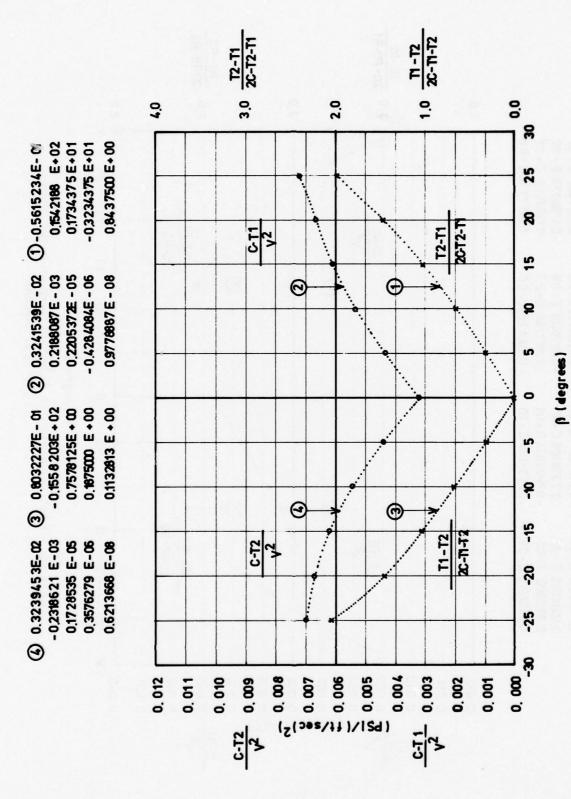


Figure 81 -Post Calibration of Tube 15 in Horizontal-Tangential Plane

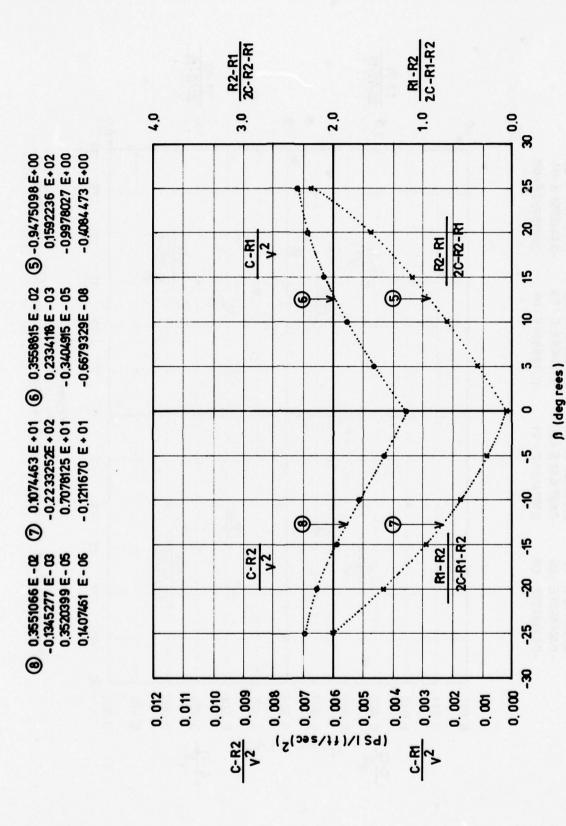


Figure 82 -Post Calibration of Tube 15 in Vertical-Radial Plane

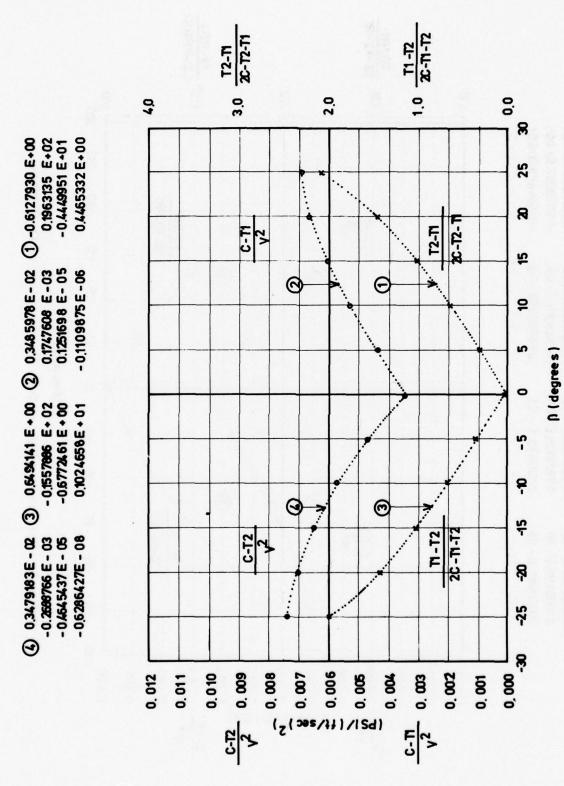


Figure 83 - Post Calibration of Tube 16 in Horizontal-Tangential Plane

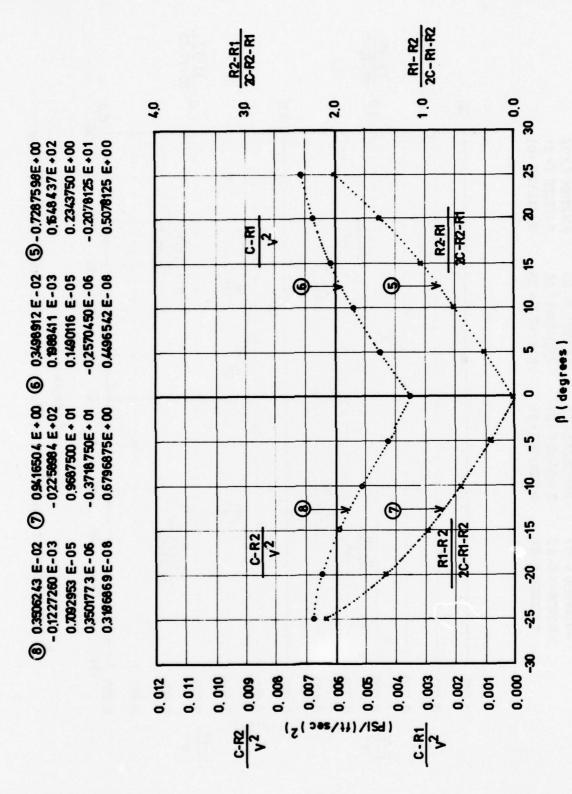


Figure 84 - Post Calibration of Tube 16 in Vertical-Radial Plane

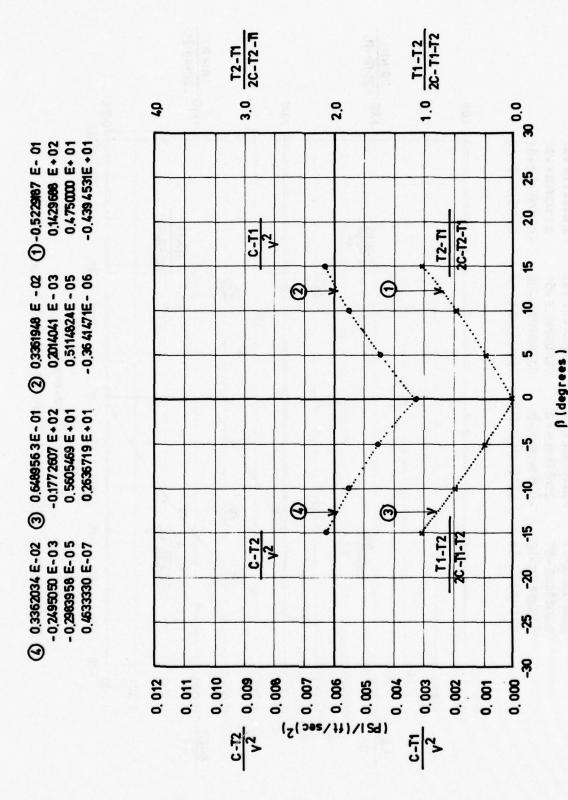


Figure 85 - Post Calibration of Tube 17 in Horizontal - Tangential Plane

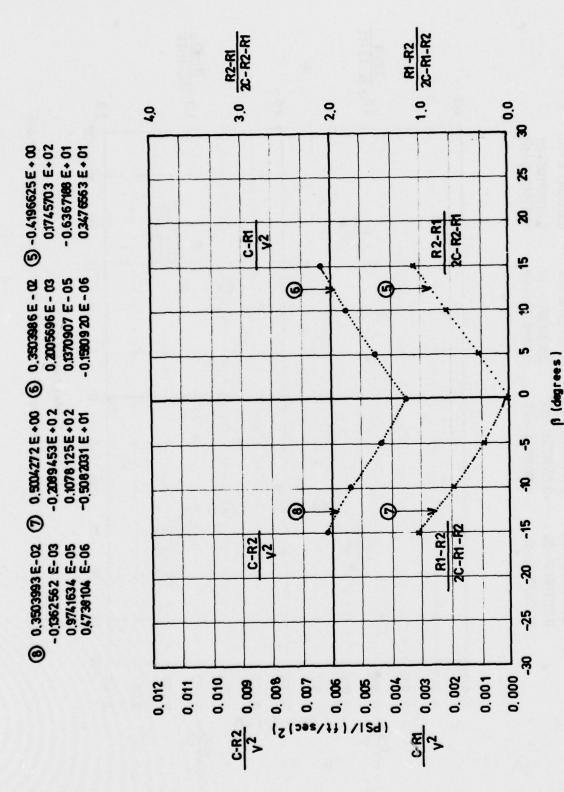


Figure 86 - Post Calibration of Tube 17 in Vertical-Radial Plane

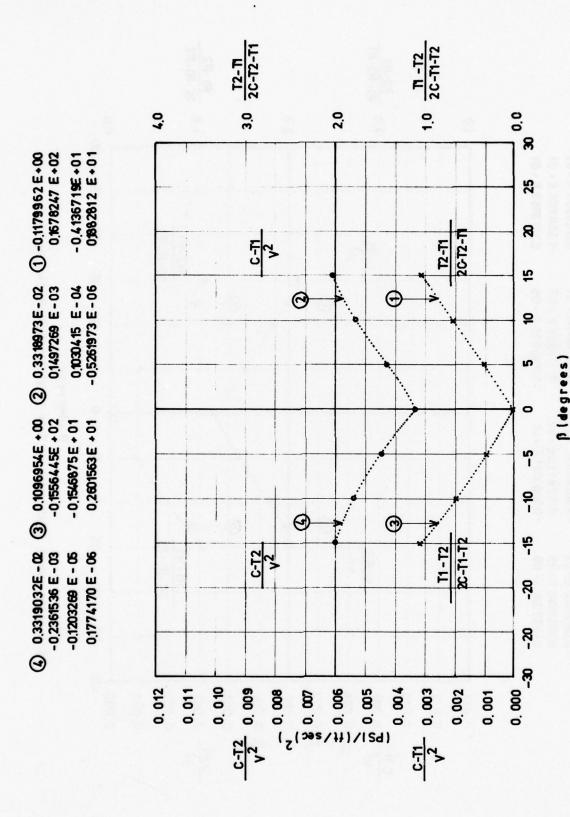


Figure 87 -Post Calibration of Tube 20 in Horizontal-Tangential Plane

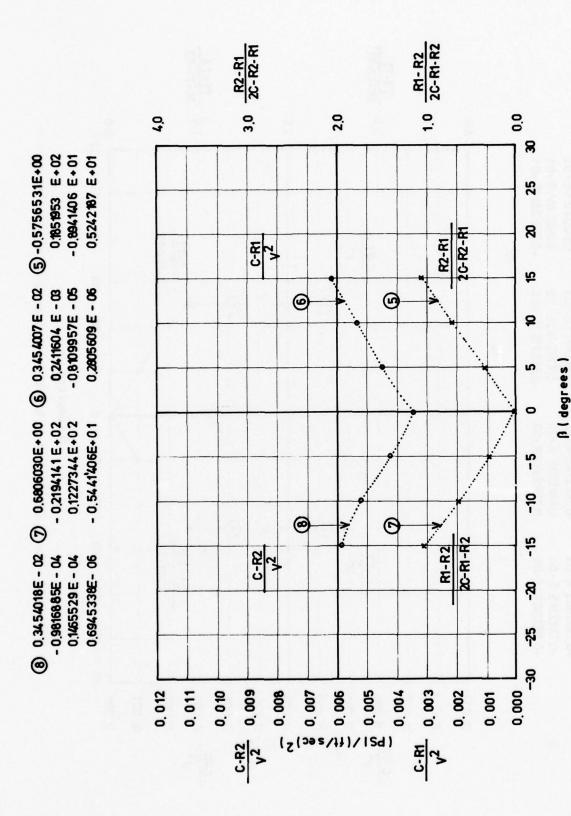


Figure 88 - Post Calibration of Tube 20 in Vertical-Radial Plane

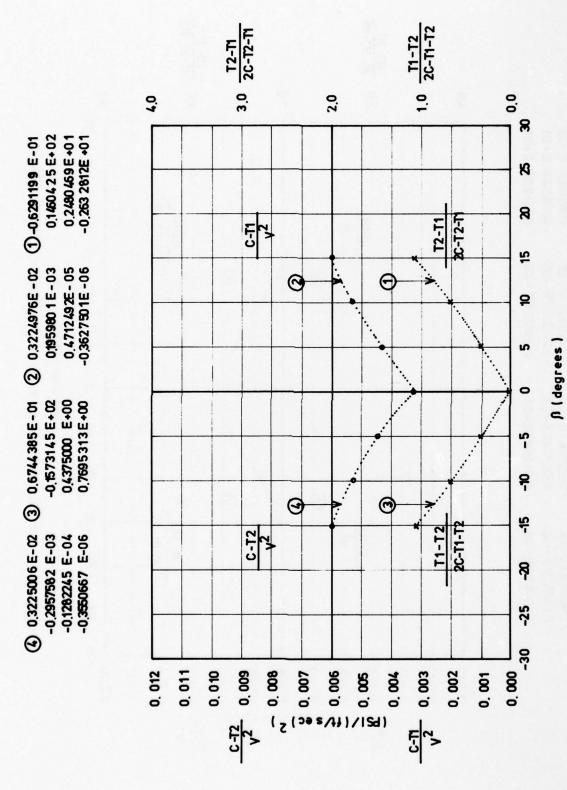


Figure 89 - Post Calibration of Tube 21 in Horizontal-Tangential Plane

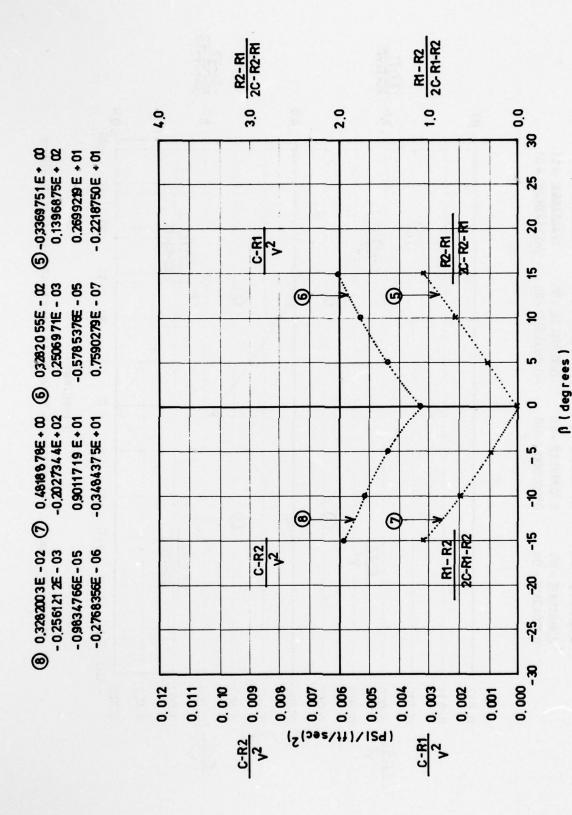


Figure 90 - Post Calibration of Tube 21 in Vertical-Radial Plane

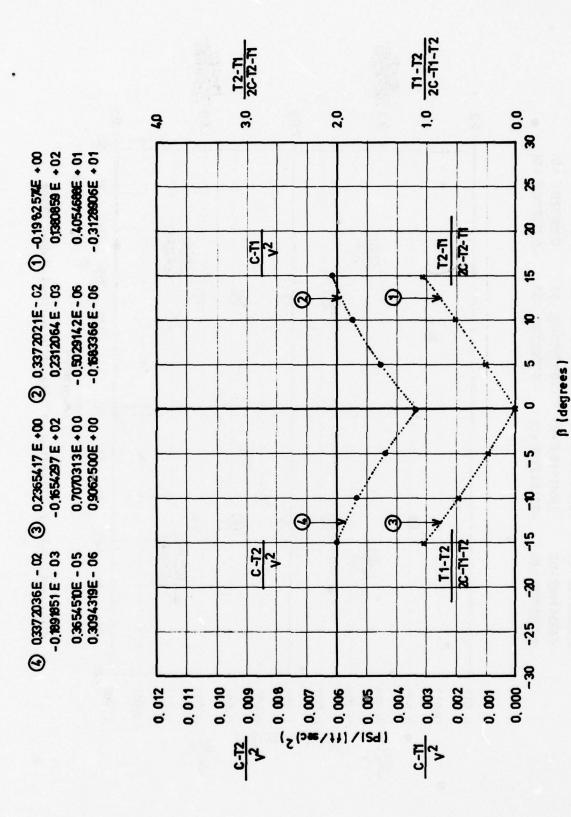


Figure 91 -Post Calibration of Tube 22 in Horizontal-Mangential Plane

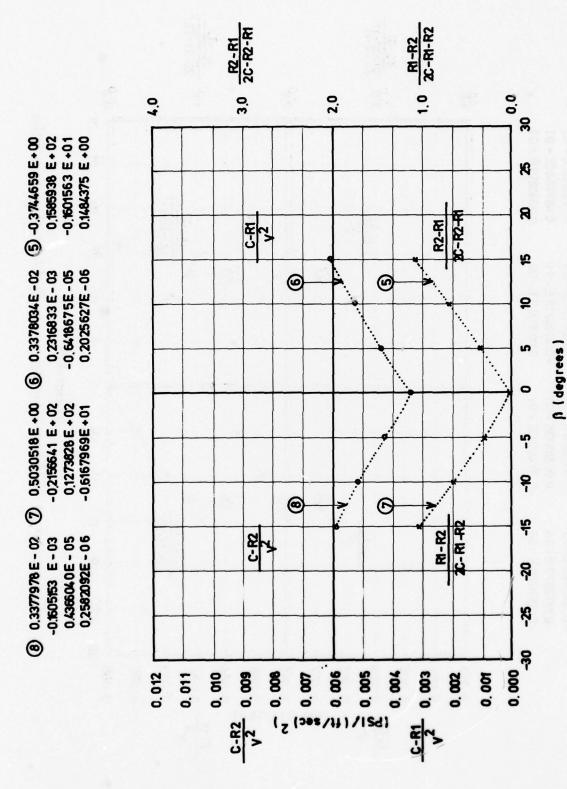


Figure 92 -Post Calibration of Tube 22 in Vertical-Radial Plane

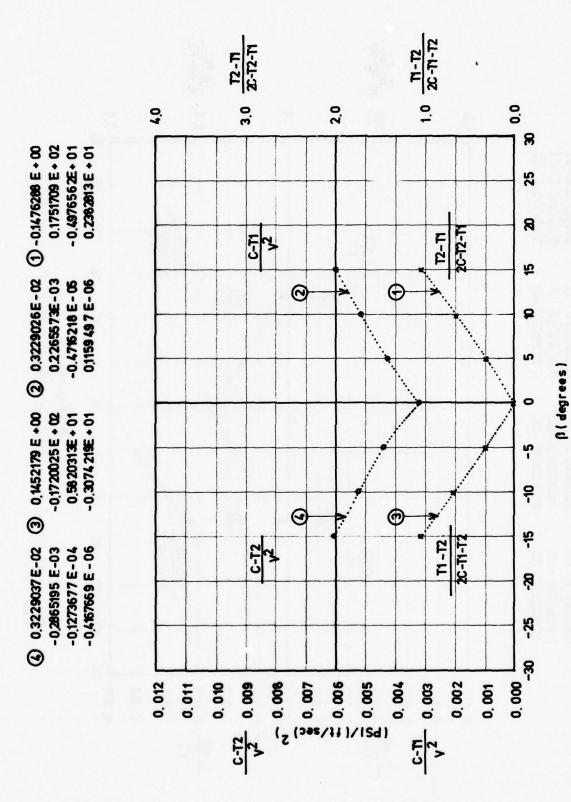


Figure 93 -Post Calibration of Tube 23 in Horizontal-Tangential Plane

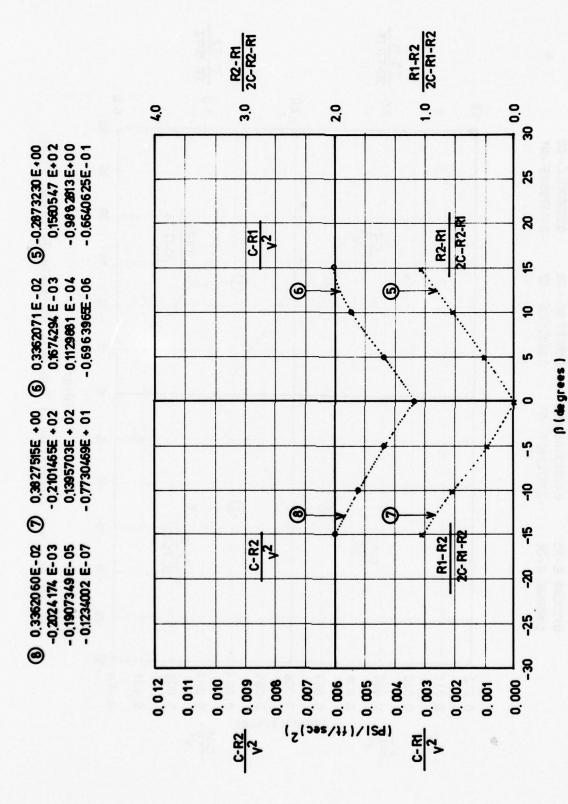


Figure 94 -Post Calibration of Tube 23 in Vertical-Radial Plane

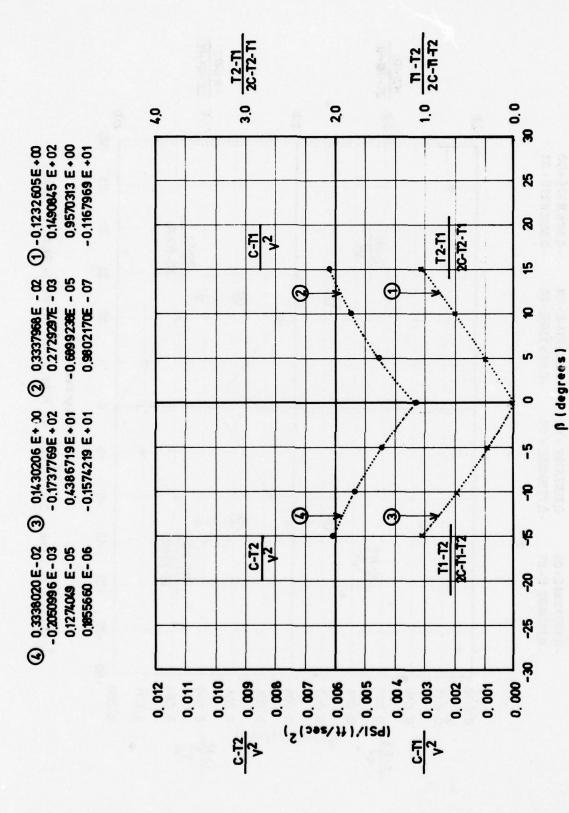


Figure 95 - Post Calibration of Tube 24 in Horizantal-Tangential Plane

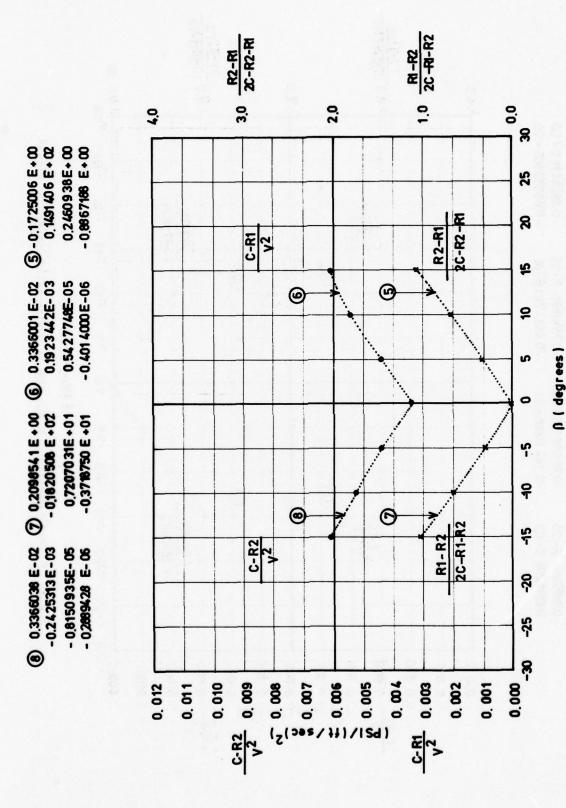


Figure 96 -Post Calibration of Tube 24 in Vertical-Radial Plane

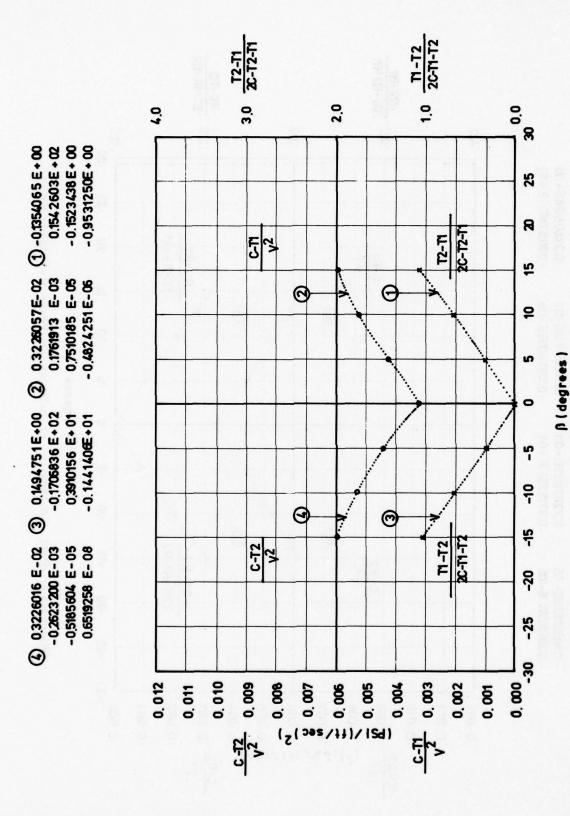


Figure 97-Post Calibration of Tube 26 in Horizontal-Tangential Plane

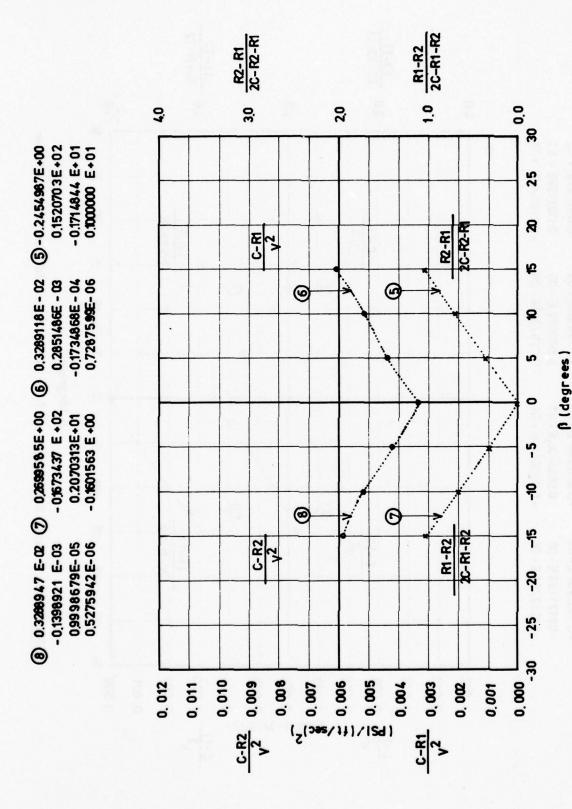


Figure 98 -Post Calibration of Tube 26 in Vertical-Radial Plane

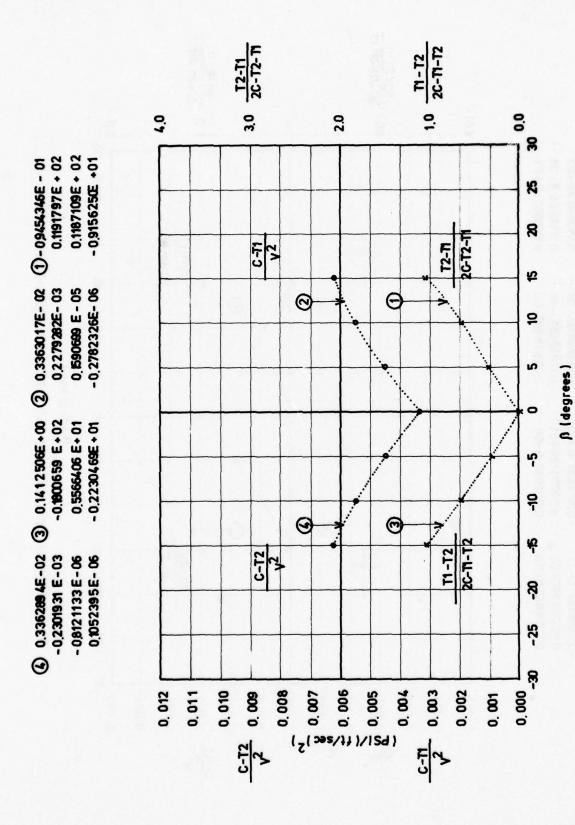


Figure 99 - Post Calibration of Tube 27 in Horizontal-Tangential Plane

124

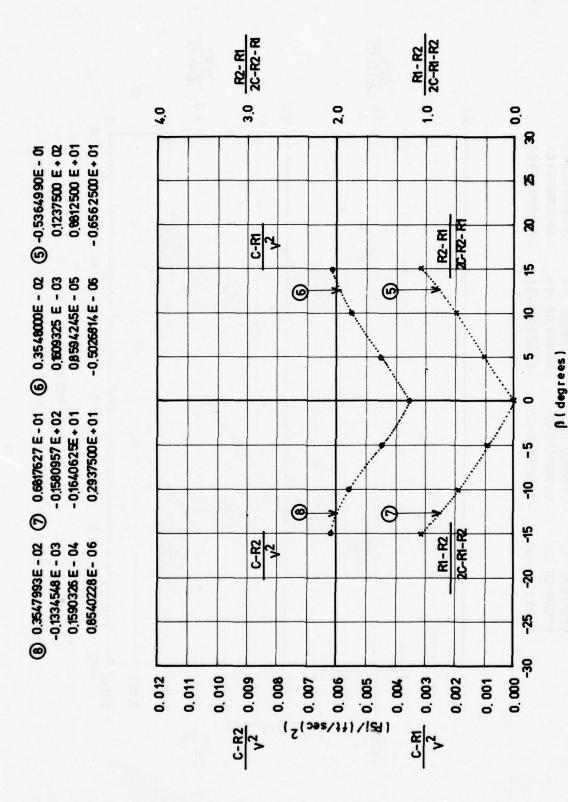


Figure 100 -Post Calibration of Tube 27 in Vertical-Radial Plane

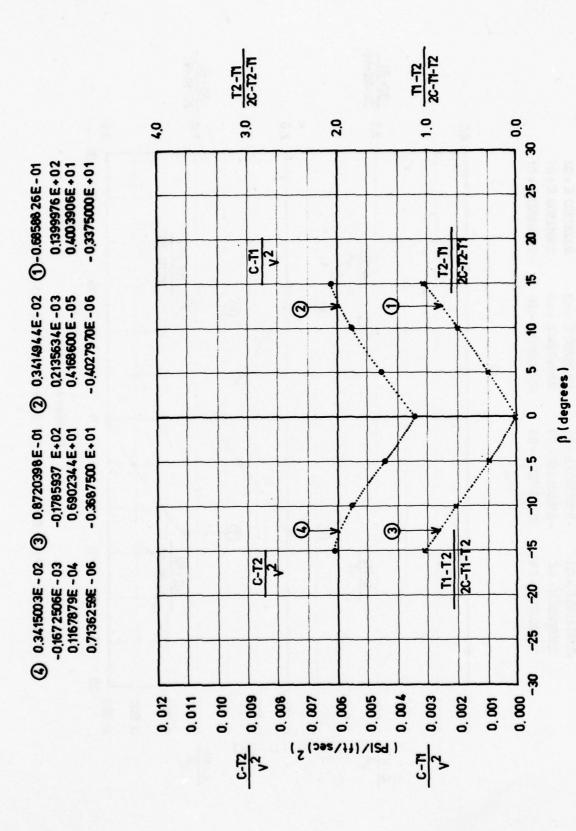


Figure 101 -Post Calibration of Tube 28 in Horizontal -Tangential Plane

126

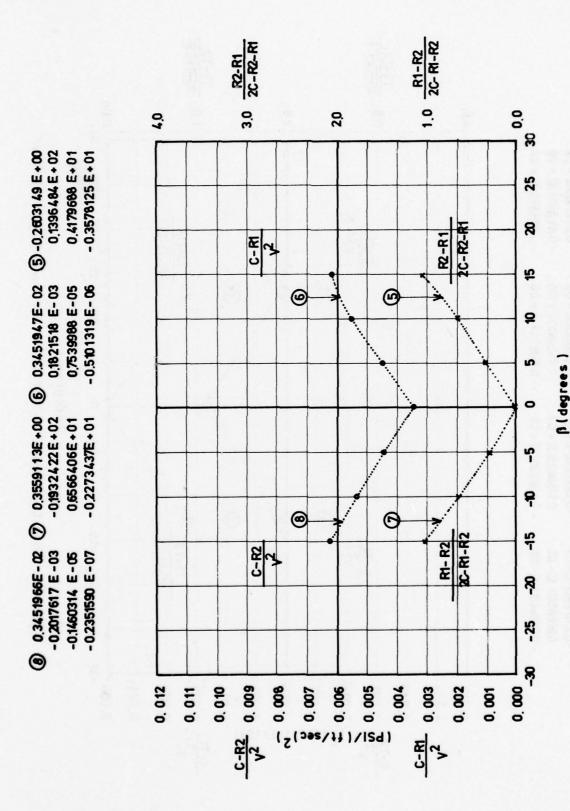


Figure 102 -Post Calibration of Tube 28 in Vertical-Radial Plane

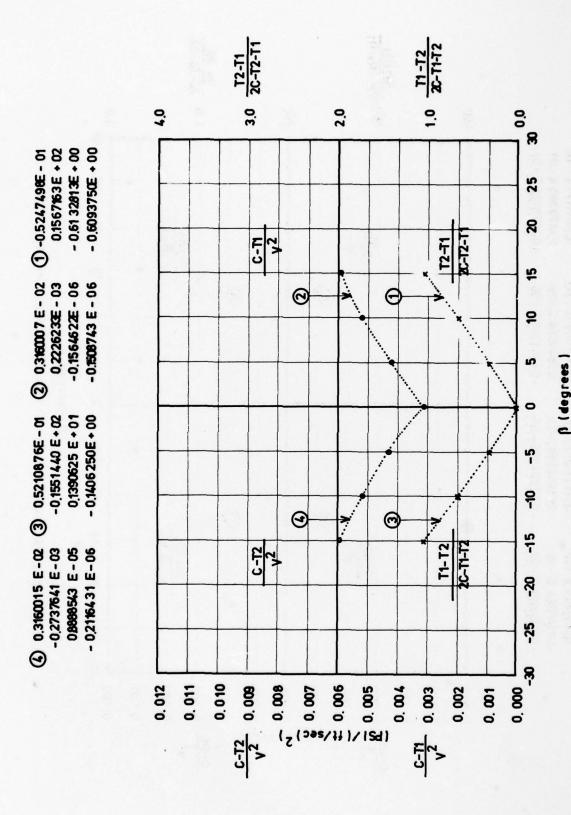


Figure 103 -Post Calibration of Tube 29 in Horizontal-Tangential Plane

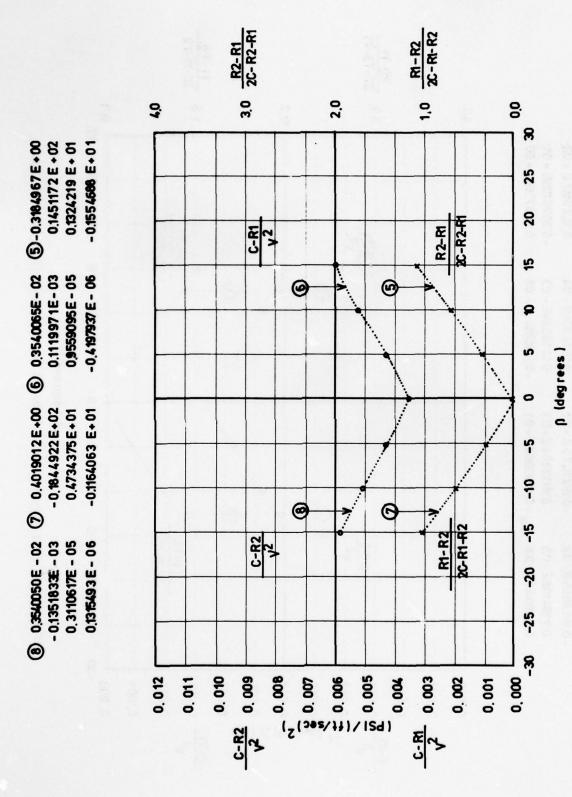


Figure 104-Post Calibration of Tube 29 in Vertical -Radial Plane

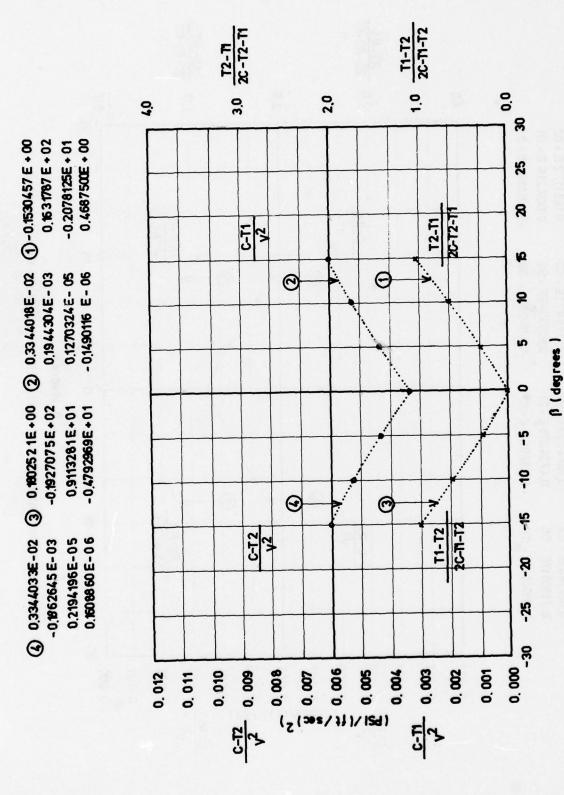


Figure 105 -Post Calibration of Tube 30 in Horizontal-Targential Plane

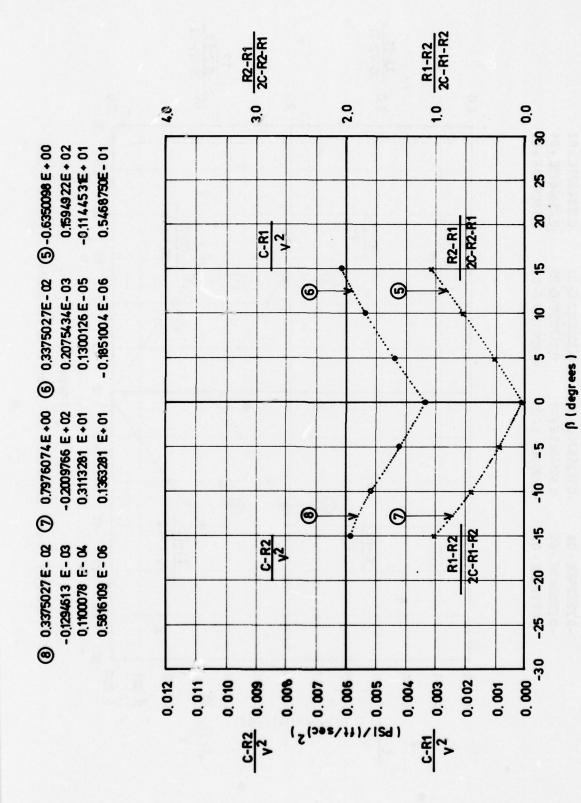


Figure 106 -Post Calibration of Tube 30 in Vertical-Radial Plane

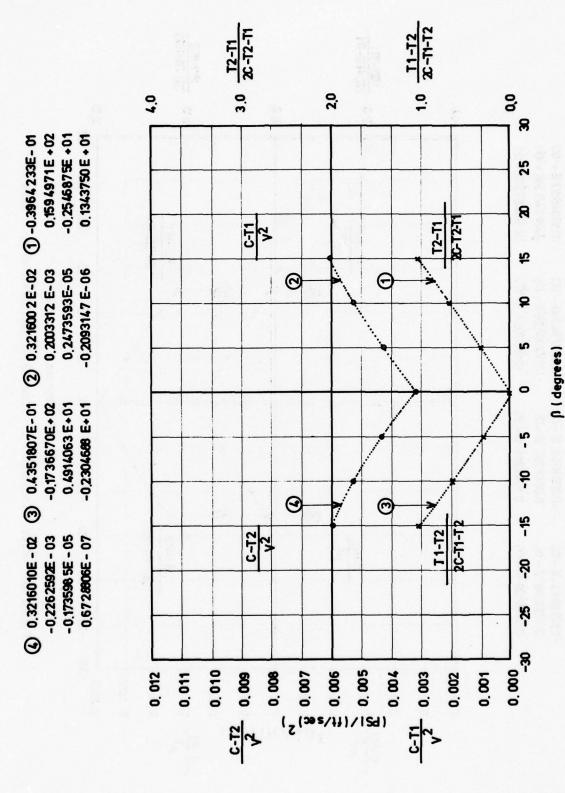


Figure 107 - Post Calibration of Tube 31 in Horizontal-Tangential Plane

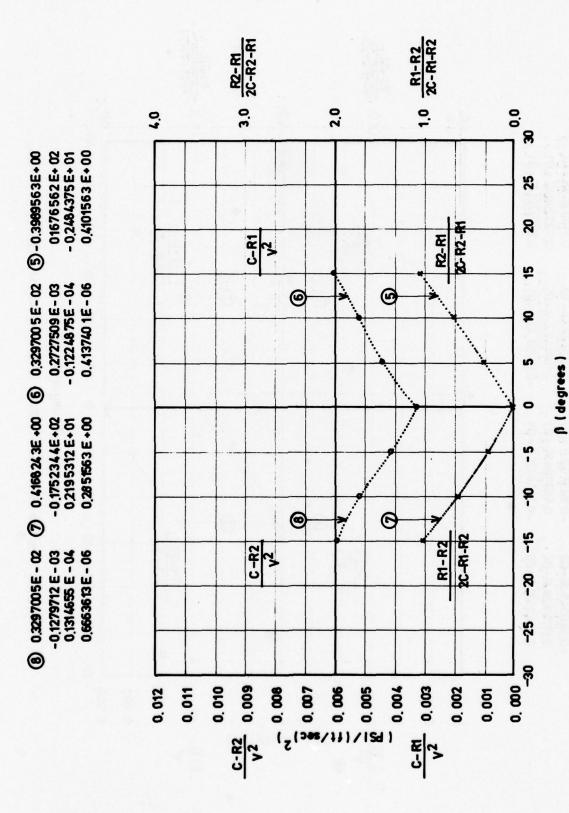
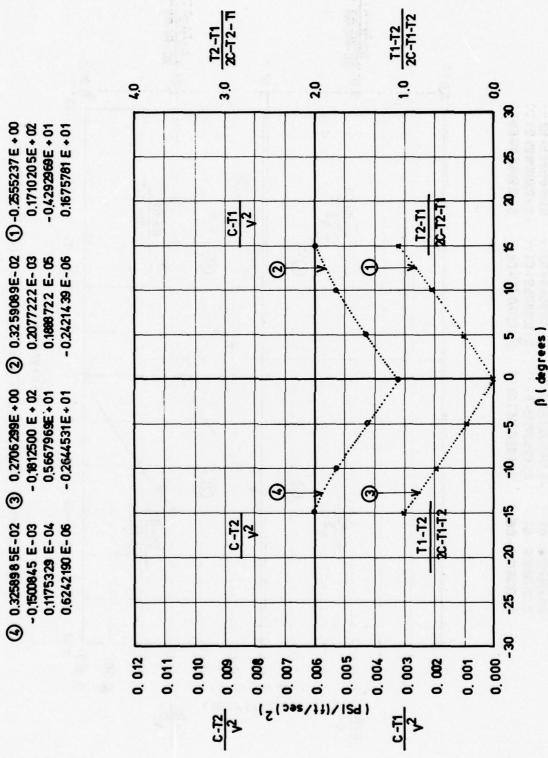


Figure 108-Post Calibration of Tube 31 in Vertical-Radial Plane



Figue 109 -Post Calibration of Tube 32 in Horizontal-Tangential Plane

134

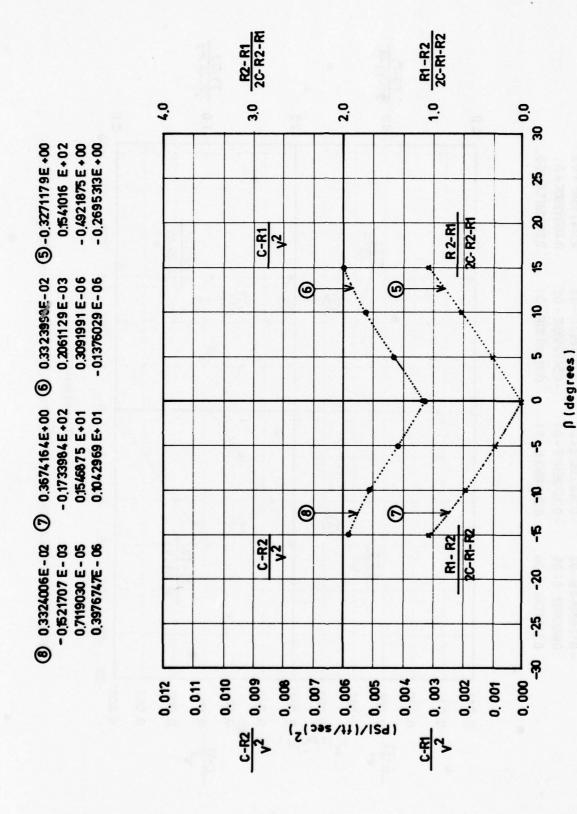


Figure 110 - Post Calibration of Tube 32 in Vertical-Radial Plane

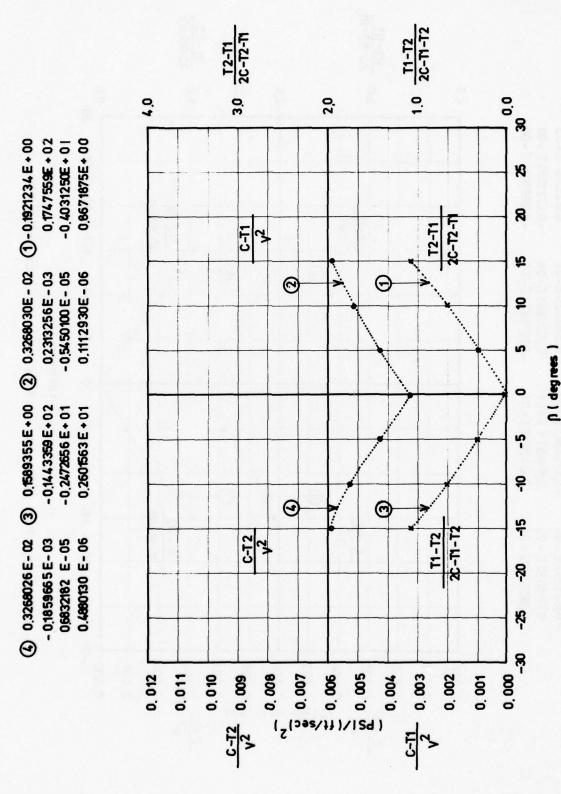


Figure 111 -Post Calibration of Tube 33 in Horizontal-Tangential Plane

136

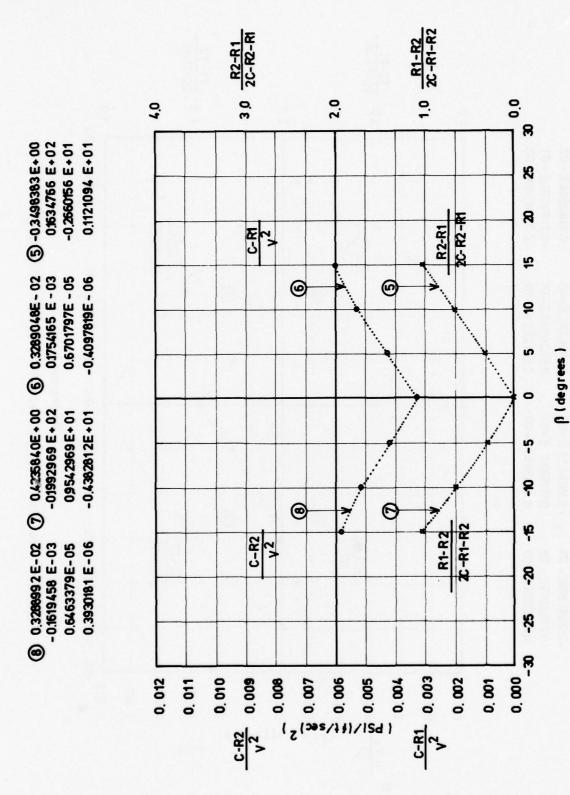


Figure 112 -Post Calibration of Tube 33 in Vertical-Radial Plane

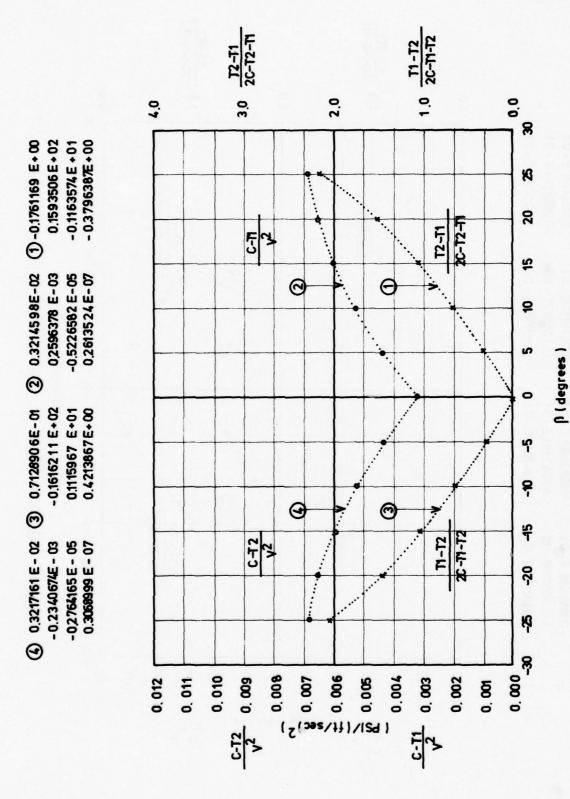


Figure 113 - Post Calibration of Tube 34 in Harizontal-Tangential Plane

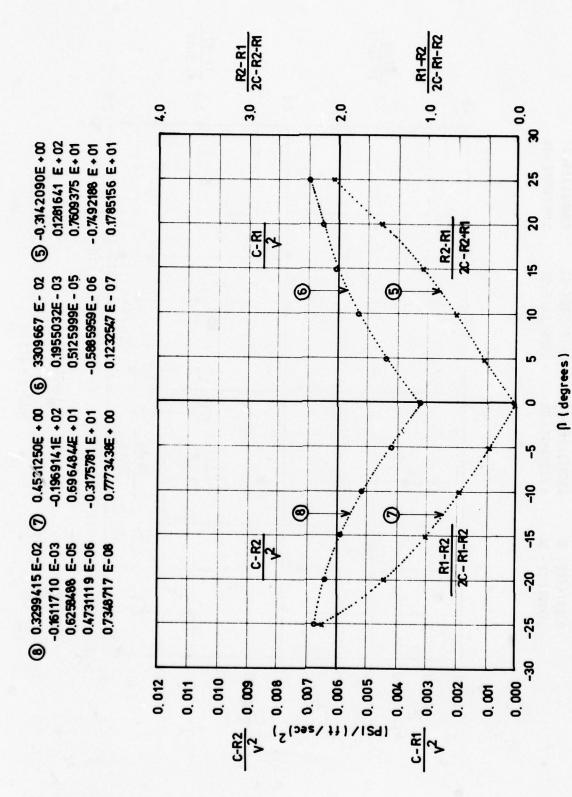
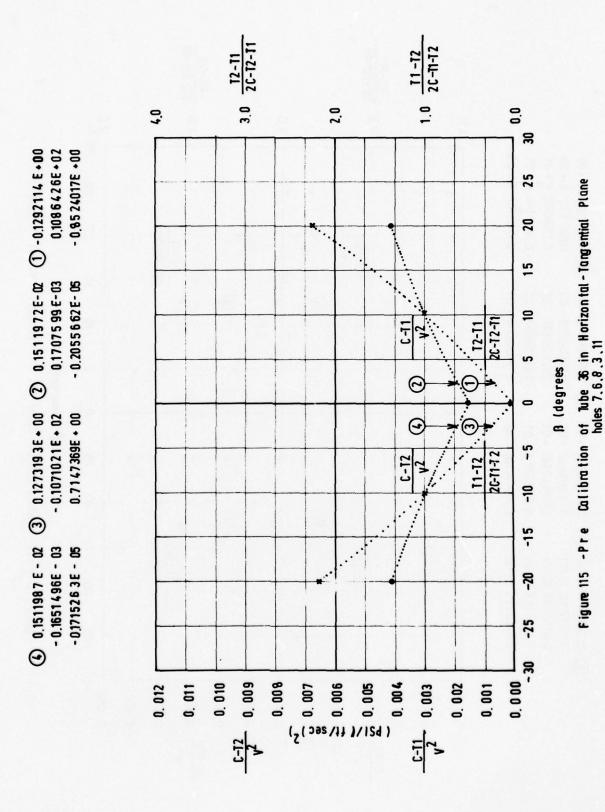


Figure 114-Post Calibration of Tube 34 in Vertical-Radial Plane



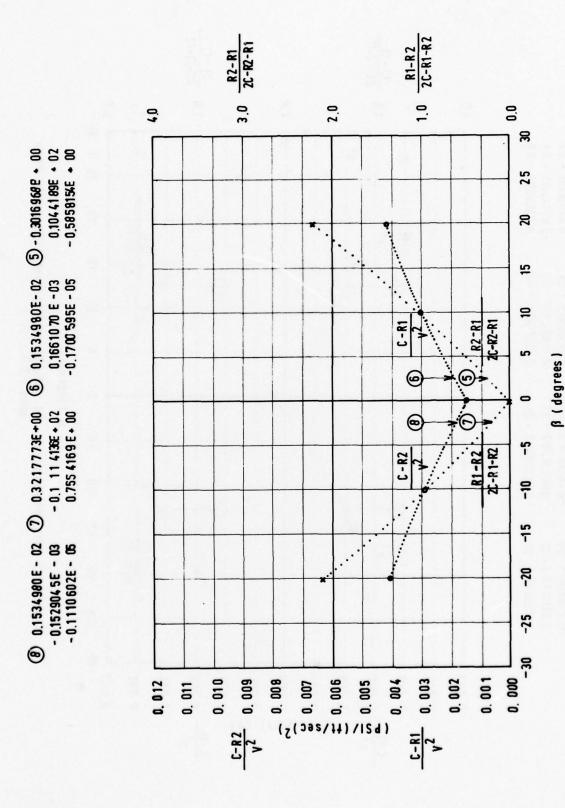
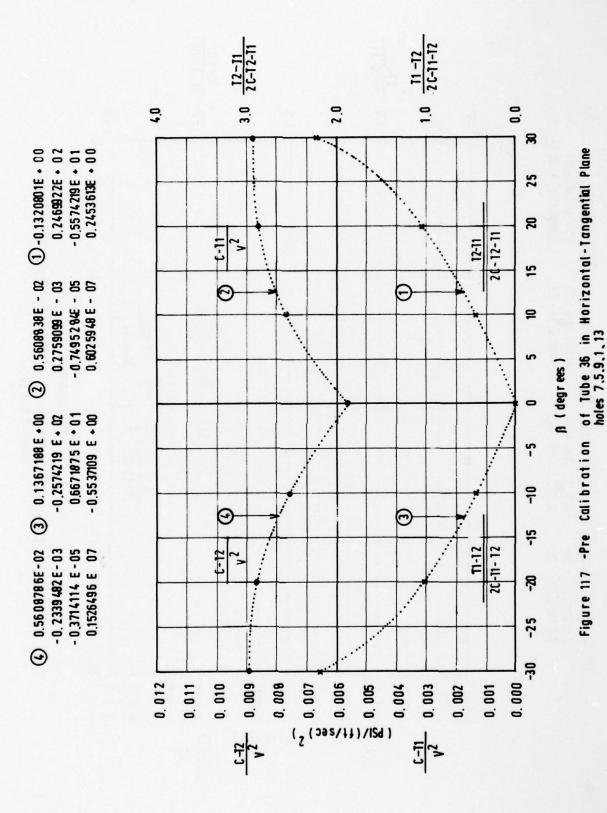


Figure 116-Pre Calibration of Tube 36 in Vertical-Radial Plane holes 7.6.8 .3.11

141



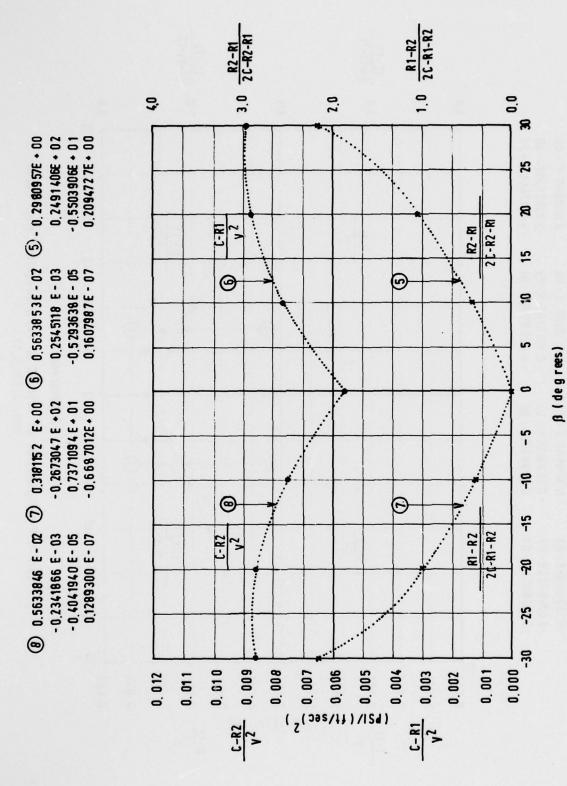


Figure 118 - Pre Calibration of Tube 36 in Vertical - Radial Plane holes 7.5, 9.1, 13

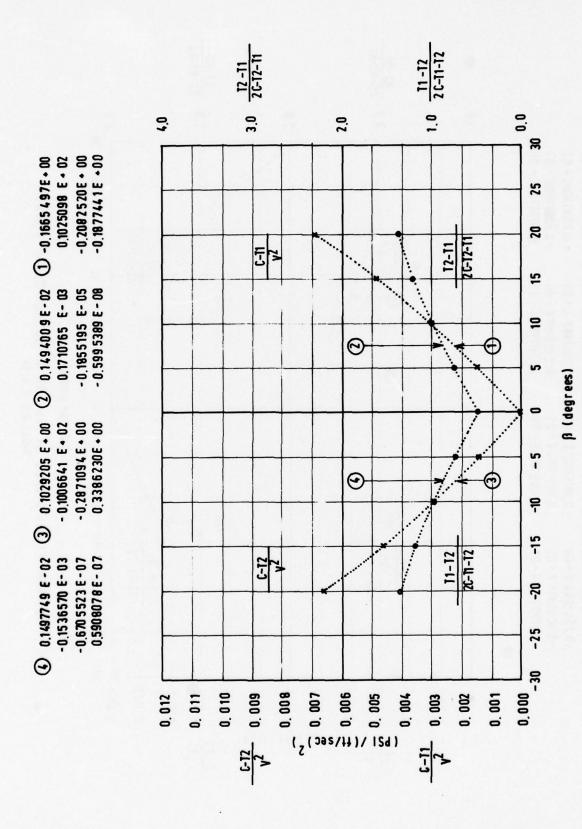


Figure 119-Pre Calibration of Tube 37 in Horizontal.-Tangential Plane holes 7.6,8,3,11

144

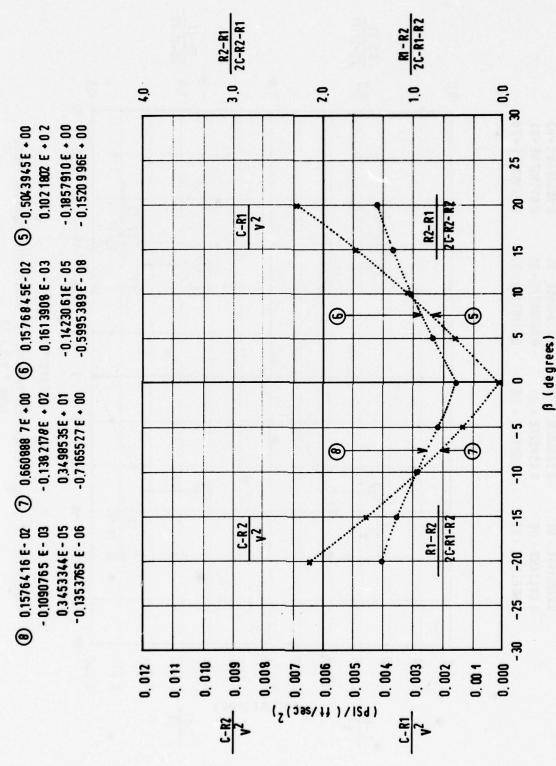
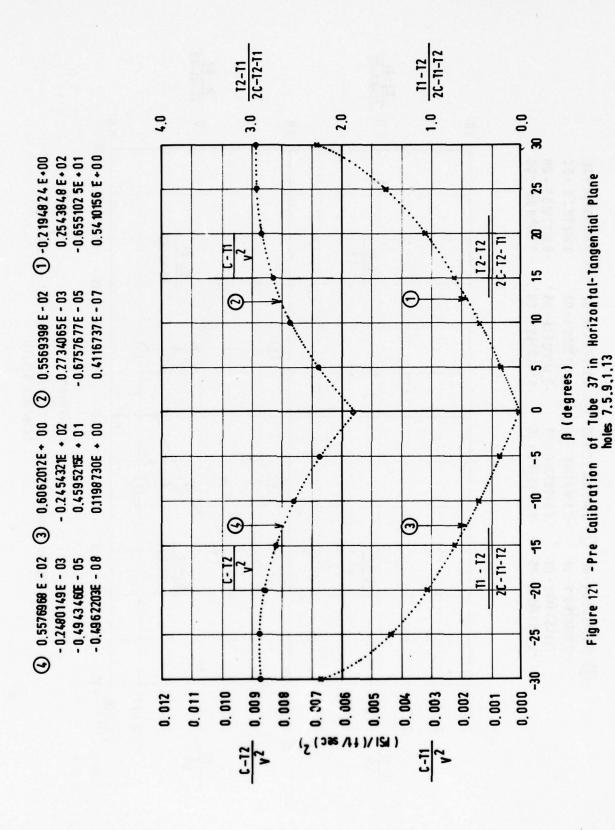
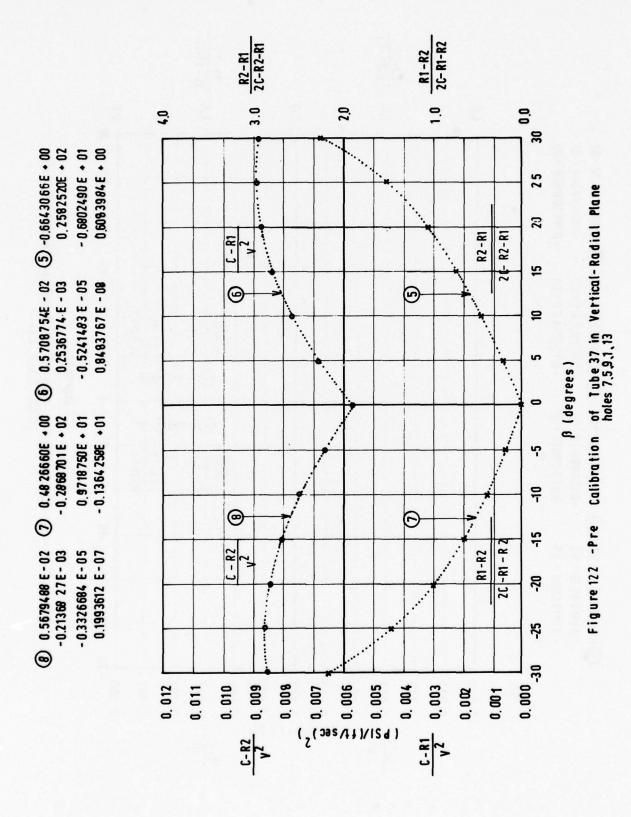


Figure 120 - Pre Calibration of Tube 37 in Vertical-Radial Plane holes 7.6,8,3,11





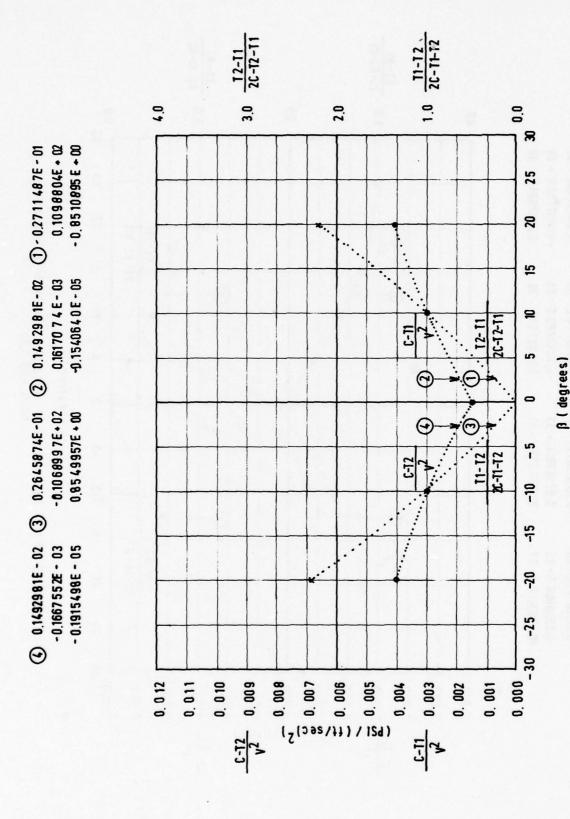
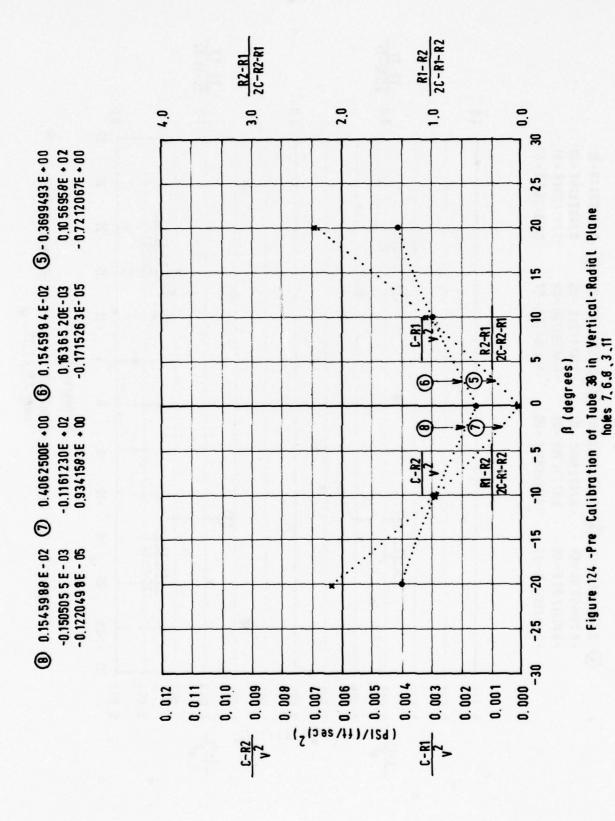
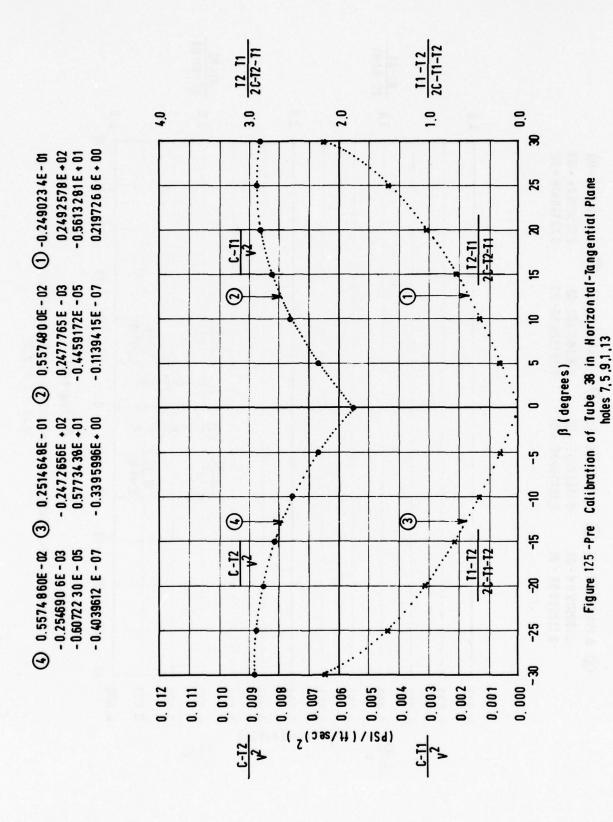


Figure 123 - Pre Calibration of Tube 38 In Horizontal-Tangential Plane holes 7.6.8.3.11

148





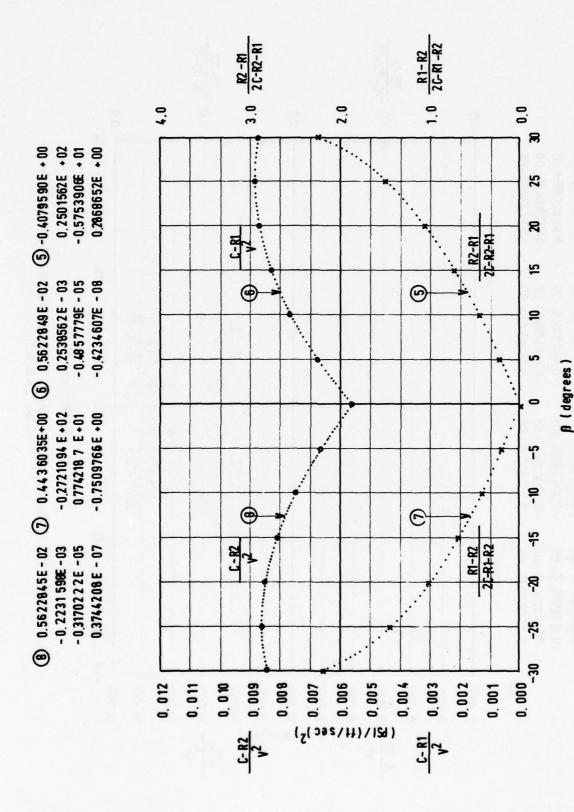


Figure 126-Pre Calibration of Tube 38 in Vertical-Radial Plane holes 7.5,9,1,13

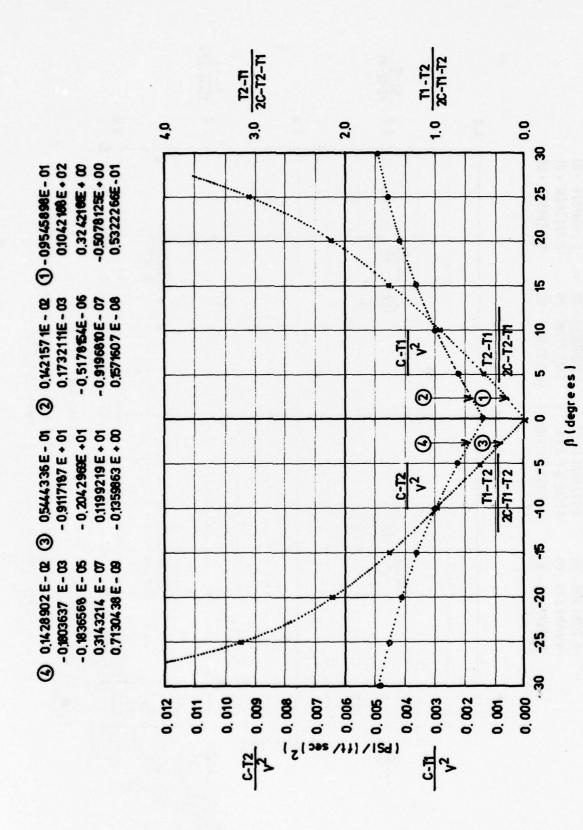
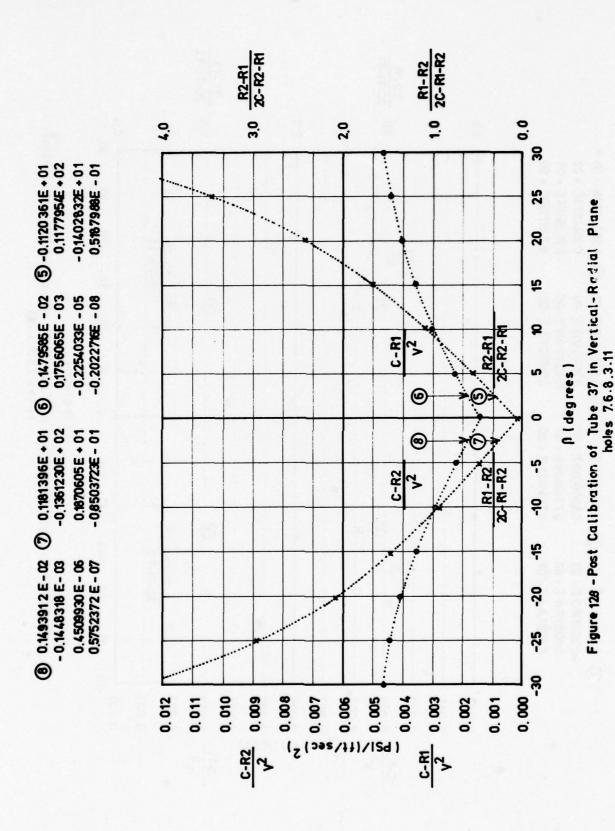


Figure 127 -Post Calibration of Tube 37 in Harizontal-Tangential Plane holes 7.6.8.3.11

152



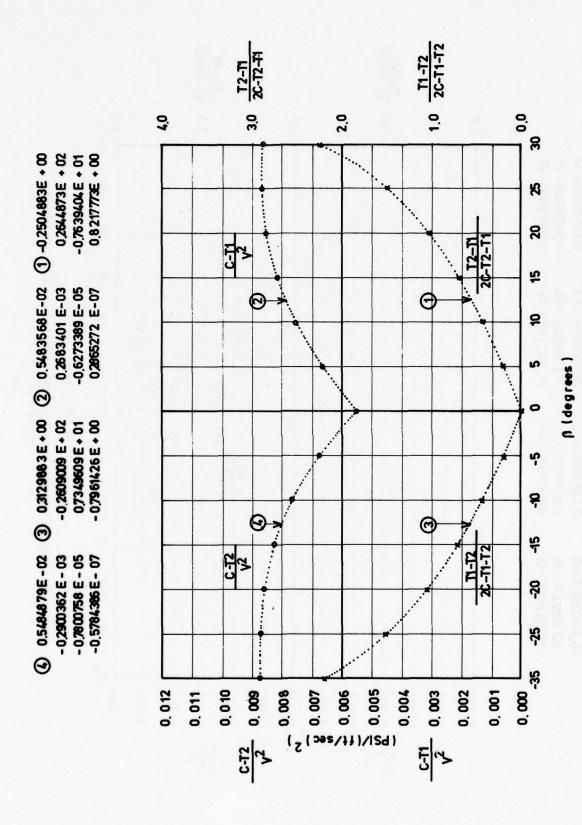


Figure 129 - Post Calibration of Tube 37 in Horizontal-Tangential Plane holes 7.5.9.1.13

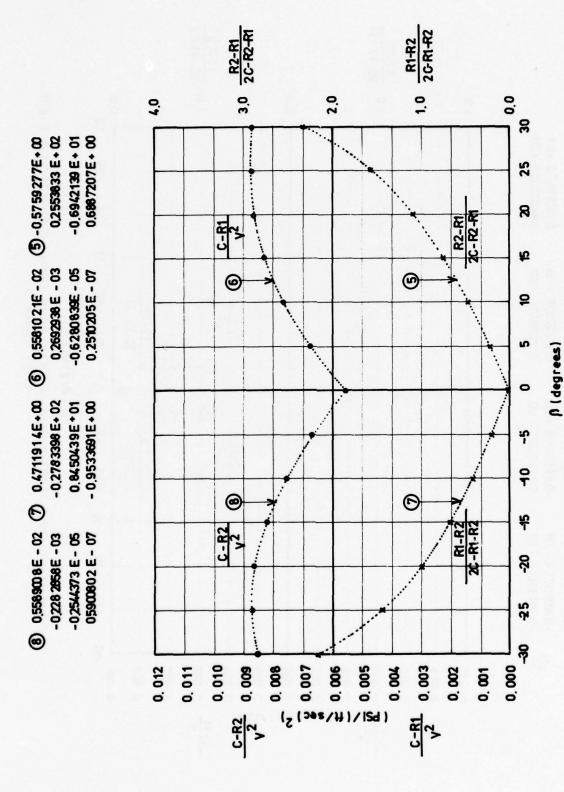


Figure 130 - Post Calibration of Tube 37 in Vertical-Radial Plane holes 7.5.9.1.13

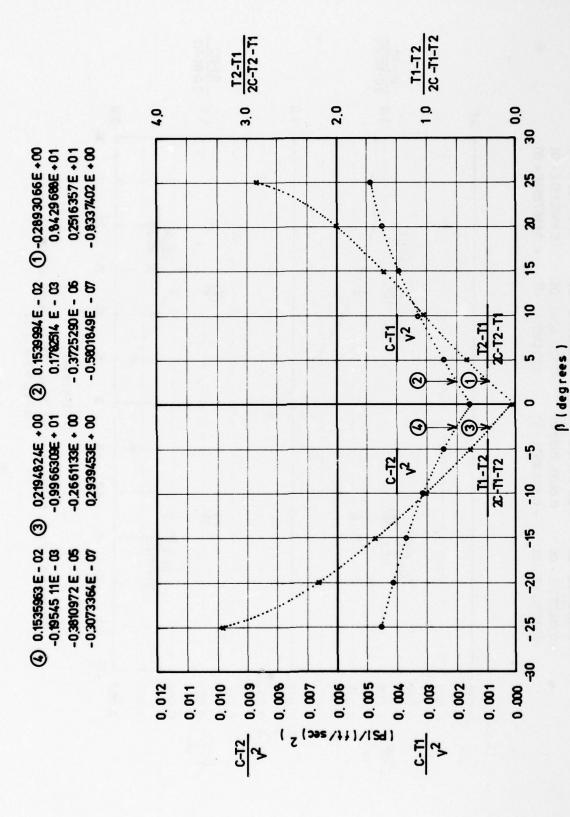


Figure 131 - Post Calibration of Tube 38 in Horizontal-Tangential Plane holes 7.6.8.3.11

156

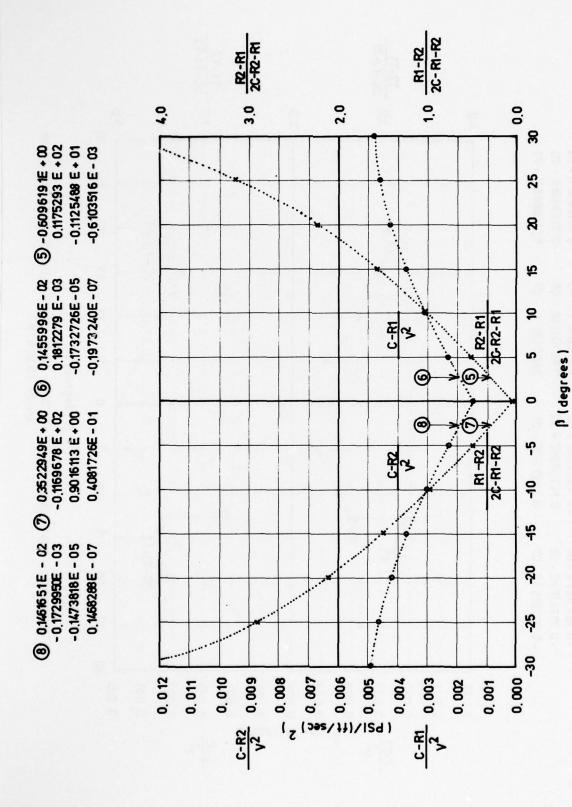


Figure 132 - Post Calibration of Tube 38 in Vertical-Radial Plane holes 7.6.8.3.11

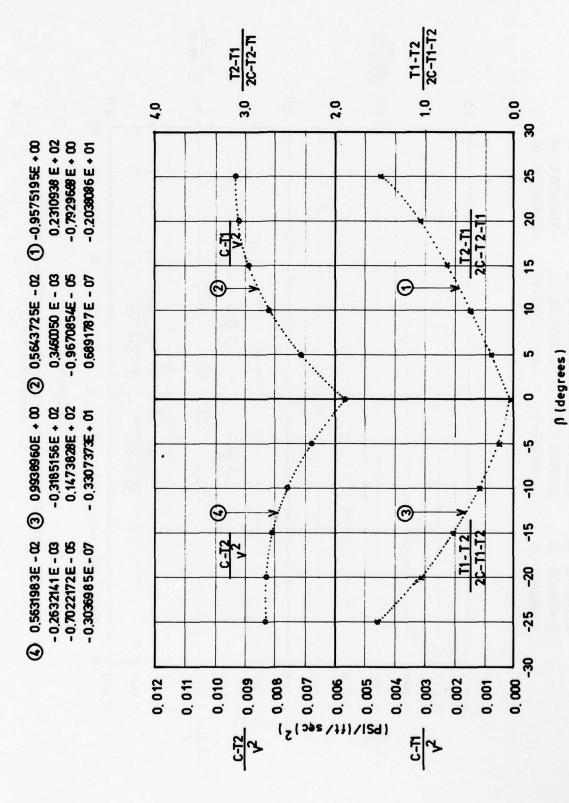


Figure 133 -Post Calibration of Tube 38 in Horizontal-Tangential Plane holes 7.5.9.1.13

158

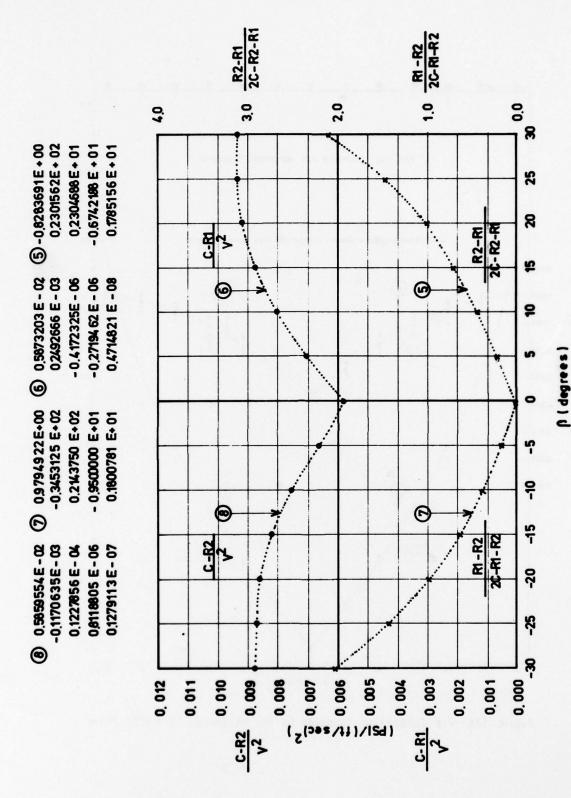


Figure 134 - Post Calibration of Tube 36 in Vertical-Radial Plane holes 7.5.9.1.13

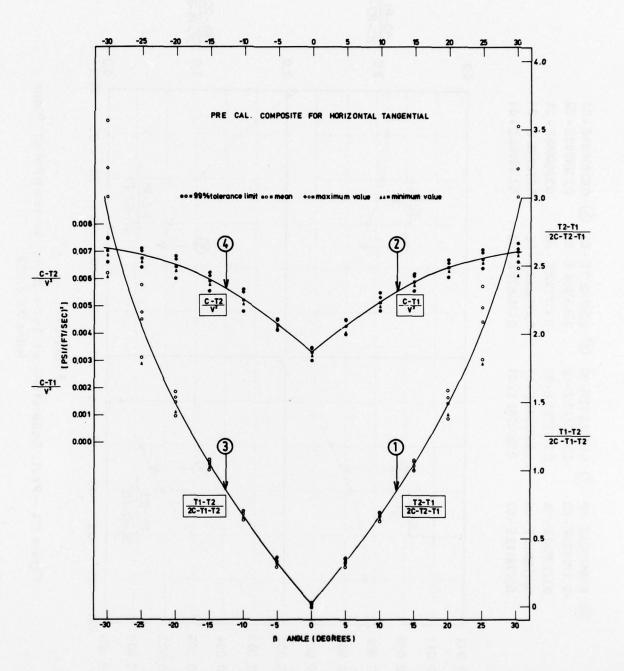


Figure 135 - Pre Calibration Composite for the Horizontal/Tangential Plane

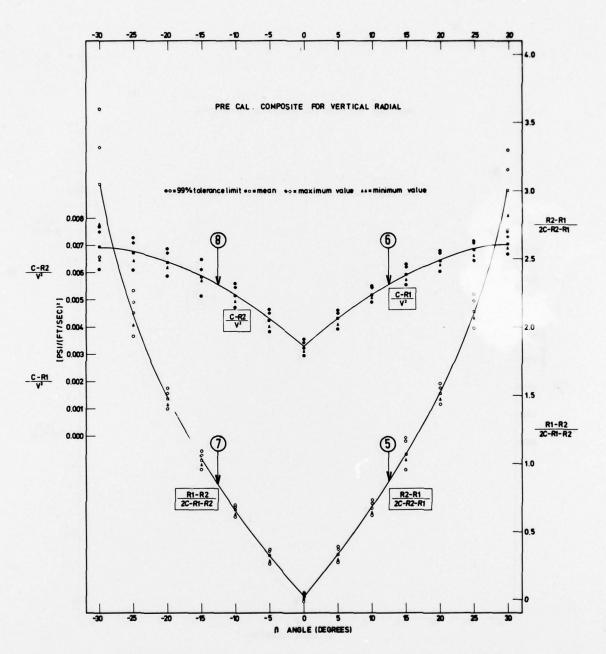


Figure 136-Pre Calibration Composite for the Vertical/Radial Plane

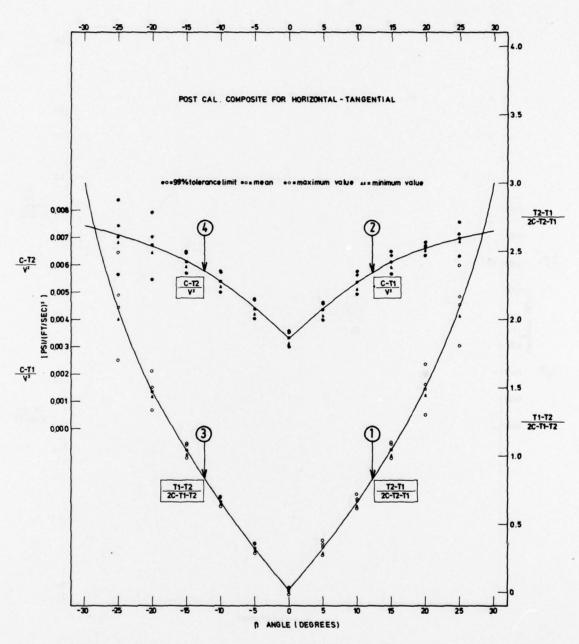


Figure 137- Post Calibration Composite for the Horizontal/Tangential Plane

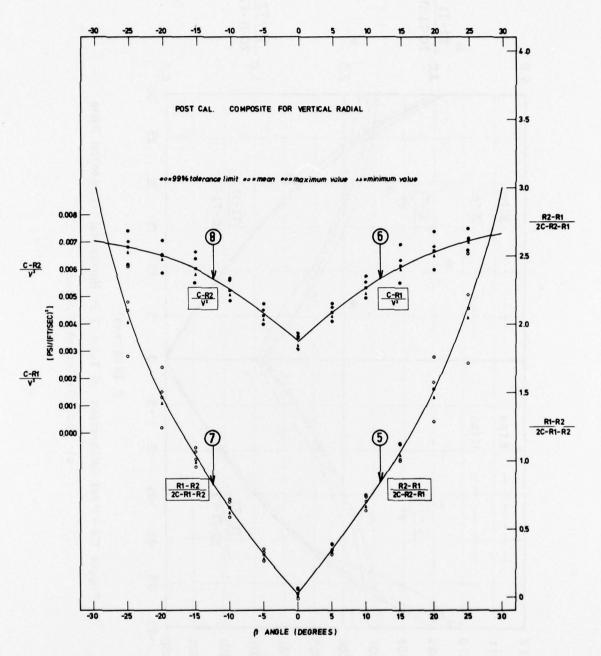


Figure 138 -Post Calibration Composite for the Vertical / Radial Plane

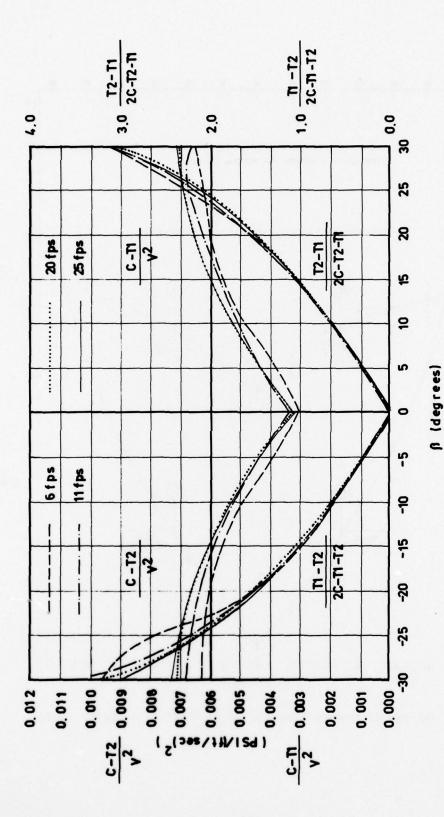


Figure 139 – Post Calibration of Tube 13 in Horizontal-Tangential Plane at Four Different Speeds

APPENDIX A

PROCEDURE FOR DERIVING VELOCITY COMPONENT RATIOS FROM PRESSURE MEASUREMENTS

Column	Identification	Derivation
1	C-Tl	Pressure at hole C minus pressure at hole Tl, converted to inches of water pressure.
2	C-T2	Pressure at hole C minus pressure at hole T2, converted to inches of water pressure.
3	T2-T1	= (C-T1) - (C-T2) $=$ Col. 1 - Col. 2
4	SC-IS-II	= (C-T1) + (C-T2) = Col. 1 + Col. 2
5	T2-T1 2C-T2-T1	$= \frac{(C-T1) - (C-T2)}{(C-T1) + (C-T2)} = Col. 3 / Col. 4$
6	$oldsymbol{eta_{LT}}$	Angle of water flow in the LT plane. Read from calibration curve at value of T2-T1
		in Col. 5. If the value of Col. 5 is negative, read the curve labeled $\frac{\text{Tl-T2}}{2\text{C-Tl-T2}}$.
7	C-TI V _{LT}	Read from calibration curve at value of $\beta_{\rm LT}$ in Col. 6, if the value of Col. 5 is positive. Otherwise, omit.
8	V _{LT}	Read from calibration curve at value of $\beta_{\rm LT}$ in Col. 6, if the value of Col. 5 is negative. Otherwise, omit.
9	V _{LT} ²	$= \frac{C-T1}{(C-T1)/(V_{LT}^{2})} = Col. 1 / Col. 7$
		if Col. 5 is positive, or
		$= \frac{C-T2}{(C-T2)/(V_{LT}^{2})} = Col. 2 / Col. 8$
		if Col. 5 is negative.
10	Y _{LT}	Component of the water velocity in the LT plane. = $\sqrt{V_{LT}^2}$ = square root of Col. 9.
n	cos ÂLT	= cos of angle in Col. 6.

Column	Identification	Derivation
12	sin ALT	= sin of angle in Col. 6.
13	v _r	Longitudinal component of the water velocity derived from V _{LT} .
		$= V_{LT} \times \cos \beta_{LT} = \text{Col. 10 x Col. 11.}$
14	v _T	Tengential component of the water velocity. = V _{LT} x sin β_{LT} = Col. 10 x Col. 12.
	4.72	
15	C-Rl	Pressure at hole C minus pressure at hole Rl, converted to inches of water pressure.
16	C-R2	Pressure at hole C minus pressure at hole R2, converted to inches of water pressure.
17	R2-R1	= (C-R1) - (C-R2) = Col. 15 - Col. 16
18	2C-R2-R1	= (C-R1) + (C-R2) = Col. 15 + Col. 16
19	R2-R1 2C-R2-R1	$= \frac{(C-R1) - (C-R2)}{(C-R1) + (C-R2)} = Col. 17 / Col. 18$
20	FIR	Angle of water flow in the LR plane. Read from calibration curve at value of R2-R1 in Col.
		19. If the value of Col. 19 is negative, read the curve labeled R1-R2 2C-R2-R1 2C-R2-R1 2C-R1-R2
21	C-R1	Read from calibration curve at value of $\beta_{ m LR}$
	V _{LT}	in Col. 20, if the value of Col. 10 is positive. Otherwise, omit.
22	C-R2	Read from calibration curve at value of $oldsymbol{eta}_{\mathrm{LR}}$
	V _{LT} ²	in Col. 20, if the value of Col. 19 is negative. Otherwise, omit.
23	V _{LR} ²	$= \frac{C-71}{(C-R1)/(V_{LR}^2)} = Col. 15 / Col. 21$
		if Col. 19 is positive, or
	(5) 117 storio 118 120 sq. (5) 170 sq.	$= \frac{C-R2}{(C-R2)/(V_{LR}^2)} = \text{Col. 16 / Col. 22}$
		if Col. 19 is negative.

Column	Identification	Derivation
24	V _{LR}	Component of the water velocity in the LR plane
		= $\sqrt{V_{LR}^2}$ = square root of Col. 23.
25	cos β_{LR}	= cos of angle in Col. 20.
26	sin ALR	= sin of angle in Col. 20.
27	A ^{r5}	Longitudinal component of the water velocity derived from VIR.
		$= V_{LR} \times \cos \beta_{LR} = \text{Col. } 24 \times \text{Col. } 25.$
28	V _R	Radial component of the water velocity.
		$= V_{LR} \times \sin \beta_{LR} = \text{Col } 24 \times \text{Col. } 26.$
29	V	Model speed in ft/sec.
30	v _x /v	Longitudinal component of the water velocity expressed as a ratio of ship speed.
		$= 1/2 \left(\nabla_{\underline{L}_1} + \nabla_{\underline{L}_2} \right) / \nabla$
		= (Col. 13 + Col. 27) / (2 x Col. 29)
31	v _ r /v	Tangential component of the water velocity expressed as a ratio of ship speed.
		= Col. 14 / Col. 29
32	v _R /v	Radial component of the water velocity expressed as a ratio of ship speed.
		= Col. 28 / Col. 29

V_/V is positive in the aft direction.

 V_{c}/V is positive in the counterclockwise direction.

Vp/V is positive toward the shaft centerline.

r/R and Θ are the polar coordinates of the point in the TR plane at which the wake is measured. r is the radial distance of the point from the centerline of the propeller shaft; R is the design propeller radius. Θ is the position angle measured from the top of the propeller disc in a counterclockwise direction.

CALC	ULATI	ON OF	WAKE	CALCULATION OF WAKE SURVEY	DATA OBTAINED WITH PITOT TUBE RAKE NO.	TAINE	D WITH	PITO	T TUB	E RAK	E NO.		MODEL	11	1	TEST		,
Col.	-	7	3	7	5	9	7	8	6	10	=	12	13	14				Pitot
2	11-3	21-3		12-11 26-12-11	11-21-32	וורן	15/21	21-3	V _U 2	Π _Λ	cos P _{LT}	sinfl	17,	1,	. ON	7/R	66	Tu be
-															-			
1															1			
~															~			
4															7			
2															5			
9															٩			
1															7			
8															80			
6															6			
2															9			
50	15	9	17	-18	19	70	12	n	23	77	25	92	11	82	53	30	3	32
No.	C-R1	C-R2	R2-R1	2C-R2-R1	R2-R1 2C-R2-R1	PLR	C-R-1	V-R2	V _{LR} 2	VLR	SOS PLR	Sinfle	4 _{L2}	۲. ۳	>	V, X	VXIV VIV YRIV	7R/7
_																		L.,
1																		
3																		
4																		
2															_			
9																		
1																		
8																		Ĺ
6																		

APPENDIX B

CALIBRATION CONSTANTS

I. FORM OF CALIBRATION EQUATION

 $Y = A_1 + A_2X + A_3X^2 + A_4X^3 + A_5X^4$

II. CALIBRATION CURVE LABELS FOR THE HORIZONTAL/TANGENTIAL PLANE

Curve Number

1

<u>X</u>

 $\frac{T_2 - T_1}{2C - T_2 - T_1}$

<u>Y</u>

β

2

β

 $\frac{C - T_1}{v^2}$

3

 $\frac{T_{1} - T_{2}}{2C - T_{1} - T_{2}}$

β

4

3

 $\frac{C - T_2}{v^2}$

III. CALIBRATION CURVE LABELS FOR THE VERTICAL/RADIAL PLANE

Curve Number

5

<u>X</u>

 $\frac{R_2 - R_1}{2C - R_2 - R_1}$

<u>Y</u>

β

6

β

 $\frac{C - R_1}{v^2}$

7

 $\frac{R_1 - R_2}{2C - R_1 - R_2}$

E

8

β

 $\frac{C - R_2}{v^2}$

DTNSRDC ISSUES THREE TYPES OF REPORTS

- 1. DTNSRDC REPORTS, A FORMAL SERIES, CONTAIN INFORMATION OF PERMANENT TECHNICAL VALUE. THEY CARRY A CONSECUTIVE NUMERICAL IDENTIFICATION REGARDLESS OF THEIR CLASSIFICATION OR THE ORIGINATING DEPARTMENT.
- 2. DEPARTMENTAL REPORTS, A SEMIFORMAL SERIES, CONTAIN INFORMATION OF A PRELIMINARY, TEMPORARY, OR PROPRIETARY NATURE OR OF LIMITED INTEREST OR SIGNIFICANCE. THEY CARRY A DEPARTMENTAL ALPHANUMERICAL IDENTIFICATION.
- 3. TECHNICAL MEMORANDA, AN INFORMAL SERIES, CONTAIN TECHNICAL DOCUMENTATION OF LIMITED USE AND INTEREST. THEY ARE PRIMARILY WORKING PAPERS INTENDED FOR INTERNAL USE. THEY CARRY AN IDENTIFYING NUMBER WHICH INDICATES THEIR TYPE AND THE NUMERICAL CODE OF THE ORIGINATING DEPARTMENT. ANY DISTRIBUTION OUTSIDE DTNSRDC MUST BE APPROVED BY THE HEAD OF THE ORIGINATING DEPARTMENT ON A CASE-BY-CASE BASIS.